THE MACROSCOPIC FUNDAMENTAL DIAGRAM IN URBAN NETWORK: ANALYTICAL THEORY AND SIMULATION

A Thesis
Presented to
The Academic Faculty

by

Yi Zhou

In Partial Fulfillment
of the Requirements for the Degree
Master of City Planning in the
School of City and Regional Planning

Georgia Institute of Technology
August 2013

A STUDY OF THE MACROSCOPIC FUNDAMENTAL DIAGRAM IN URBAN NETWORK BY ANALYTICAL THEORY AND SIMULATION

Approved by:

Dr. Catherine Ross, Advisor
School of City and Regional Planning
Georgia Institute of Technology

Dr. Jorge Laval
School of Civil and Environmental Engineering
Georgia Institute of Technology

Dr. Jiawen Yang
School of City and Regional Planning
Georgia Institute of Technology

Date Approved: Jul 1st, 2013

[To the students of the Georgia Institute of Technology and whoever that has provided advise and help in the writing for this thesis]

ACKNOWLEDGEMENTS

I wish to thank Dr. Jorge Laval, a professor in the School of Civil and Environmental Engineering, Georgia Institute of Technology and also a committee member for this thesis, for sharing his earlier java programming scripts for traffic simulation in an urban network. The programming for the simulations adopted in this thesis has benefited greatly from his idea of applying the CA(L) model to predict vehicle trajectories in the urban network.

TABLE OF CONTENTS

LIST OF TABLES

LIST OF FIGURES

LIST OF SYMBOLS AND ABBREVIATIONS

$A(t), A_i(t)$	Number of vehicles that have arrived in the system/ the node(i) by time t
$L(t), L_i(t)$	Number of vehicles that have left the system/ the node(i) by time t
$O(t), O_i(t)$	Number of trips that have originated within the system/ the node(i) by time t
$U(t), U_i(t)$	Number of trips that have originated outside the system/ the node(i) by time t
$E(t), E_i(t)$	Number of trips that have ended within the system/ the node(i) by time t
$D(t), D_i(t)$	Number of trips that have ended outside the system/ the node(i) by time t
κ	Jamming density on the triangular Fundamental Diagram
q_c	Maximum capacity on the triangular Fundamental Diagram
v_f	Free-flow speed on the triangular Fundamental Diagram
$-w$	Wave speed on the triangular Fundamental Diagram
k_c	Critical density on the Fundamental Diagram
G	Green time in a signal cycle
R	Red time in a signal cycle
C	The time length of a signal cycle
q	Generalized average circulating flow in the system
k	Generalized average density in the system
v	Generalized average speed in the system
$\|A\|$	The area of a defined rectangle area A on the space-time plane
$t(A)$	Total travelled time in a defined rectangle area A on the space-time plane
$d(A)$	Total travelled distance in a defined rectangle area A on the space-time plane
P_L	Left turning rate at an intersection for vehicles
P_R	Right turning rate at an intersection for vehicles

P_S	Straight-moving rate at an intersection for vehicles
L	Length of a road
δ	Offset between two traffic signals at both ends of a road
γ	Number of intersections a moving observer has passed on a road link
$p(n)$	Possibility for a vehicle to terminate its trip endogenously within n steps of movement
γ_{max}^{f}	The maximum number of intersections a backward moving observer can pass on a road link without being stopped red signal in the forward moving process
γ_{max}^{b}	The maximum number of intersections a backward moving observer can pass on a road link without being stopped red signal in the backward moving process
t_{tored}^{γ}	The time between a vehicle has arrived at an intersection and the signal at that intersection becomes red after its arrival
D_γ	The arrival time of a vehicle at the γth intersection in the current cycle at that intersection
m, m_b	The remainder after D_1 is divided by cycle time C in the forward/backward moving process
h_N	The location of the Nth "cycle-jumping" intersection (Define of "cycle-jumping is shown in Section 4.2")
ρ	The probability that an endogenous trip starts from a length cell on the road during one time step in simulation
π	The probability that a driver will choose to exit the system endogenously if he finds an exit opportunity
λ	The density of exit opportunities for endogenous exiting along the road
MFD	Macroscopic Fundamental Diagram
FD	Fundamental Diagram
CA(L) model	Cellular automata linear model
c.o.v.	Coefficient of variance

SUMMARY

The Macroscopic Fundamental Diagram (MFD) is a diagram that presents a relationship between the average flow (production) and the average density in an urban network. Ever since the existence of low scatter MFD in urban road network was verified, significant efforts have been made to describe the MFD quantitatively. Due to the complexity of the traffic environment in urban networks, an accurate and explicit expression for the MFD is not yet developed and many recent research efforts for MFD rely on computer simulations. On a single corridor, an analytical approximation model for the MFD exists. However, this thesis expanded this theory in two directions. First, we specialize the method for models with equal road length on the corridor, which greatly reduces the complexity of the method. We introduce the adoption of seven straight cuts in approximation. Computer simulations are conducted and show a high compatibility with the approximated results. However the analytical approximation can only be applied with the assumption of constant circulating vehicles in the system without turnings and endogenous traffics. Secondly, we show that turnings and endogenous traffic can bring various impact on the shape of the MFD, the capacity, the critical density, the variance in density and cause a phenomenon of clustered traffic status along the MFD curve. Furthermore, the simulation using stochastic variables reveals that the variance in turning rates and endogenous traffic don't have significant impact on the MFD. This discovery enables studies to focus on scenarios with deterministic parameters for those factors. While traditional objective of engineering for network is to maximize capacity and widen the range for the maximum capacity, our results indicate that traffic

stability at the maximum performance is poor if the system does not stay constantly in equilibrium status. This thesis provides insights into the factors that affect the shape of the MFD by analytical approximation and simulation.

CHAPTER 1

INTRODUCTION

1.1 Introduction to the MFD Research

The Macroscopic Fundamental Diagram (MFD) is deemed as an important tool to evaluate the traffic performance within an urban area at a macroscopic scale and the characteristics of capacity in an urban network. The MFD represents a consistent and reliable relationship between the average flow and density within a defined network system. In traffic flow theory, traffic parameters of density, flow and speed are linked together based on "fundamental diagram" (FD), which characterize the traffic at a specific location. Traffic can be measured by the MFD if the average of the highly scattered flow and density data from each individual spots can be plotted as a low-scatter MFD curve and reflect the average traffic property for a local network. However, due to the correlation between successive arterial links and the diversity in traffic conditions in road networks, it is hard for researchers to accurately formulate the MFD.

In the past, a majority of progress in traffic flow theory has been made for evaluating and predicting the performance for single components such as an intersection or a section of a highway. There are few proposals for dealing with the property for a system that is composed of components that are connected closely with each other. As proved by Greenshields (Greenshields, 1935), on a single street level, the flow can be expressed as a function of density, and this relationship can be graphed as the fundamental diagram (FD). The first theoretical proposition of a unimodal relation between flow and density in a network has been developed by Godfrey (1969). And this idea has also been initiated by Herman and Prigogine in the two-fluid model (1979), which posits that the average speed in urban network was a function of the fraction of stopped vehicles in the system. This theory was later refined by Herman and Ardekani (1984) that the fraction of stopped vehicles can be further functioned by the average density.

However, situation becomes more complex when we consider if this simple relationship can be extended to urban road networks. The first empirical evidence that the model of MFD can be observed in congested urban networks is presented by Geroliminis and Daganzo (2007) (2008). It collects disaggregated lane data from 500 fixed sensors and 140 taxi mobile sensors in Yokohama, Japan. The flow and density are averaged with a weight of road lengths and the derived plots present a clear macroscopic flow-density relationship (see Figure 1.1). The study in Yokohama shows an important relationship between the existence and property of MFD and the distribution of congestion in the network. Although this result doesn't indicate the universal existence of MFD, it suggests that it is possible to relate the average flow and density in certain networks. In the work at Yokohama, sufficient regularity is postulated including slow-varying and uniformly distributed demand, and homogeneous network infrastructure. However, some later studies show that strict homogeneity isn't necessary for define MFD (Helbing, 2009) (Mazloumian, Geroliminis, & Helbing, 2010) (Geroliminis & Sun, 2011). Yet, more studies and experiments are required to identify the type of networks that can be well characterized by invariant and low-scattered MFD.

Other studies have pointed out that networks with heterogeneous distribution of traffic characteristics tend to exhibit networks flows far below those with homogeneity conditions (Daganzo, Gayah, & Gonzales, 2011). It is also proved analytically that the variations in the parameters for a corridor could suppress the maximum performance on it (Geroliminis & Boyaci, 2012). A recent study successfully relates the average flow with average density and the inhomogeneity of density with a two dimensional generalization (Knoop, 2012). Furthermore, another empirical study of Buisson and Ladier (2009) in Toulouse, France, shows hysteresis effect that loops the MFD curvature can be observed when disturbance to network appears. This phenomenon was explained by Gayah and Daganzo (2011) by a two-bin system model. They proved the loading process and the recovering process in the network may generate asymmetric path for density pairs and thus cause congestion not to be distributed uniformly in the system, if with fixed transfer rate between two "bins" in the system. The imbalance in congestion

distribution cannot be eliminated even in the most homogeneous network with the same road length and symmetric signal designs. They also point out that if drivers can adapt to avoid congested routes within the network, that behavior will effectively exclude the occurrence of hysterics loops in the MFD and improve the uniformity in congestion distribution.

However, due to the requirements for large amount of data collection in urban network, the existing data collected for the MFD studies is very scarce. Many researches are still using simulation for urban network to predict the shape and formula for local MFDs. In current researches, there are still very few theories providing analytical methods to forecast the MFD. As far as the writer has concerned, one of the most significant analytical models for the MFD prediction is suggested by Daganzo and Geroliminis, which adopts variational theory to approximate an upper boundary for the MFD. The reliability of this method is validated with urban traffic data collected in Yokohama and San Francisco (2008). This thesis will evaluate this model by simulation and discuss on the potential refinements with this model.

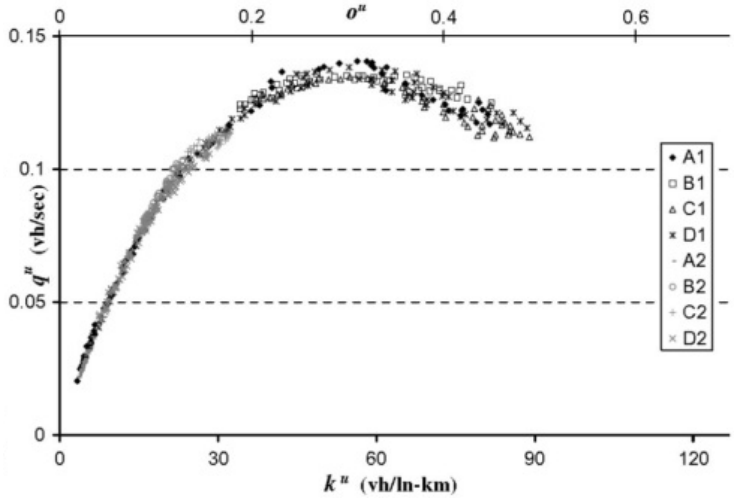

Figure 1.1 Deriving flow-density curve from detector data in Yokohama
Source: (Geroliminis & Daganzo, 2008)

1.2 Statement of the Research Objectives

Daganzo and Geroliminis has proposed an approximation method for MFD (2008) derived from variational theory. This model works on a ring with a fixed number of vehicles circulating, i.e. when a vehicle exits the system another vehicle enters the system. It can also be applied for the road links that are composed of one-way roads connected to each other end by end under the assumption of a constant number of circulating vehicles on the link. In this scenario, the model demands a very little turning rate in and out of the system and the trip for each vehicle in the system should not be ended within the system. It is posited that MFD can be well approximated for homogeneous road links with slow-changing traffic demand. However, the model carries drawbacks because it tends to overestimate the flow when predicting the real-world situations and its assumptions of constant vehicles, no endogenous trips, and very little turning rates are hard to be met in real practice. This model doesn't reflect the impact of other factors, such as driver adaptions and heterogeneity for the inputs and outputs in a network.

The thesis focuses on the approximation model (2008) by Daganzo and Geroliminis and evaluates its prediction by simulation. The approximation model assumes "virtual" observers that move forward or backward and stop only at traffic lights. The average speed and maximum passing rate is estimated for each observer and develop an approximated cut for each of them. Under this model, if the first intersection where the observer is forced to stop is very far from the starting point, a majority of cuts is required for prediction of the MFD. However, when the road link is homogeneous in length and signal settings, it is not necessary to include all the cuts as described in the approximation model because some of them are completely beyond others and not used for making the upper envelope for the MFD. A refinement is proposed in this thesis to filter those redundant cuts. Moreover, the inclusion of a limited number of cuts enables us to explicitly formulate the MFD. One of the thesis objectives is to simplify the model by reducing the redundant cuts in the assumption for a homogeneous road link. The identification of those effective cuts is significant because it indicates that the characteristic of the MFD on a homogenous single-way road link is determined by a few intersections on it.

Then the thesis attacks on the situations where the assumptions for the approximation model are not held. The thesis discusses the scenarios with the turning rates, the existence of endogenous generated and ended traffic, the adaption behavior of drivers, the slow-movers in the traffic stream and their effects on the MFD. The MFDs simulated in these various scenarios are compared with the approximation for the MFDs. Although in this thesis these comparisons are not to give explicit formula and parameters for these impacts, they provide useful information on how these factors can impact on the shape of the MFD and lay a base for future studies to quantify those impacts. A summary of the research objectives with this thesis is shown as follows:

(1) Improvements on the existing approximation model by reducing the number of effective cuts required in the approximation process. The explicit formula for these identified effective cuts is given.

(2) The approximated results are compared with the simulations to check the compatibility between them. It is expected that the result of the two should be consistent with each other because both variational theory and the cellular automata model used for simulation are rested on the assumption of infinite acceleration and deceleration rate and a triangular FD.

(3) The existence and the shape of the MFD are tested in networks where turning rates are allowed for vehicles to transfer between road links. The simulated MFD is compared with the MFD approximated by variational theory.

(4) The effect of endogenous traffic on the MFD is tested by introducing vehicles that start their trip within a street or end their trip within a street. The simulated MFD is compared with the approximation model.

1.3 Planning of the Research

A flow chart representing the research planning of the thesis is given in Figure 1.2. The research begins with reviewing literature for the MFD and the literature provides information in three aspects: (1) a few traffic models in the earlier research for the MFD; (2) the required data and parameters we need to collect from our modeling process: speed, density and flow; (3) how the data are processed to make an aggregation for MFD. The analytical traffic models applied within this thesis include the reservoir theories, the cellular automata model, and the upper approximation method for MFD. The reservoir theory (Daganzo C. , 2007)describes the network as a correlated combination of simple components such as an intersection or a roundabouts and traffic flow are seen as liquids that pass through or are temporarily stored in those components. The cellular automata model (CA) (Daganzo C. , 2004) provides a discrete way to simulate the change in traffic with time. The MFD approximation model (Daganzo & Geroliminis, 2008) introduces a method to predict the MFD analytically on a road link. The detailed description of these literatures can be viewed in Chapter 2.

The research runs java programs for obtaining the MFDs that are based on the simulation and approximation methods provided in the literature review. The models are constructed in three different scenarios: (1) on a road link; (2) in a one-way network; (3) in a two-way network. The flow and density are measured in the models and exported in text format and can be imported into the Matlab. Three dimensional heat maps featuring the simulated flows are plotted to provide a better comparison between the simulation and the analytical approximation.

A comparison between the approximated MFD and the simulated results is a major tool that we use to validate the refinement with the approximation model and produce the MFDs for those situations where the assumption for the approximation model doesn't apply. The programming with java displays the simulated results and the approximation for the MFD simultaneously to facilitate the comparison.

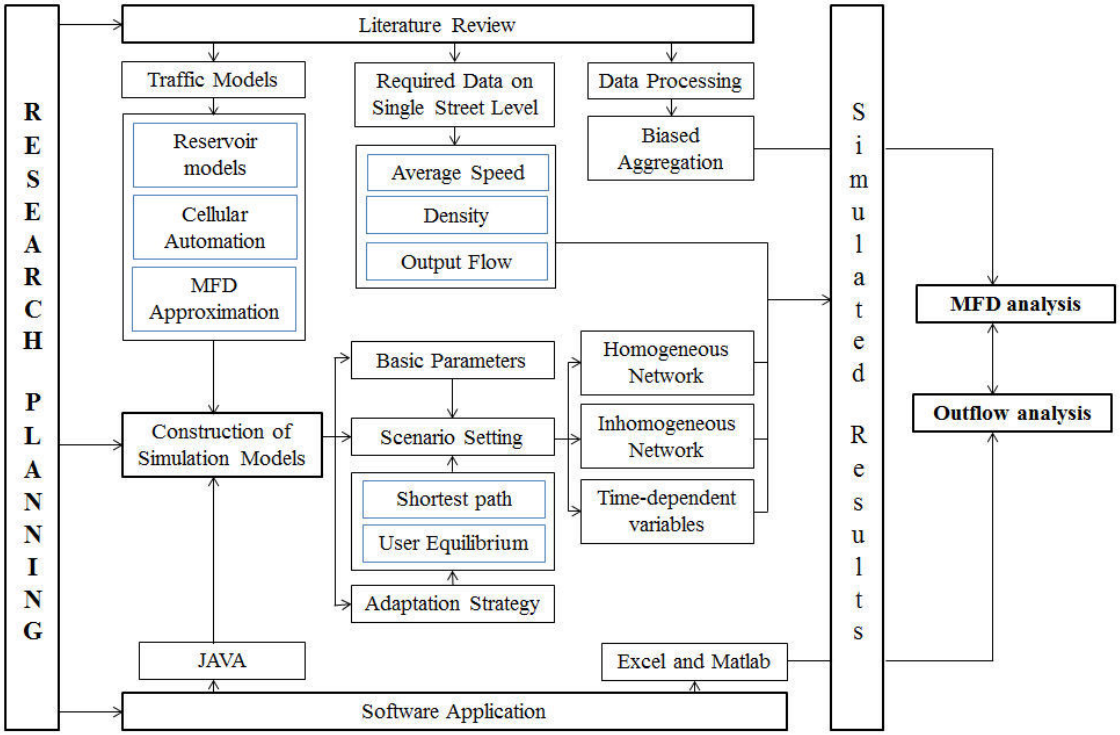

Figure 1.2 Planning of research

1.4 Outline of the Thesis

This thesis is organized into 6 chapters and is outlined as follows.

Chapter 1 Introduction: This chapter provides a basic description of the research conducted in this thesis. It first summarizes the history and recent progress in the MFD research. The thesis defines the objective of the research as a discussion on the refinement and applications for the Daganzo's approximation model.

Chapter 2 Literature review: This chapter reviews the analytical traffic models. It briefly reviews three models: the reservoir theory, the CA model for vehicle trajectory prediction and the approximation model. The mathematical mechanics behind these models are briefly explained in this chapter and the equations that will be applied for the simulation are presented. This chapter sets the platform for the common understanding of the discussion of traffic flow characteristics in the thesis.

Chapter 3 Assumptions and methodology: The basic assumptions that the thesis and simulation relies on is described in this chapter. It explains the homogeneous settings we assume for the network and the road link. It also provides a general description for methodology, which is an extension of the equations quoted from Chapter 2. It describes the calculation for generalized flow and density, the driver adaptation strategy, and the parameter and environmental settings in the model.

Chapter 4 Applications with road links: This chapter discusses the application of VT theory with the model of a chain of roads. It assumes a homogeneous length of the roads, exogenous traffic, and a zero turning rate. This chapter suggests a refinement on the MFD approximation of Daganzo (2008) by reducing redundant cutting lines from the model. It has proved that these cuts can be ignored without degrading the accuracy of the original model. The reliability of the improved MFD approximation is verified based on the CA(L) model.

Chapter 5 Applications with urban networks: This chapter conducts the simulation and analysis for homogeneous networks with turning rates and endogenous traffic. It explores the potential shifts of the MFD when turning rate and endogenous traffic applies in the network. The MFDs generated in this chapter are compared with those generated with the same parameters in Chapter 4. The sensitivity of the system to the effects of driver adaption and slow movers in traffic stream are also discussed in this chapter.

Chapter 6 Conclusions and recommendations: This chapter summarizes the result observed from the previous chapters. It also gives an outlook for potential future studies with MFD that haven't been completed in this thesis.

CHAPTER 2

LITERATURE REVIEW

2.1 Reservoir Theories

2.1.1 Types of Flow

The reservoir theory (2007) treats the flow in the system as liquid and traffic nodes as reservoirs that can retain liquids. The network is seemed as a correlated net of traffic nodes that can serve as "reservoirs". In this theory, it categorizes the traffic demands into 4 types based on their generation and destination. If the total number of vehicles traveling on link i at time t is denoted as $n_i(t)$, it is the difference of cumulative number of vehicles to have arrive and left link i by time t: $n_i(t) \equiv A_i(t) - L_i(t)$. The exogenous portions of $A_i(t)$ and $L_i(t)$ are respectively denoted $O_i(t)$ and $E_i(t)$, shorthand for the trips that originated and ended within link i. Similarly the endogenous portions are denoted $U_i(t)$ and $D_i(t)$, shorthand for upstream arrivals and downstream departures. It's trivial that: (Daganzo C. , 2007)

$$A_i(t) \equiv O_i(t) + U_i(t) \tag{2.1a}$$

$$L_i(t) \equiv E_i(t) + D_i(t) \tag{2.1b}$$

2.1.2 Relationship Between Exit Flow and Circulating Flow

Two simplest single-reservoir models are shown in Figure 2.1. On a freeway link of length l with no endogenous traffic, the traffic won't get congested unless a restricted flow is applied. The exit flow from this structure is the same as the triangular FD. In comparison, on a closed loop of length l with no exogenous traffic, the exit flow is smaller than the congested flow with FD. Suppose the average trip length d is homogeneous, the exit flow can be expressed as $g = (l/d)Q$. In the loop, the congested status can be obtained by modulating the input flow.

Most traffic systems fall between the above two extreme cases, where the maximum sustainable accumulation v can be achieved without exit restriction falls somewhere on the

declining branch of the FD (see Figure 2.2). When the traffic demand is applied slowly, the exit flow g can be roughly seen as the MFD for the system. (Daganzo C. , 2007)

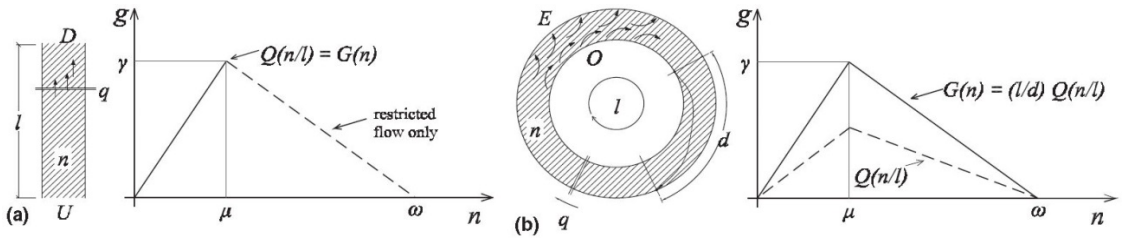

Figure 2.1 Outflow versus vehicle number diagrams for simple reservoir models
Source: (Daganzo C. , 2007)

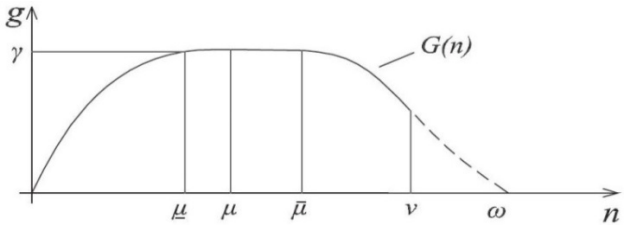

Figure 2.2 A generic exit function
Source: (Daganzo C. , 2007)

2.1.3 Drivers' Exiting Rate

Suppose that drivers look for "exit opportunities" on a road at various exits and take the first exit that satisfies their need. Let the opportunity density along the road be $\lambda(x)$ and the possibility for each opportunity to satisfy their need be $\pi \ll 1$. Let $N(x)$ be the cumulative number of opportunities along a road from a reference point $x = 0$, so $N(x) = \int_0^x \lambda(y)dy$. Set intervening opportunity $N(x, y) = N(y) - N(x)\ if\ y > x$, where N is the total opportunity. Then the probability for the driver to exit between x and y is defined as

$$p(x, y) = 1 - (1 - \pi)^{N(x,y)} \qquad (2.2).$$

2.2 Cellular Automation Model

The cellular automata linear CA(L) model (Daganzo C. , 2004) is one of the many vehicle prediction models. The simplest car–following (CF) models relates speed and spacing by a linear rule, with a time tag. Let $x^n(t), v^n(t)$ be the position and speed of car n at time t, and $s^n(t) = x^{n-1}(t) - x^n(t)$ be the spacing in front of car n at time t. And we further define v_f as the free-flow speed, $1/\kappa$ be the jam spacing. The model assumes that drivers sample their spacing at times $t_i = i\tau$ and adjust the speed to $v_{i,i+1}^n = V(s_i^n) = min\left(s_i^n - 1/\tau\kappa\,, v_f\right)$ during this interval. Under this model assumption, the jam spacing is preserved at all times. The final vehicle position can be formulated as $x_{i+1}^n = min\left(x_i^n + v_f\tau, x_i^{n-1} - 1/\kappa\right)$.

The kinematic wave (KW) model is consistent with the CF model by choosing appropriate parameters. The KW model assumes that the wave speed in the congested regime is $w = -1/\tau\kappa$. Let $N(t,x)$ denote the number of vehicles that have passed point x by time t. The initial vehicle positions are given by a Lipschitz-continuous and non-decreasing function, $N(0,x)$, such that $N(0,x) - N(0,x+\Delta x) \le \delta\Delta x$ for all x and Δx. The vehicle position is given by:

$$\begin{cases} x^n(t) = x^n(0) + tV\left(x^{n-1}(0) - x^n(0)\right) & if\ t \le \tau \\ x^n(t) = min\left\{x^n(0) + tv_f, x^{n-1}(t-\tau) - \delta\right\} & if\ t \ge \tau \end{cases}$$

If we only concern the position of vehicles at the lattice times $\{t_i = i\tau\}$, the equation can be turned into a discrete version of the KW model $x_{i+1}^n = min\left\{x_0^n + (i+1)\tau v_f, x_i^{n-1} - 1/\kappa\right\}$.

The parameters in the CA(L) model are correspondent to the KW model. In CA(L) model, the space is discretized in increments $1/\kappa$, and the model works with dimensionless distance $z = \kappa x$ and lattice number $z_j = j$. Define a dimensionless quantity $\omega = \tau v_f \kappa$, then the trajectory of vehicle can be expressed as: $z_{i+1}^n = min(z_i^n + \omega, z_i^{n-1} - 1)$. If ω is a positive integer, and the data $\{z_i^0, z_0^n\}$ are also integer, the position of the vehicle will always fall on the lattice lines. CA(L)=CF=KW for the associated ILVP of any LVP. (Daganzo C. , 2004)

2.3 Analytical Approximation for the MFD

Daganzo and Geroliminis have shown an approximation method for the MFD without relying on simulation (2008), which can be applied to a single street with no turns and a constant number of vehicles at all times. The problem is treated with variational theory. It uses a relative capacity function to give the maximum flow rate at which vehicles can pass an observer moving along the street with any average speed v. By the triangular FD, the maximum passing rate r is defined by $r(v) = -k_c(v - v_f)$.

A second element of VT is the set of moving observer paths on the (t, x) plane which travels at an average speed within the range of $[-w, v_f]$. Suppose $\mathcal{P}$ is a valid path, $v_{\mathcal{P}}$ is the average speed for the complete path, and $\Delta(\mathcal{P})$ is the path's cost evaluated from $r(\mu)$. By definition, $\Delta(\mathcal{P})$ is the change in vehicle numbers that could possibly be seen by the observer $\mathcal{P}$. Thus the quantity $R(u) = lim_{t_0 \to \infty} inf_{\mathcal{P}}\{\Delta(\mathcal{P}): u_{\mathcal{P}} = u\}/t_0$ represents the upper bound to the average rate at which traffic can overtake an observer that travels with average speed u during a long period. It is trivial that $R(u)$ is a least-cost path problem and $R(0)$ is the system capacity. It has been shown by Daganzo (2005) that the optimal path always exists piece-wise linearly: either following an intersection line or else slanting up or down with slope v_f or $-w$.

Since a ring's MFD, $q = Q(k)$ is concave and given by $q = inf_{\mathcal{P}}\{ku + R(u)\}$, the MFD is the lower envelope of the 1-parameter family of lines on the (k, q) plane defined by $q = ku + R(u)$ (see Figure 2.3). Because evaluating $R(u)$ for all u can be tedious, three families of practical cuts that jointly bound the MFD is proposed. The first family uses a stationary observer at the most constraining intersection. It leads to the first cut: $q \leq min\{q_c G_i/C_i\}$, where q_c is the capacity, G_i is the green phase, and C_i is the signal cycle length at the ith intersection. The second family uses forward moving observers which move forward at speed v_f except when delayed by a red phase at an intersection. Assume that all the red time R_i have been extended at the front end by an amount of time f_i, during which the observer can be passed at capacity q_c. Thus the second family of cuts are $q \leq kv(f_i) + \sum q_c f_i$. The third family uses backward moving

observers which move at wave speed $-w$ except stopped by the red signal. Also assume that the red time R_i have been extended at the front end by an amount of time g_i, during which the observer can be passed at the capacity q_c. And further let h_i be the time it spends in moving at speed $-w$, during which it can be passed at rate $r_i(-w)$. So the third family of cuts are $q \leq kv(g_i) + \sum(q_c g_i + r_i(-w)h_i)$. (Daganzo & Geroliminis, 2008)

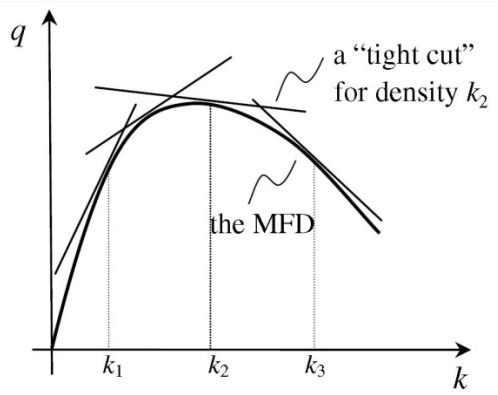

Figure 2.3 The MFD defined by 1-parameter family of cuts
Source: (Daganzo & Geroliminis, 2008)

2.4 Generalized Definition of Network Flow and Density

If we denote the generalized network flow as q and the generalized network density as k, q and k can be expressed by the total travelled distance within the time-space area and the total time vehicles spend within the time-space area separately. We use the generalized flow and density as the average network flow and density in this thesis. The generalized formula for them is proposed by Edie to avoid the sensitivity of these properties to the variations in the individual vehicles. They are formulated as follows: (Edie, 1965) (Edie, 1974)**:**

$$q = \frac{total\ distance\ travelled\ by\ all\ vehicles}{time - space\ area} = \frac{d(A)}{|A|} \tag{2.3}$$

$$k = \frac{total\ time\ costed\ on\ all\ vehicles}{time - space\ area} = \frac{t(A)}{|A|} \tag{2.4}$$

CHAPTER 3

ASSUMPTIONS AND METHODOLOGY

3.1 Basic Assumptions for Networks

3.1.1 Signalized Intersections

In this thesis, a road is defined as a single-lane road controlled by traffic signals with fixed cycle at both its ends. The network modeled in this thesis is consisted of such single road links. Other intersection types such as roundabouts, unsignalized intersections, are not considered here.

The signalization is simplified into a two-phase design: red and green. And we assume that network is homogeneous with signal design that signals retains the same cycle C, green time G and red time R for all the intersections in the network. Yellow phase and all-red phase are not considered in this ideal and simplified model. Trivially, at an intersection, when EW direction is in the green phase, the NS direction is in the red phase, and vice versa. During green time, the vehicles are allowed to make forward movements as well as left turns and right turns. In addition, U-turn is not allowed at intersections. During red time, all vehicles have to stop and no movement is allowed.

In a network, the turning rates at each intersection are not necessarily be the same. When a single vehicle is making movement decisions at an intersection, we shorthand its rate to turn left as P_L, its rate to turn right as P_R, and its rate to keep straight as P_s. By definition of the turning rates, $P_L + P_R + P_s = 1$. At each intersection, when two vehicles bounding for opposite directions are trying to turn and enter a same road, the right-turn movement is prioritized. And we consider no time lost or speed slow-downs at intersections.

Congestions will occur when the first vehicle at the intersection fails to enter any other roads because they are all jammed. A queue will accumulate along the road until the first vehicle can move on.

3.1.2 Homogeneity in Network Geometry and Signal Design

To narrow focus on the effect of turning rates and endogenous traffic in a homogenous road network, we assume that all roads are lined in a grid network with fixed length L both in the east-west direction and north-south direction. In other words, all blocks in the network are identical and square. The length and space of the intersections are neglected in the model. A sketch for such a network composed of single-way roads is shown in Figure 3.1(a) and a network composed of double-way roads is shown in Figure 3.1(b).

Since the network is controlled by signalizations of same phase settings, we can further define a fixed offset δ between each pair of neighboring traffic signals. An offset δ means that the signal at the end of the road can start a cycle faster than the signal at the entrance of the road by time δ. If the offset for one direction is δ, the offset for the opposite direction is $C-\delta$. And we also assume that the offset δ in the network is homogeneous in EW and NS directions.

On a typical road in the network, there is at most one lane per direction. This assumption is used to avoid the complex situations such as the lane-changing, choice of lane, and turning controls at intersection. The overpassing by taking the lane on the opposite direction is also prohibited in the model.

3.1.3 Parameter Assumptions for Fundamental Diagram

We assume that all roads in the network conform to one triangular FD. As shown in Figure 3.1(c), the FD is assumed to be with capacity q_c, jam density κ, free-flow speed v_f and backward wave speed $-w$. The critical density k_c represents the density at which the capacity q_c is reached and it can be calculated by $k_c = q_c/v_f = \kappa - q_c/w$.

The thesis makes the following settings for the parameters. The jam density κ in the network is supposed to be 150 veh/km (because the theoretical jam density is around 168 veh/km). The flow capacity q_c on a single lane is assumed to be 1800 veh/hr and the critical density k_c is assumed as 30 veh/km. Under this setting, v_f =60 km/hr and $-w$ =-15 km/hr.

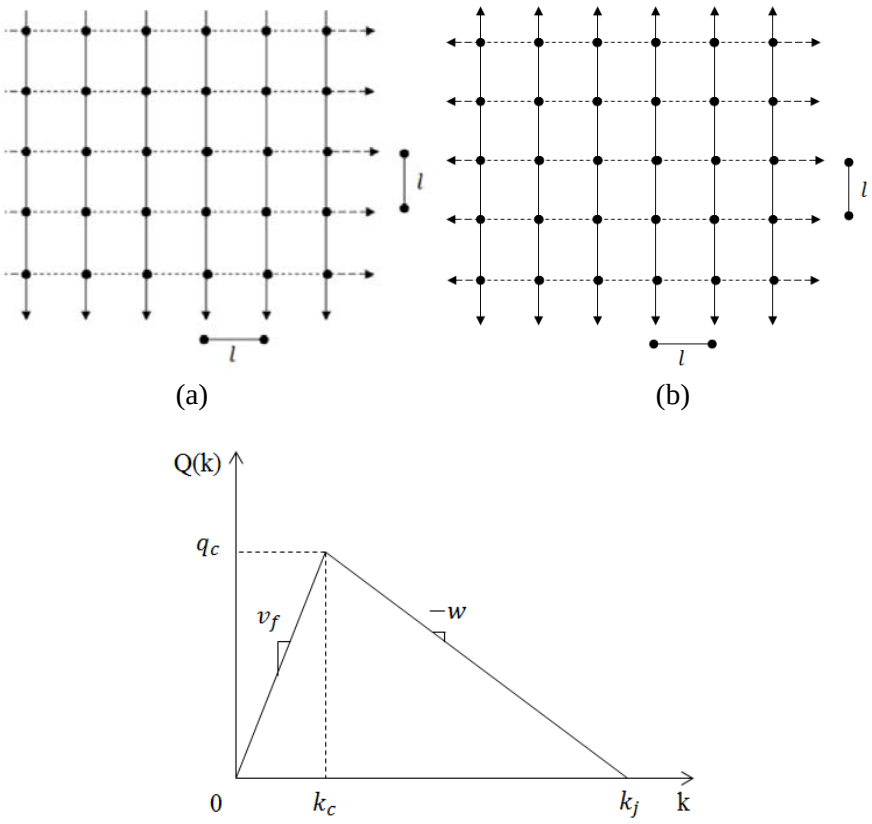

Figure 3.1 Idealized network for simulation and the assumed triangular FD

3.2 General methodology

3.2.1 Simulation with CA model

According to the CA(L) model by Daganzo (Section 2.2), the space and time are discreted in the model. A road segment can be latticed into multiple cells and the length for each cell is the jam spacing κ. Since the CA(L) model is a discrete model that only works for integer parameters, we assume that the road length is multiple to δ. By the CA(L) model, the length of the time unit can be expressed as $(-\delta/w)$. The location of the nth vehicle at the $(i+1)th$ time lattice is determined by:

$$z_{i+1}^{n} = min(z_i^n + \omega, z_i^{n-1} - 1) \tag{3.1}$$

$$where: \omega = \frac{v_f}{-w}$$

By the assumptions for FD in Section 3.1.3, the time unit is 1.6 seconds and $\omega = 4$. For each time step, the locations of the vehicles are updated on all roads by Equation (3.1). A normal vehicle will forward for 4 unit of length on a road if no leading vehicle is ahead of it within that distance. Otherwise, the vehicle will forward to one unit behind the leading vehicle.

The measurement of the flow and the density is performed for every 200 time steps, i.e. 320 seconds. When a vehicles moves, the forwarded units of its movement are recorded. From when a vehicle enters the system, the time steps during which it stays in the system is accumulated and the forwarded moving steps it has travelled is accumulated in each statistical cycle. Using Equation (2.3) and (2.4), we denote the accumulated forwarded units for all vehicle movements during 320 seconds as m and accumulated time steps travelled by all vehicles as n. We can have the average flow and density on the road as follows:

$$q = \frac{m * \frac{1}{150}}{(Street\ units * \frac{1}{150}) * (\frac{320}{3600})} = \frac{m * 3600}{Street\ units * 320} \quad \left(\frac{veh}{hr}\right) \tag{3.2}$$

$$k = \frac{n * \left(\frac{1.6}{3600}\right)}{(Street\ units * \frac{1}{150}) * (\frac{320}{3600})} = \frac{n * 150}{Street\ units * 200} \quad \left(\frac{veh}{km}\right) \tag{3.3}$$

In order to get a fully developed MFD ranging from totally free-flow status to totally congested status, simulations manipulated in the following phases: Firstly, we start with a network or road link with no traffic. Then the input flow rate into the system is gradually increased until maximum. Note that the maximum input flow rate doesn't guarantee that the system will become self-gridlock with jam density. Secondly, when the maximum input flow is reached, we further add a restriction on the output. The restriction on the output is intensified slowly until the density of the system reaches near jam density. In this way, we can get a

complete congested branch of the MFD. The density at which the restriction begins to be applied is the location of critical density

3.2.2 Driver Adaptation at Intersections

A vehicle could enter another road when three conditions are met: (1) there is no other leading vehicles before that vehicle. (2) if the vehicle forwards with a maximum forward step of 4 units, it's location will exceed the road length. (3) the signal downstream is in green phase at that time step. However, there are two situations that the vehicle will be forced to stop at the end of the road instead of entering the next road. The first situation is that the road to enter is jammed. The second situation is that the vehicle is about to make a left turn but at the same time another vehicle of opposite direction is making a right turn. In these situations, the vehicle will wait until the next time step and again make an independent choice for the road it wants to enter.

Since the network is structured as single-lane per direction, a stopped vehicle will jam all traffic behind it. We reasonably assume that drivers are likely to consider another route instead of stopping stoutly for the chance to enter a jammed road. The drivers' adaptation ensures that traffics will tend to use less congested roads when congestion begins to appear. All simulations in the thesis adopt drivers' adaptation except for Section 5.4.

3.2.3 Identification of Equilibrium Status

Analytically, the traffic flow characteristics can accurately represent the MFD only when the traffic reaches equilibrium status. The equilibrium means that the number of vehicles in the system keeps constant. In the simulation, we translate that as the input of vehicles into the system should be the same as the output. For every 200 steps, the accumulated output and input number of vehicles are compared to decide if the system has reached an equilibrium status. By Equation (3.4), both endogenous and exogenous components should be added to ensure that the inputs equals the outputs. The simulation records data only when the equilibrium is achieved.

$$A(t) = L(t) = O(t) + U(t) = E(t) + D(t) \tag{3.4}$$

3.2.4 Generation and Termination of Endogenous Traffics

Endogenous traffics are those traffics that either originate in the network system or terminate in the system. The generation of endogenous traffic assumes that vehicles can come from blocks and enter the road when the road cell it tries to enter through is vacant. The rate of endogenous traffic is controlled by a parameter ρ, which represents the probability for a vehicle to enter the system from a single road cell on the road within a time step. If ρ along a road is high, it means that the block bordering that road is a traffic producer.

The model of endogenous termination is based on the "exit opportunity" model by Daganzo (2007) in Section 2.1.3. We assume a homogeneous exit rate $\pi = 0.02$ for all drivers. And we assume the distribution density of the exit opportunity on roads is λ. The roads in trip-attracting areas should be featured with a higher density λ for exit opportunity. Supposing that a car is moving n steps along a road with an opportunity density λ, the probability for it to exit within this movement is

$$p(n) = 1 - (1 - \pi)^{\lambda n} = 1 - 0.98^{\lambda n} \tag{3.5}$$

When a car makes a movement, we use a Bernoulli model with the parameter $p(n)$ to determine whether the car will terminate its travel within a certain movement. If the travel of the car is terminated with this movement, the probability that the vehicle will exit by road cell i is then determined by Equation (3.6).

$$p_i = \frac{0.98^{(i-1)\lambda} - 0.98^{i\lambda}}{p(n)} \tag{3.6}$$

CHAPTER 4

APPLICATION WITH ROAD LINKS

In Chapter 4, the approximation and the characteristics of MFD are discussed in the scenario of a road link. In this scenario, the turnings in and out of the link are not allowed and MFD is affected by the length of the street and the phase design of the signalization. This chapter proves that in a homogeneous road link, there are at most seven cuts necessary for defining a MFD. The approximations for MFD are compared with the simulation results by the cellular automata model to show that the upper approximation can predict the shape of MFD with little errors.

4.1 Existing Approximation Model for MFD

This section will demonstrate a simplification for the approximation for MFD (Daganzo & Geroliminis, 2008), so that it requires fewer cuts without degrading the quality of prediction. The simplification assumes a homogeneous road chain, which means that each road on the link is of the same length L. As indicated by the analytical approximation, a moving observer that travels in one way with the maximum possible speed except when it is stopping at an intersection is required. We define the maximum number of intersections that a forward observer can travel through without being stopped by red signal as γ_{max}^{f}, and similarly, the maximum number of intersections that a backward observer can travel through without being stopped by red signal as γ_{max}^{b}. As shown in Figure 4.1(a), a stop must be performed at one of the intersections that are not behind the $\gamma_{max}^{f}th$ (or the $\gamma_{max}^{b}th$) intersection. The total delay at an intersection is the time before the next green phase. We shorthand the cut formed by stopping at the ith intersection as (i, F) or (i, B) depending on whether the moving direction is forward or backward. And furthermore, the cut formed by always staying at the first intersection is called S-cut in this thesis. The S-cut is horizontal in q-k diagram with an intercept of $\frac{G}{C} q_c$. Figure 4.1(b) shows how the MFD is approximated by those cuts.

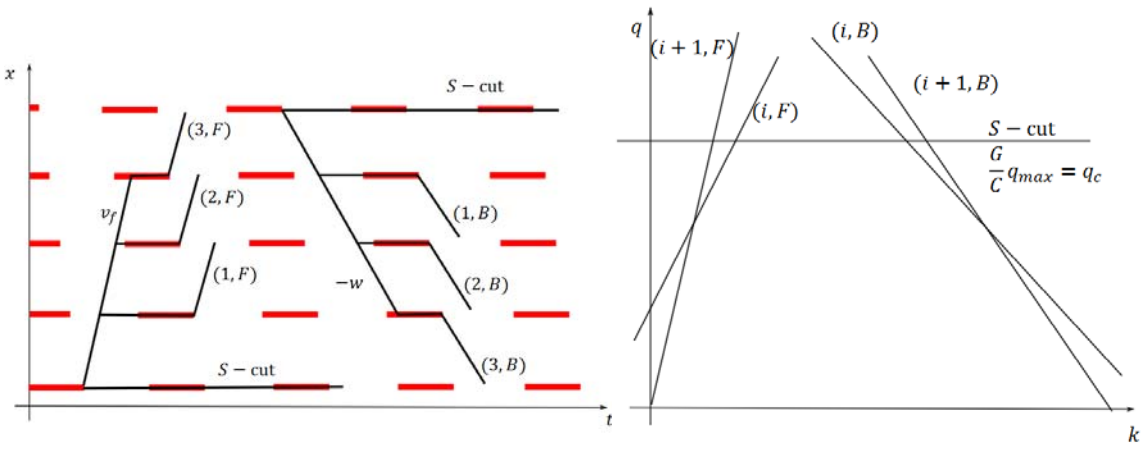

(a) (b)

Figure 4.1 Moving path and cuts for MFD approximation in variational theory
Source: (Geroliminis & Boyaci, 2012)

By the definition of cuts, the slope of a cut is the average speed of travelling and the intercept of the cut is the average cost of travelling, i.e. the average maximum overpassing rate. We first demonstrate the simplification for the forward cuts. For the forward cuts, the travelling costs are the maximum capacity q_c multiplied by the delayed time at the intersection during the green phase. We define t_{tored}^{i} as the time between the observer arrives at the ith intersection and the signal turns red. If the vehicle is stopped by a red signal, $t_{tored}^{i} = 0$. Thus, for the two cuts $(i-1, F)$ and (i, F) which are formed by observers stopping before the $\gamma_{max}^{f} th$ intersection, we can write their corresponding forms in the q-k diagram as:

$$q_{i-1} = ku_{i-1} + r_{i-1} \tag{4.1}$$

$$q_i = ku_i + r_i \tag{4.2}$$

Where

$$u_{i-1} = \frac{(i-1)L}{\frac{(i-1)L}{v_f} + t_{tored}^{i-1} + R} \tag{4.3}$$

$$r_{i-1} = \frac{t_{tored}^{i-1}}{\frac{(i-1)L}{v_f} + t_{tored}^{i-1} + R} q_c \tag{4.4}$$

$$u_i = \frac{iL}{\frac{iL}{v_f} + t_{tored}^i + R} \tag{4.5}$$

$$r_i = \frac{t_{tored}^i}{\frac{iL}{v_f} + t_{tored}^i + R} q_c \tag{4.6}$$

If the cuts (4.1) and (4.2) are not parallel, the y-coordinate for the intersection of cuts $(i-1, F)$ and (i, F) is

$$q_{(i-1)\cap i} = \frac{r_{i-1}u_i - r_i u_{i-1}}{u_i - u_{i-1}} = \frac{it_{tored}^{i-1} - (i-1)t_{tored}^i}{t_{tored}^{i-1} - (i-1)t_{tored}^i + R} q_c \tag{4.7}$$

4.2 Phenomenon of "Cycle-jumping"

The "cycle-jumping" phenomenon means that a vehicle's delay at an intersection is longer than at its previous intersection. This phenomenon only occurs when $\frac{G}{C} > 0.5$. The intersections at which the cycle-jumping happens are called "cycle-jumping" intersections in this thesis, and similarly the cuts formed by observers that stop at "cycle-jumping" intersections are called "cycle-jumping" cuts. Notice that two consecutive intersections can be both "cycle-jumping. All the intersections in a road chain can be categorized into two types: "cycle-jumping" and non-"cycle-jumping".

To explore the features of the "cycle-jumping" intersections, we introduce a new parameter $D_\gamma = \frac{\gamma L}{v_f} + \gamma\delta$ for a forward observer which stops at the γth intersection. D_γ is useful because $D_\gamma mod C$ represents the time that has passed in a signal cycle before the observer has reached the γth intersection. As a result, the parameter in Equation (4.3) to (4.6) can be replaced by $t_{tored}^\gamma = G - (D_\gamma mod C)$. By definition of D_γ and the assumption that the road chain is homogeneous in length, $D_\gamma = \gamma D_1$, and $D_1 = L/v_f + \delta$. To facilitate calculation, we denote D_1 as $D_1 = nC + mC$, where $n \in \mathbb{Z}$ and $0 < m < 1$. And we can rewrite:

$$t_{tored}^\gamma = G - \gamma mC + \lfloor \gamma m \rfloor C \quad (\gamma < \gamma_{max}^f) \tag{4.8}$$

We introduce a new parameter h_N to represent the location of the Nth "cycle-jumping" intersection. We will demonstrate in Equation (4.10) to (4.16) that the Equation (4.9) is the expression for h_N.

$$h_N = \left\lceil \frac{N}{\frac{D_1}{C} - \left\lfloor \frac{D_1}{C} \right\rfloor} \right\rceil = \left\lceil \frac{N}{m} \right\rceil \tag{4.9}$$

In Equation (4.9), N can be any natural number and the value of h_N is dependent on N. Suppose for a given N, there exist integers $\gamma - 1$ and γ, which satisfy $h_{N-1} \leq \gamma - 1 < \gamma < h_N$. Noticing that $m < 1$, one can find

$$N - 1 < h_{N-1}m \leq (\gamma - 1)m < \gamma m \leq (h_N - 1)m < N < h_N m < N + 1 \tag{4.10}$$

By Equation (4.10), we rewrite Equation (4.8) as

$$t_{tored}^{\gamma-1} = G - (\gamma - 1)mC + \lfloor(\gamma - 1)m\rfloor C = G - (\gamma - 1)mC + (N - 1)C \tag{4.11}$$

$$t_{tored}^{\gamma} = G - \gamma mC + \lfloor \gamma m \rfloor C = G - \gamma mC + (N - 1)C \tag{4.12}$$

$$t_{tored}^{h_N-1} = G - (h_N - 1)mC + \lfloor(h_N - 1)m\rfloor C = G - (h_N - 1)mC + (N - 1)C \tag{4.13}$$

$$t_{tored}^{h_N} = G - h_N mC + \lfloor h_N m \rfloor C = G - h_N mC + NC \tag{4.14}$$

Comparing Equation (4.11) and (4.12), Equation (4.13) and (4.14) separately, we have:

$$t_{tored}^{\gamma} - t_{tored}^{\gamma-1} = -mC < 0 \tag{4.15}$$

$$t_{tored}^{h_N} - t_{tored}^{h_N-1} = (1 - m)C > 0 \tag{4.16}$$

Inequality (4.16) proves that the delay at the Nth intersection is always greater than the delay at its previous intersection. So Equation (4.9) is the expression for h_N. On the other hand, Inequality (4.15) shows that the difference of delay between a non-"cycle-jumping" intersections and its previous one is always negative. In other words, when the delay enlarges, the intersection in calculation is a "cycle-jumping" intersection, and vice versa. We call it "cycle-jumping" intersection in this thesis because compared to the non-"cycle-jumping" intersections it will add an additional cycle length to the delay.

4.3 Effective Cuts for the MFD Approximation

In this section, we show that not all cuts in variational theory for MFD approximation are effective for the MFD. The MFD is dependent on a very limited subset of cuts. We focus our discussion on the formation for the free-flow branch of MFD. In the following comparison, we know that for any two consecutive intersections, only one of them is effective for shaping MFD, and the identification of the effective cut is dependent on whether the latter one is "cycle-jumping". We have made 2 pairs of comparisons: (1) Two cuts formed by stopping at a "cycle-jumping" intersection and by stopping at one intersection before the "cycle-jumping" intersection. (2) Two cuts formed by stopping at a non-"cycle-jumping" intersection and one intersection before the non-"cycle-jumping" intersection.

Situation (1): Cut $(h_N - 1, F)$ compared with cut (h_N, F)

Using Equation (4.7) and Equation (4.9), the y-coordinate of the intersection for the cut $(h_N - 1, F)$ and the cut (h_N, F) is

$$\begin{aligned} q_{(h_N-1)\cap h_N} &= \frac{h_N t_{tored}^{h_N-1} - (h_N-1)t_{tored}^{h_N}}{t_{tored}^{h_N-1} - (h_N-1)t_{tored}^{h_N} + R} q_c \\ &= \frac{h_N(G-(h_N-1)mC+(N-1)C) - (h_N-1)(G-h_N mC+NC)}{G-(h_N-1)mC+(N-1)C-(h_N-1)(G-h_N mC+NC)+R} q_c \\ &= \frac{-h_N C + G + NC}{-h_N C + C + NC} q_c = \left(1 + \frac{R}{(h_N - 1 - N)C}\right) q_c \end{aligned} \tag{4.17}$$

Because $h_N = \left\lceil \frac{N}{m} \right\rceil$ and $0 < m < 1$, we deduce $h_N > N$. If $h_N = 1 + N$, the cut $(h_N - 1, F)$ and the cut (h_N, F) are parallel to each other. In this case, the effective cut between them should be the one with the smaller intercept on the y-axis. If $h_N > 1 + N$, it is trivial the two cuts intersect above the S-cut. In this case, the line with the larger slope will be effective in shaping the MFD curve.

If $h_N > 1 + N$, then by Equation(4.3) and (4.5), we have

$$u_{h_N-1} = \frac{(h_N-1)L}{\frac{(h_N-1)L}{v_f} + t_{tored}^{h_N-1} + R} = \frac{L}{\frac{L}{v_f} + \frac{G-(h_N-1)mC+(N-1)C+R}{h_N-1}}$$

$$= \frac{L}{\frac{L}{v_f} + \left(\frac{N}{h_N - 1} - m\right) C} \tag{4.18}$$

$$u_{h_N} = \frac{h_N L}{\frac{h_N L}{v_f} + t_{tored}^{h_N} + R} = \frac{L}{\frac{L}{v_f} + \frac{G - h_N mC + NC + R}{h_N}}$$

$$= \frac{L}{\frac{L}{v_f} + \left(\frac{N+1}{h_N} - m\right) C} \tag{4.19}$$

To compare Equation (4.18) and (4.19), we just need to check the right of the equations. Under assumption that $h_N > 1 + N$, and we have $\frac{N}{h_N - 1} < \frac{N+1}{h_N}$. So $u_{h_N - 1} > u_{h_N}$.

If $h_N = 1 + N$, then by Equation(4.4) and (4.6), we have:

$$r_{h_N - 1} = \frac{t_{tored}^{h_N - 1}}{\frac{(h_N - 1)L}{v_f} + t_{tored}^{h_N - 1} + R} q_c = \frac{G - (h_N - 1)mC + (N-1)C}{\frac{(h_N - 1)L}{v_f} + G - (h_N - 1)mC + (N-1)C + R} q_c$$

$$= \frac{G - NmC + (N-1)C}{N\left(\frac{L}{v_f} - mC + C\right)} q_c = \left(\frac{-R}{N} - mC + C\right) \frac{q_c}{\frac{L}{v_f} - mC + C} \tag{4.20}$$

$$r_{h_N} = \frac{t_{tored}^{h_N}}{\frac{h_N L}{v_f} + t_{tored}^{h_N} + R} q_c = \frac{G - h_N mC + NC}{\frac{h_N L}{v_f} + G - h_N mC + NC + R} q_c$$

$$= \left(\frac{-R}{N+1} - mC - C\right) \frac{q_c}{\frac{L}{v_f} - mC + C} \tag{4.21}$$

$$r_{h_N} - r_{h_N - 1} = \frac{R q_c}{N(N+1)\left(\frac{L}{v_f} - mC + C\right)} > 0 \tag{4.22}$$

In either case, if the $h_N th$ intersections are "cycle-jumping" intersections, only one cut between $(h_N - 1\,, F)$ and (h_N, F) is effective for MFD approximation and it is $(h_N - 1\,, F)$. In fact, this result implies that "cycle-jumping" cuts can never be effective in MFD shaping. If there exist a set of consecutive "cycle-jumping" intersections, we only need to take the first "non-cycle jumping" intersections immediately before the "cycle-jumping" intersections.

Situation (2): Cut (γ, F) compared with cut $(\gamma - 1, \mathrm{F})$, and $r \notin \left\{\left\lceil \frac{N}{m} \right\rceil | N \in \mathbb{N}\right\}$.

In this situation, we notice that in Equation (4.10) that $\lfloor \gamma m \rfloor = \lfloor (\gamma - 1)m \rfloor$. As a result, we can rewrite Equation (4.8) as

$$t_{tored}^{\gamma-1} = G - (\gamma - 1)mC + \lfloor \gamma m \rfloor C \ \left(\gamma < \gamma_{max}^{f}\right) \tag{4.23}$$

$$t_{tored}^{\gamma} = G - \gamma mC + \lfloor \gamma m \rfloor C \ \left(\gamma < \gamma_{max}^{f}\right) \tag{4.24}$$

Using Equation (4.7), the y-coordinate for the intersection of the cuts $q_{\gamma-1}$ and q_{γ} is

$$\begin{aligned} q_{(\gamma-1)\cap\gamma} &= \frac{\gamma t_{tored}^{\gamma-1} - (\gamma-1)t_{tored}^{\gamma}}{\gamma t_{tored}^{\gamma-1} - (\gamma-1)t_{tored}^{\gamma} + R} q_c \\ &= \frac{\gamma(G - (\gamma-1)mC + \lfloor \gamma m \rfloor C) - (\gamma-1)(G - \gamma mC + \lfloor \gamma m \rfloor C)}{\gamma(G - (\gamma-1)mC + \lfloor \gamma m \rfloor C) - (\gamma-1)(G - \gamma mC + \lfloor \gamma m \rfloor C) + R} q_c \\ &= \frac{G + \lfloor \gamma m \rfloor C}{C + \lfloor \gamma m \rfloor C} q_c \end{aligned} \tag{4.25}$$

It is trivial that

$$\frac{G + \lfloor \gamma m \rfloor C}{C + \lfloor \gamma m \rfloor C} q_c \geq \frac{G}{C} q_c \tag{4.26}$$

Furthermore,

$$u_{\gamma-1} = \frac{L}{\frac{L}{v_f} + \frac{t_{tored}^{\gamma-1} + R}{\gamma - 1}} = \frac{L}{\frac{L}{v_f} - mC + \frac{1 + \lfloor \gamma m \rfloor}{\gamma - 1} C} \tag{4.27}$$

$$u_{\gamma} = \frac{L}{\frac{L}{v_f} + \frac{t_{tored}^{\gamma} + R}{\gamma}} = \frac{L}{\frac{L}{v_f} - mC + \frac{1 + \lfloor \gamma m \rfloor}{\gamma} C} \tag{4.28}$$

Equation (4.26) implies that the intersection is above the S-cut, and the cut with larger slope is the effective cut. And Equation (4.27) and (4.28) proves that $u_{\gamma-1} < u_{\gamma}$. So the cut (γ, F) should be the effective cut. This result indicates that if there exist a set of consecutive non-"cycle-jumping" cuts, the only effective cut is the last one of them.

As a conclusion of Situation (1) and (2), the effective cuts are those non-"cycle-jumping" cuts at the junction of "cycle-jumping" and non-"cycle-jumping" intersections. In other words,

they are “non-cycle jumping” intersections immediately before the “cycle-jumping” intersections. If we denote the set of cuts formed by stopping at “cycle jumping” intersections as $\{(i,F)\}$ and denote the set of cuts formed by stopping at “non-cycle jumping” intersections as $\{(j,F)\}$, the set of effective cuts is $\{(i-1,F)\} \cap \{(j,F)\}$.

4.4 Refined Model of Approximation

4.4.1 Forward Moving Cuts

From the above discussion, we can see that only two parameters are required for MFD approximation for the free-flow branch: $\frac{G}{C}$ and $m = \frac{D_1}{C} mod 1$. When the green time is no more than 50% of the signal cycle, i.e. $\frac{G}{C} \leq 0.5$, there is no “cycle-jumping” cut. If $\gamma_{max}^{f} > 1$, since $G \leq 0.5C$ and $D_1 = nC + mC$, we get $0 < m < 0.5$. Set $\gamma - 1 = \left\lfloor \frac{G}{mC} \right\rfloor$, then $(\gamma-1)m < \frac{G}{C} \leq 0.5$, and $\gamma m = (\gamma-1)m + m < 0.5 + m < 1$. By Equation (4.24) and $\gamma m < 1$, we can further get $t_{tored}^{\gamma} = G - \gamma mC$. Now, $\gamma = \left\lceil \frac{G}{mC} \right\rceil$ and $\gamma mC > G$, so $t_{tored}^{\gamma} < 0$. This conflicts with the definition of t_{tored}^{γ} and implies that the forward observer is stopped by the red signal at the γth intersection. And obviously this is the first intersection that the observer is stopped by the red signal, i.e. $\gamma_{max}^{f} = \gamma = \left\lceil \frac{G}{mC} \right\rceil \leq \left\lceil \frac{1}{m} \right\rceil$. Since all intersections before the $\gamma_{max}^{f} th$ intersection are also before the $\left\lceil \frac{1}{m} \right\rceil th$ intersection, so none of the intersections can be “cycle jumping”. According to the conclusions in Section 4.3, the effective forward cuts are $(\gamma_{max}^{f} - 1\ , F)$ and (γ_{max}^{f}, F).

When the green phase is greater than 50%, the following various situations need to be checked for each different value of m.

(i) $\frac{G}{C} > 0.5$ and $\left(\left\lfloor \frac{\frac{G}{C}}{\frac{D_1}{C} mod 1} \right\rfloor + 1 \right) \left(\frac{D_1}{C} mod 1 \right) < 1$

In this situation, there is no "cycle-jumping" cut. The effective cuts in this situation is exactly the same as those when $\frac{G}{C} \leq 0.5$. This fact can be proved as follows.

We take integer $\gamma = \left\lfloor \frac{\frac{G}{C}}{\frac{D_1}{C} mod 1} \right\rfloor + 1$. And since $m = \frac{D_1}{C} mod 1$, the inequality can be written as $\gamma m < 1$ and $\gamma = \left\lfloor \frac{G}{mC} \right\rfloor + 1$. If $\gamma < \gamma_{\max}^{f}$, we can further have $t_{tored}^{\gamma} = G - (\gamma mC - \lfloor \gamma m \rfloor C)$. Since $\frac{G}{mC}$ can either be an integer or not, suppose first $\frac{G}{mC}$ isn't an integer. Since $\gamma m < 1$, $t_{tored}^{\gamma} = G - \gamma mC = G - \left(\left\lfloor \frac{G}{mC} \right\rfloor + 1 \right) mC = G - \left\lceil \frac{G}{mC} \right\rceil mC < 0$. Then suppose $\frac{G}{mC}$ is an integer, and we find $t_{tored}^{\gamma} = G - \gamma mC = G - \left(\frac{G}{mC} + 1 \right) mC = -mC < 0$. In either case, a conflict is constructed against the assumption $\gamma < \gamma_{max}^{f}$, so $\gamma = \gamma_{max}^{f}$. So the effective cuts in Situation (i) are also $(\gamma_{max}^{f} - 1, F)$ and (γ_{max}^{f}, F).

(ii) $\frac{G}{C} > 0.5$, and $m = \frac{D_1}{C} mod 1 = 0$

It is easy to notice that situation (ii) is a very particular case where the forward observer reaches each intersection immediately after the signal turns from red to green. As a result, the delayed time at each intersection is always the same, which can be expressed as $t_{tored}^{\gamma} = G$. We can write the cuts $(\gamma - 1, F)$ and (γ, F) in the form of Equation (4.1) to (4.6), and the parameters are shown as follows.

$$u_{\gamma-1} = \frac{(\gamma-1)L}{\frac{(\gamma-1)L}{v_f} + C}, r_{\gamma-1} = \frac{G}{\frac{(\gamma-1)L}{v_f} + C} q_c, u_{\gamma} = \frac{\gamma L}{\frac{\gamma L}{v_f} + C}, r_{\gamma} = \frac{G}{\frac{\gamma L}{v_f} + C} q_c \tag{4.29}$$

By Equation (4.7), the y-coordinate of the intersection is

$$q_{(\gamma-1)\cap\gamma} = \frac{r_{\gamma-1}u_{\gamma} - r_{\gamma}u_{\gamma-1}}{u_{\gamma} - u_{\gamma-1}} = \frac{\frac{G}{\frac{(\gamma-1)L}{v_f} + C} * \frac{\gamma L}{\frac{\gamma L}{v_f} + C} - \frac{G}{\frac{\gamma L}{v_f} + C} * \frac{(\gamma-1)L}{\frac{(\gamma-1)L}{v_f} + C}}{\frac{\gamma L}{\frac{\gamma L}{v_f} + C} - \frac{(\gamma-1)L}{\frac{(\gamma-1)L}{v_f} + C}} q_c$$

$$= \frac{G}{C} q_c \tag{4.30}$$

Obviously, $u_{\gamma-1} < u_{\gamma}$, and the effective cut should be formed by an observer traverse the most intersections without stop. Since $\gamma_{max}^{f} = +\infty$, we have:

$$\lim_{i\to+\infty} u_i = \lim_{i\to+\infty} \frac{L}{\frac{L}{v_f} + \frac{C}{i}} = v_f \tag{4.31}$$

$$\lim_{i\to+\infty} r_i = \lim_{i\to+\infty} \frac{G}{\frac{iL}{v_f} + C} q_c = 0 \tag{4.32}$$

So the only effective forward cut is $(+\infty, F)$, which can be formulated as $q = kv_f$

(iii) $\frac{G}{C} > 0.5$, and $\left(\left\lfloor \frac{\frac{G}{C}}{\frac{D_1}{C} mod 1} \right\rfloor + 1\right)\left(\frac{D_1}{C} mod 1\right) \geq 1$

This situation can involve more than two effective forward cuts in determining the MFD shape. If we recall the definition of h_N in Section 4.3, the potential effective cuts should be selected from $\{(h_N - 1, F)\}$. To further simplify the model, we notice that the cuts $(h_{N_1} - 1, F)$, $(h_{N_2} - 1, F)$, and $(h_{N_3} - 1, F)$ may intersect at the same point under certain conditions. If we write a cut with the parameter defined in Equation (4.33) and (4.34), and then replace N with N_1, N_2 and N_3. We can get the intersection between them as expressed in Equation (4.35)and (4.36).

$$u_{h_N-1} = \frac{L}{\frac{L}{v_f} - mC + \frac{NC}{\left\lceil \frac{N}{m} \right\rceil - 1}} \tag{4.33}$$

$$r_{h_N-1} = \frac{\frac{G + (N-1)C}{\left\lceil \frac{N}{m} \right\rceil - 1} - mC}{\frac{L}{v_f} - mC + \frac{NC}{\left\lceil \frac{N}{m} \right\rceil - 1}} q_c \tag{4.34}$$

If we replace N with N_1, N_2 and N_3, the intersection between every two cuts are:

$$q_{h_{N_1}-1 \cap h_{N_2}-1} = \left(1 + \frac{\left(\left\lceil \frac{N_1}{m} \right\rceil - \left\lceil \frac{N_2}{m} \right\rceil\right)(G - C)}{C\left(N_2\left(\left\lceil \frac{N_1}{m} \right\rceil - 1\right) - N_1\left(\left\lceil \frac{N_2}{m} \right\rceil - 1\right)\right)}\right) q_c \tag{4.35}$$

$$q_{h_{N_1}-1 \cap h_{N_3}-1} = \left(1 + \frac{\left(\left\lceil \frac{N_1}{m} \right\rceil - \left\lceil \frac{N_3}{m} \right\rceil\right)(G-C)}{C\left(N_3\left(\left\lceil \frac{N_1}{m} \right\rceil - 1\right) - N_1\left(\left\lceil \frac{N_3}{m} \right\rceil - 1\right)\right)} \right) q_c \tag{4.36}$$

If the three cuts intersect at the same point, Equation (4.35) and (4.36) should equal. By calculation, it can be verified that the condition in Equation (4.37) should be met.

$$N_3\left(\left\lceil \frac{N_1}{m} \right\rceil - \left\lceil \frac{N_2}{m} \right\rceil\right) + N_1\left(\left\lceil \frac{N_2}{m} \right\rceil - \left\lceil \frac{N_3}{m} \right\rceil\right) = N_2\left(\left\lceil \frac{N_1}{m} \right\rceil - \left\lceil \frac{N_3}{m} \right\rceil\right) \tag{4.37}$$

It is proved in a simulation that if the length of red phase is long enough, all "cycle-jumping" cuts before γ_{max}^{f} can meet Equation (4.37). The simulation supposes a red phase of 20%C and is run with m values from 0.21 to 0.79, because otherwise it is obviously that there will be no "cycle-jumping" intersections. The design code of the test in Matlab is shown in Figure 4.2. The running result shows that no exception is found. We can further improve the approximation model by just using the first cut before the "cycle-jumping" cuts and the last cut before the "cycle-jumping" cuts. In other words, in situation (iii) we need at most three cuts: $\left(\left\lceil \frac{1}{m} \right\rceil - 1, F\right)$, $\left(max_{N:\left\lceil \frac{N}{m} \right\rceil \le \gamma_{max}^{f}} \left(\left\lceil \frac{N}{m} \right\rceil - 1\right), F\right)$, and $(\gamma_{max}^{f} - 1, F)$.

```
clear;
for m=0.21:0.01:0.79
    n(1)=ceil(1/m);a=0;
    for i=2:100
        n(i)=ceil(i/m);
    end
    for i=2:100
        if n(i)-n(i-1)==1
            continue;
        else
            for j=(i+1):100
                if n(j)-n(j-1)~=1
                    break;
                end
            end
            for k=(j+1):100
                if n(k)-n(k-1)~=1
                    break;
                end
            end
            if (k-j)*n(i)+(i-k)*n(j)+(j-i)*n(k)~=0
                a=n(k);break;
            end
        end
    end
    if a==0
        continue;
    end
    b=a+1;
    for l=1:a
        mr=m*l;
        if mod(mr,1)>=0.8-eps
            b=l;break;
        end
    end
    if a<b
        c='Exeption found!'
    end
end
```

Figure 4.2 m programming in MATLAB that test for the existence of exception that requires for more than three cuts for one MFD branch

4.4.2 Backward Moving Cuts

As shown in the previous sections to deal with the forward moving cuts, the effective backward cuts defining the congested branch of MFD can be obtained in a similar way. If we rotate Figure 4-1(a) to its reverse and then mirror it along the x-axis, it makes the same scenario for a forward moving observer except that the maximum moving speed is changed from v_f to w and the offset is changed from δ to $C - \delta$. So if we replace the v_f by w and δ by $C - \delta$ in Equation (4.3) to (4.6), it makes the formula for q_{i-1} and q_i in related with the mirrored density. Now, we notice that the cost of the path for backward observers is different from that for forward observers. Because there is a time-based cost rate of $\left(1 + \frac{v_f}{w}\right) q_c$ when a backward observer is moving with wave speed w. As a result, the r_{i-1} and r_i must be implemented by adding another item that represents the cost when moving backward. So the function for the q_{i-1} and q_i can be modified as follows in Equation (4.38) and (4.39).

$$q_{i-1} = -ku_{i-1} + r'_{i-1} \tag{4.38}$$

$$q_i = -ku_i + r'_i \tag{4.39}$$

where

$$u_{i-1} = \frac{(i-1)L}{\frac{(i-1)L}{w} + t_{btored}^{i-1} + R}, \quad r'_{i-1} = r_{i-1} + b_{i-1}$$

$$u_i = \frac{iL}{\frac{iL}{w} + t_{btored}^{i} + R}, \quad r'_i = r_i + b_i$$

$$r_{i-1} = \frac{t_{btored}^{i-1}}{\frac{(i-1)L}{w} + t_{btored}^{i-1} + R} q_c, \quad r_i = \frac{t_{btored}^{i}}{\frac{iL}{w} + t_{btored}^{i} + R} q_c$$

$$b_{i-1} = \left(1 + \frac{v_f}{w}\right) q_c * \frac{\frac{(i-1)L}{w}}{\frac{(i-1)L}{w} + t_{btored}^{i-1} + R}$$

$$b_i = \left(1 + \frac{v_f}{w}\right) q_c * \frac{\frac{iL}{w}}{\frac{iL}{w} + t_{btored}^{i} + R}$$

The t_{btored}^{i-1} and t_{btored}^{i} utilize the same concept defined in Section 4.1 for t_{tored}^{i-1} and t_{tored}^{i} except for they are measured in the backward moving scenario. By Equation (4.7),the y-coordinate for the intersection of cuts q_{i-1} and q_i is

$$q_{(i-1)\cap i} = \frac{r'_{i-1}u_i - r'_i u_{i-1}}{u_i - u_{i-1}} = \frac{r_{i-1}u_i - r_i u_{i-1}}{u_i - u_{i-1}} + \frac{b_{i-1}u_i - b_{i-1}u_{i-1}}{u_i - u_{i-1}} \tag{4.40}$$

$$\begin{aligned} b_{i-1}u_i - b_{i-1}u_{i-1} &= \left(1 + \frac{v_f}{w}\right) q_c * \frac{\frac{(i-1)L}{w}}{\frac{(i-1)L}{w} + t_{btored}^{i-1} + R} * \frac{iL}{\frac{iL}{w} + t_{btored}^{i} + R} \\ &\quad - \left(1 + \frac{v_f}{w}\right) q_c * \frac{\frac{iL}{w}}{\frac{iL}{w} + t_{btored}^{i} + R} * \frac{(i-1)L}{\frac{(i-1)L}{w} + t_{btored}^{i-1} + R} \\ &= 0 \end{aligned} \tag{4.41}$$

Combing Equation (4.40) and (4.41), we find

$$q_{(i-1)\cap i} = \frac{r_{i-1}u_i - r_i u_{i-1}}{u_i - u_{i-1}} \tag{4.42}$$

Equation (4.42) tells that all the results proved in Section 4.3 and Section 4.4.1 for the free-flow branch holds for the approximation for the congested branch. Correspondingly, we can rewrite the result from Section 4.4.1 as follows. The parameters D_1^b, D_γ^b, and t_{btored}^{γ} for the backward movings are defined in Equation (4.43) to (4.45).

$$D_1^b = \frac{L}{w} + C - \delta = n_b C + m_b C \quad (n_b \in \mathbb{Z}, 0 < m_b < 1) \tag{4.43}$$

$$D_\gamma^b = \frac{\gamma L}{w} - \gamma(C - \delta) = \gamma D_1^b \tag{4.44}$$

$$t_{btored}^{\gamma} = G - \left(D_\gamma^b - \left\lfloor \frac{D_\gamma^b}{C} \right\rfloor C\right) \quad (\gamma \le \gamma_{max}^b - 1) \tag{4.45}$$

In Scenario (i) where $\frac{G}{C} \le 0.5$ and Scenario (ii) where $\frac{G}{C} > 0.5$ and $\left(\left\lfloor \frac{\frac{G}{C}}{\frac{D_1^b}{C} mod 1} \right\rfloor + 1\right)\left(\frac{D_1^b}{C} mod 1\right) < 1$, we require two backward cuts: $(\gamma_{max}^b - 1, B)$ and (γ_{max}^b, B). In Scenario

(iii) where $\frac{G}{C} > 0.5$ and $m^b = \frac{D_1^b}{C} mod1 = 0$, the desired effective backward cut is $(+\infty, B)$, i.e. $q = -kw + \left(1 + \frac{v_f}{w}\right) q_c$. In scenario (iv) where $\frac{G}{C} > 0.5$ and $\left(\left\lfloor \frac{\frac{G}{C}}{\frac{D_1^b}{C} mod1} \right\rfloor + 1\right)\left(\frac{D_1^b}{C} mod1\right) \geq 1$, there are two or three effective backward cuts. If we denote the $h_N^b th$ intersections as "cycle jumping" intersections in backward moving scenario and $h_N^b = \left\lfloor \frac{N}{\frac{D_1^b}{C} mod1} \right\rfloor = \left\lceil \frac{N}{m_b} \right\rceil$ $(N \in \mathbb{N})$, we need at most three cuts: $\left(\left\lceil \frac{1}{m^b} \right\rceil - 1, B\right)$, $\left(max_{N:\left\lceil \frac{N}{m^b} \right\rceil \leq \gamma_{max}^b} \left(\left\lceil \frac{N}{m} \right\rceil - 1\right), B\right)$, and $(\gamma_{max}^b - 1, B)$.

4.4.3 Approximation for the MFD with Computer Programming

Based on the discussion in Section 4.4.1, the design of generating MFD approximation for the effective forward cuts is shown in Figure 4.3. Since the approximation for the effective backward cuts is very similar to the situation with the forward cuts, they are not shown in the Figure 4.3, but they works in a very similar way as shown in the Figure. However, a complete computer coding for the MFD approximation in java that includes forward cuts, backward cuts, and S-cut can be found in Appendix A. In a simulation on the road link, the simulation program requires the input of road length, number of roads in the chain, the cycle of signals, and the green phase of signals. The parameters for FD and the assumptions for the road are configured as stated in Chapter 3. The output shows a graphed approximation for the MFD, a simulated MFD under the inputs and the residence between them. The slope and intersection for all the cuts are also exported as dat file and further processed in Matlab as shown in Section 4.5. An output that returns the slope and intercept for all the effective cuts is shown in Figure 4.4 and the coding in Matlab can be found in Appendix A.

Figure 4.4 exhibits how the approximation is graphed with simulated data and the parameters of the effective cuts. The cuts are graphed along with simulated data for the convenience of comparison. The residence between the simulated data and the approximation is returned in "Parameter and result" tab in Figure 4.4. The graphed cuts are shown in various

colors that represents different situations discussed in Section 4.4.1 and 4.4.2: the cyan lines stand for a special situation that $m_f = 0$ or $m_b = 0$; the magenta lines stand for situation (iii); the green lines stand for situation (i); and the orange lines stand for the S-cut. The simulated sample points are printed in red in free-flow status and in blue in congested status.

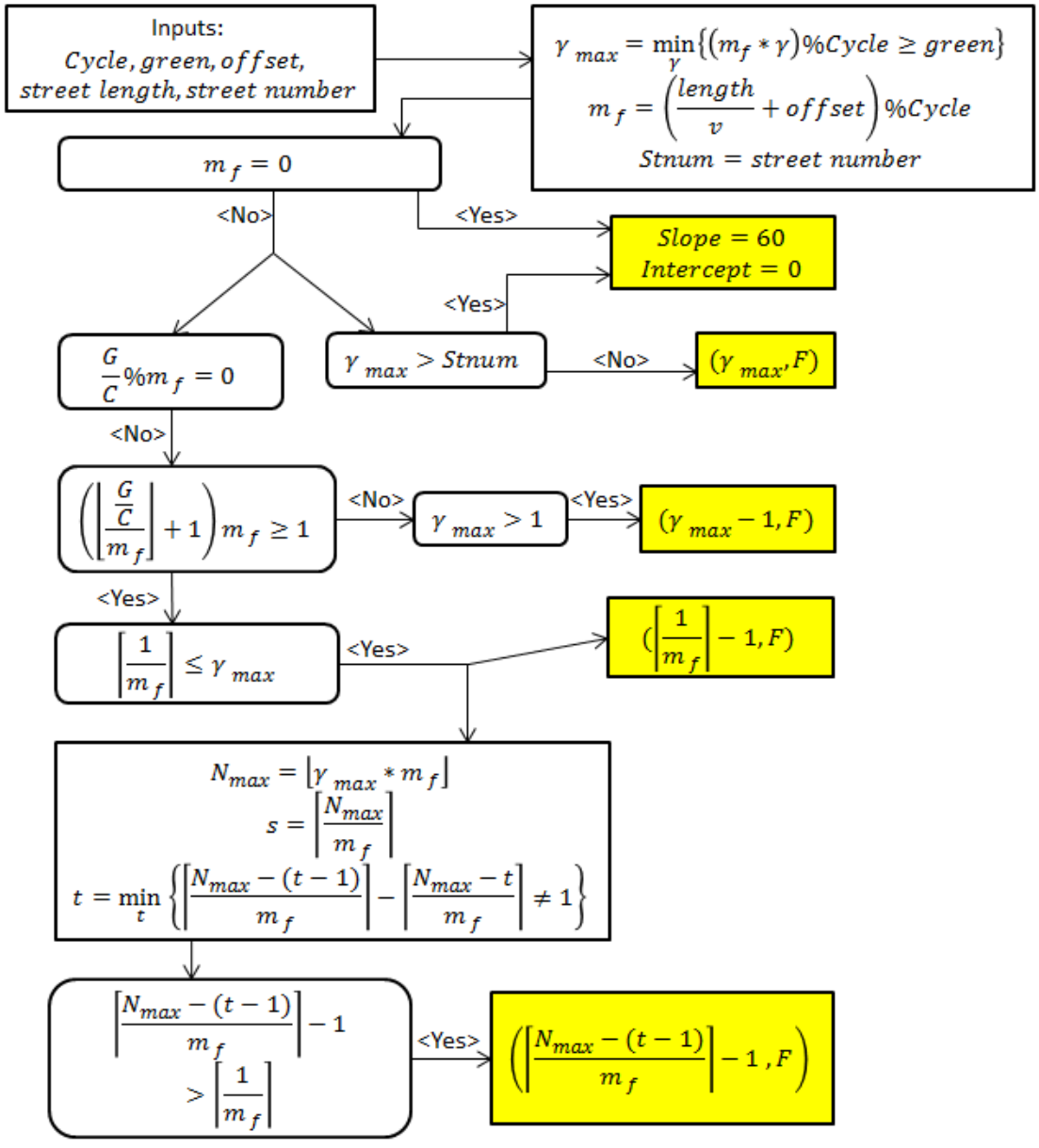

Figure 4.3 Design for programming MFD approximation

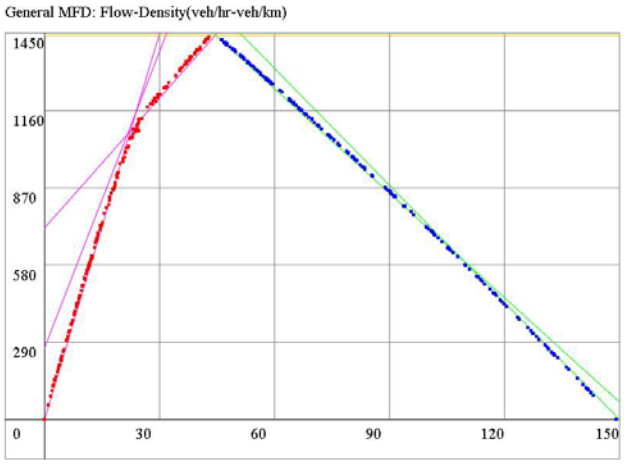

Parameter and result

Maxforward(unit)=4 trmaxforward(unit)=3 Truck Rate=0.0
Cycle(unit)=50 Green(unit)=40 Offset(unit)=20 looplocation(unit)=9
Timestepping(s)=1.6 Totalstepping=200
Boundary Input Rate=0.05 Inner Input Rate=0.0 Driver Exit Rate=0.02
Street number=10 Street length(unit)=32
Total loops=1 Loop existence rate=0.5
Maxforward=5 Maxbackward=4
m_f=0.56 m_b=0.24
slope=16.0 intercept=720.0 Stopped Intersection=1
slope=36.0 intercept=270.0 Stopped Intersection=3
slope=48.0 intercept=0.0 Stopped Intersection=5
slope=-13.0909 intercept=2029.0909 Stopped Intersection=3
slope=-14.7692 intercept=2215.3846 Stopped Intersection=4
slope=0.0 intercept=1440.0
forward cuts=3 backward cuts=2
Residence=12.6309 samples=410

(a) L=213.33m, G=80%C, C=80s, n=10, δ=32s

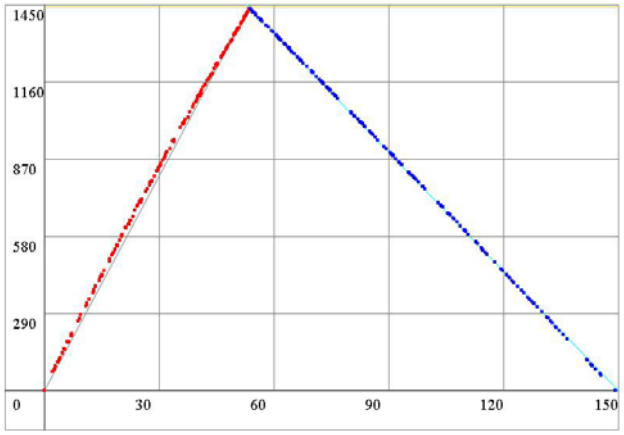

Parameter and result

Maxforward(unit)=4 trmaxforward(unit)=3 Truck Rate=0.0
Cycle(unit)=50 Green(unit)=40 Offset(unit)=32 looplocation(unit)=9
Timestepping(s)=1.6 Totalstepping=200
Boundary Input Rate=0.05 Inner Input Rate=0.0 Driver Exit Rate=0.02
Street number=10 Street length(unit)=32
Total loops=5 Loop existence rate=0.5
Maxforward=1 Maxbackward=11
m_f=0.8 m_b=1.0
slope=26.6667 intercept=0.0 Stopped Intersection=1
slope=-15.0 intercept=2250.0
slope=0.0 intercept=1440.0
forward cuts=0 backward cuts=1
Residence=17.8611 samples=410

(b) L=213.33m, G=80%C, C=80s, n=10, δ=51.2s

Figure 4.4 Results of java approximation and simulation

4.5 Results of Approximation and Simulation

4.5.1 Approximation for MFDs

We show some important features of the MFD on a road link by applying the refined approximation methods to estimate the MFDs. Figure 4.4 to Figure 4.8 show approximated flow and the corresponding effective cuts. In those figures, we categorize all the effective cuts into 6 categories described as follows and mark them with different color in the figures in this Section.

(1) Dark blue cuts are formed by observers travelled at free-flow speed/wave speed. These cuts

are effective when it is possible for observers to travel through the road chain without stopped by any red signal. (2) Magenta cuts are formed by observers that stop at the furthest intersection they can reach without stop. These cuts are determined by the maximum forward/backward intersection number under given conditions. (3) Yellow cuts are formed by stopping one intersection previous to the maximum forward/backward intersection. (4) Green cuts are formed by stopping at the last "non-cycle jumping" intersection that is previous to a "cycle-jumping" one. (5) Cyan cuts are formed by stopping at the first "non-cycle jumping" intersection that is previous to a "cycle-jumping" one. (6) Black cuts are represent the S cuts with the maximum capacity of $\frac{G}{C} q_c$.

We map the approximated MFD in a 3-d dimensional graph, which is dimensioned by density, offset/cycle, and flow. The value of flow is colored and contoured. In each figure, we fix the number of roads in the chain, and cycle and green time, but vary the road lengths. In these experiments, we choose the road length L of 100 meters, 266.67 meters, and 360 meters.

This section compares maps with different lengths in Figure 4-5. In this figure, the estimation of the MFD based on effective cuts when the signal cycle is 80 seconds and the green phase takes 80% of the total cycle time. By varying the road length from 100m to 360m, we discover that the road length decides the existence of the capacity of $\frac{G}{C} q_c$ and its range on density. The MFD follows the rules described as follows:

(1) When the offset is 0, the critical density is the exactly the same as the critical density for FD, i.e. 30 veh/km, and the capacity of $\frac{G}{C} q_c$ is always achieved at this density and offset. This statement establishes whatever the cycle, green phase length, and the road length are.

(2) When the road length is small, the range for the capacity of $\frac{G}{C} q_c$ is always 0. If $\left(\frac{\delta}{C}\right) \in \left[0, \frac{L}{wC}\right] \cup \left[1 - \frac{L}{vC}, 1\right]$, the MFDs formed by using that δ can achieve the capacity of $\frac{G}{C} q_c$ at a certain critical density. The critical density can be calculated by

$$k_{c-chain} = \begin{cases} k_c + \frac{\delta}{C}\frac{R}{L}q_c, if\ (\delta/C) \in [0, L/(wC)] \\ k_c + \left(\frac{\delta}{C} - 1\right)\frac{R}{L}q_c, if\ (\delta/C) \in \left[1 - \frac{L}{vC}, 1\right] \end{cases} \quad (4.46)$$

(3) If $L < \frac{Gwv}{w+v}$, there always exist δ at which MFD's maximum capacity is lower than $\frac{G}{C}q_c$. In this case, the maximum density point for each MFD follows a zigzag shape and the critical density varies drastically. It indicates that the offsets exert a significant impact on the shape of MFD. This observation can be justified by that the value of D_1 and D_1^b are largely dependent on the offset when $\frac{L}{w}$ and $\frac{L}{v_f}$ is very small.

(4) As the length of the road $L \geq \frac{Gwv}{w+v}$, the range of the capacity $\frac{G}{C}q_c$ begin to increase near $\frac{\delta}{C} = \frac{v}{v+w}$. Compared with Figure 4.5(a), with the increase of the roads, more MFDs in Figure 4.5(b)(c) are crossed by the black cuts across δ/C. It implies that the longer the road, there are more choice of δ that can make S-cut effective in the approximation for the MFD.

(5) By the formula for the critical density in (2), it is obvious that if $L \to \infty$, the critical density for the system will converge to k_c. In fact, if the road is long enough the MFD shape will become stable across δ/C, and it makes the MFD shape less affected by offsets.

In conclusion, the varying of the road length would bring great impact on the stability of the critical density and the stability of the MFD shape. The longer the road, the more stable will the MFD become and it will be more likely for the MFD to hold a range for the capacity of $\frac{G}{C}q_c$.

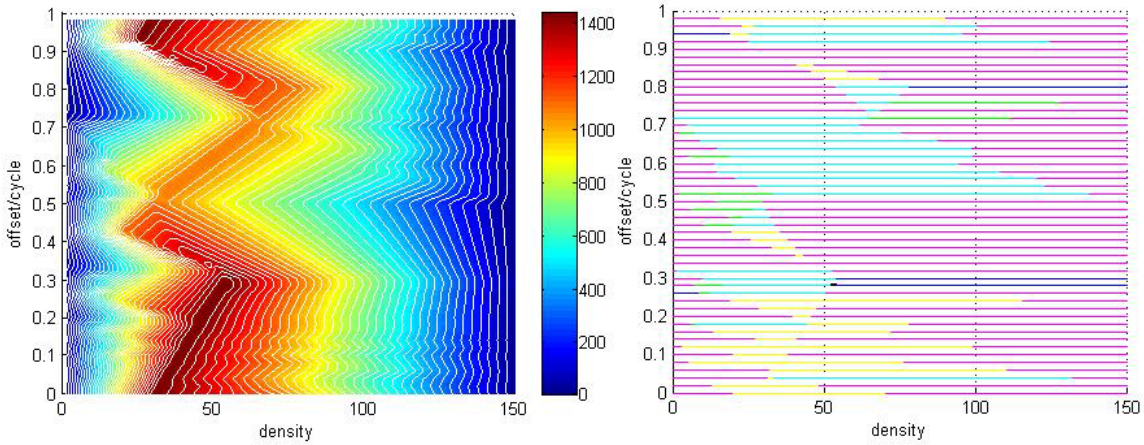

(a) L=100m, G=80%C, C=80s, n=30

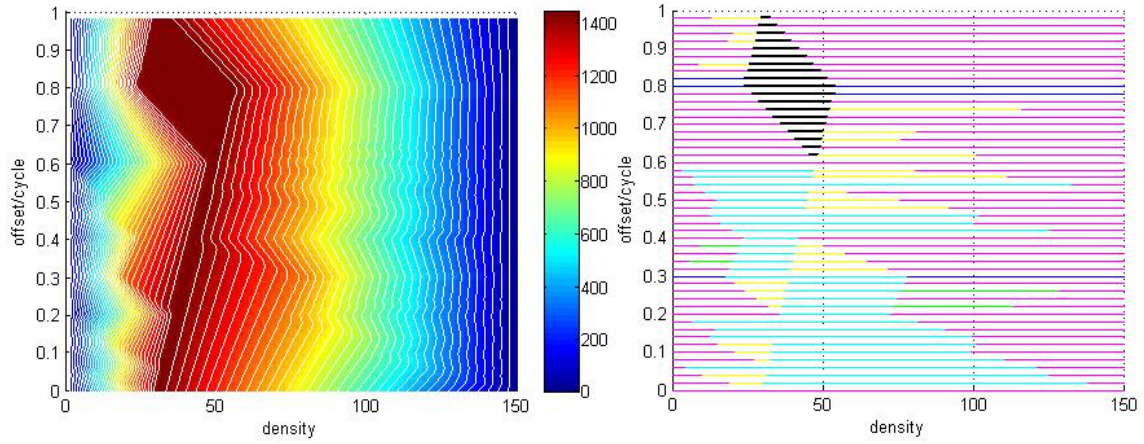

(b) L=266.67m, G=80%C, C=80s, n=30

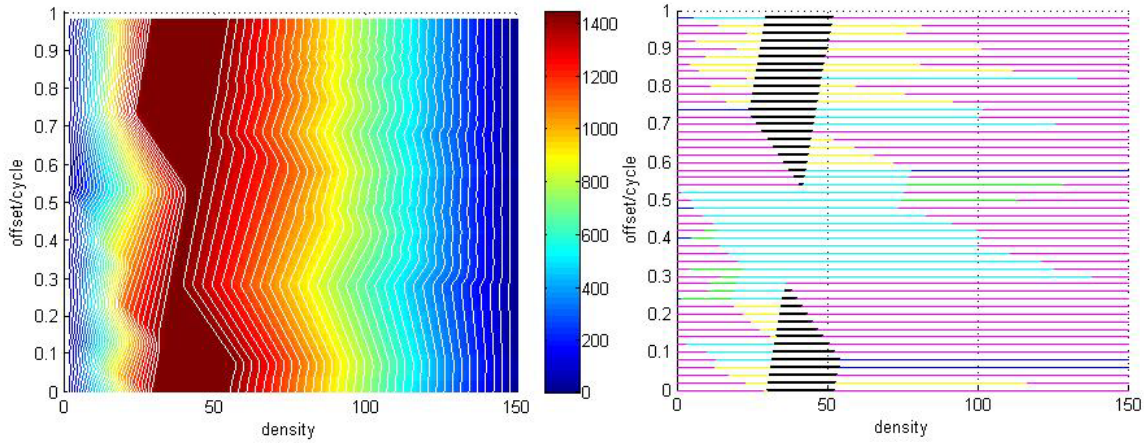

(c) L=360m, G=80%C, C=80s, n=30

Figure 4.5 Approximation of MFD based and the corresponding effective cuts with G=80%C, C=80s, and n=30

Utilizing the result shown in Figure 4.5, we run a series of simulations with similar parameter settings but vary with the chain length, cycle, and green phase percentage separately in

Figure 4.6 to Figure 4.8. Figure 4.6 applies all conditions that we have used to generate Figure 4.5, except that we changed the number of roads in the road chain from 30 to 4. It has tested the shape of MFD for road links of very small scale. It turns out that the heat maps in Figure 4.6 are roughly the same shape as those in Figure 4.5. Noises have been observed due to the fact that a road link of small scale bring more opportunities for an observer to travel through the system without being stopped and thus expand the range for maximum flows. It verifies that the number of roads isn't the major factor that impacts the pattern of the MFD map in a great way, but may trigger small noises on the edge of the original pattern. The reduction of the roads in the system may expand the range of maximum flows by introducing more dark blue cuts and produce more sawteeth on the MFD contours as shown in Figure 4.6.

Figure 4.7 shows the scenario where the cycle length is changed from 80 seconds to 96 seconds. It works with larger signal cycles, but we have verified that the maps generated using a cycle of 96 seconds are exactly the same as those that are generated using a cycle of 80 seconds with a proportionally modified length. This result can be justified because if the road length is also magnified by 96/80=1.2 folds, the parameters for D_1 and D_1^b calculation are exactly the same as the situation with a cycle of 80s. For example, the map in Figure 4-7(a) is the same as the one that generated with cycle=80s, L=83.33m.

In Figure 4.8, we set the green phase as 50% of the cycle length, instead of 80%. According to the proofs shown in Section 4.3, it is easy to observe that there are no "cycle-jumping" cuts in this scenario. Compared to Figure 4.5, the black area becomes much larger and the effective length of S-cut that used in the MFD formation is widened. This observation can be explained by that the S-cut for $\frac{G}{C}q_c$becomes lower. The green time is an essential factor in deciding the importance of S-cuts in shaping MFD.

As a conclusion for this section, the optimal performance of the road chain is heavily dependent on three factors: the green phase, road length and offset. The green phase determines the maximum capacity $\frac{G}{C}q_c$ that the road chain can ever obtain. The road length determines

whether a positive range for that capacity can be obtained. The offset allows an option of a signal design that maximize the density range for the capacity $\frac{G}{C} q_c$.

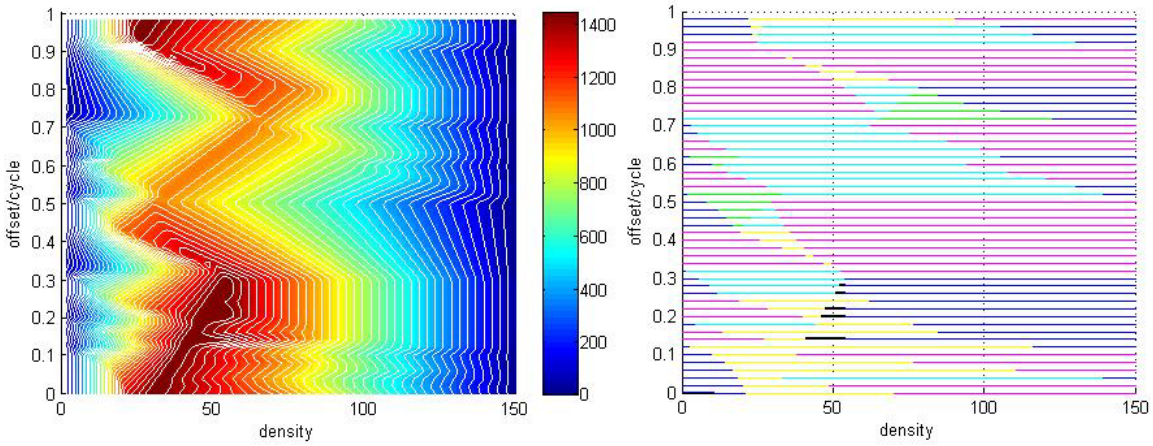

(a) L=100m, G=80%C, C=80s, n=4

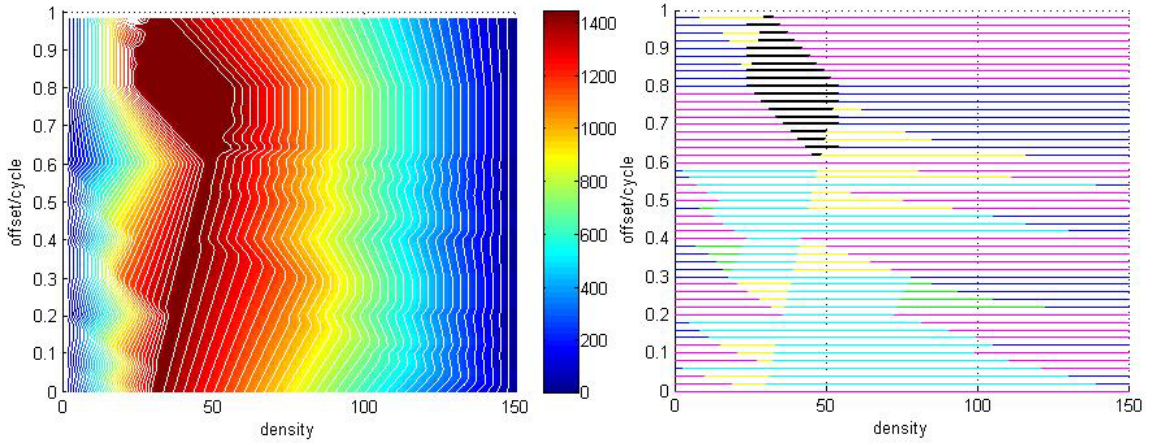

(b) L=266.67m, G=80%C, C=80s, n=4

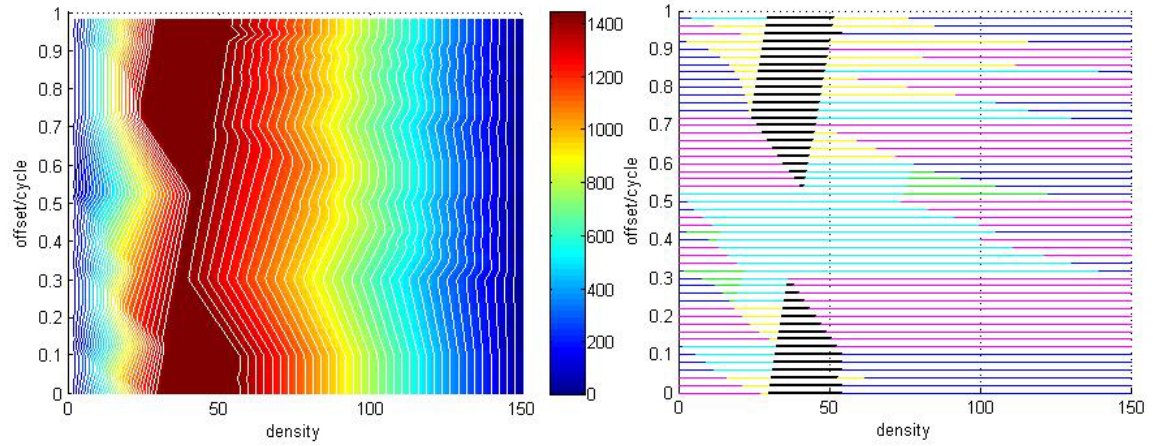

(c) L=360m, G=80%C, C=80s, n=4

Figure 4.6 Approximation of MFD based on VT theory and the corresponding effective cuts with G=80%C, C=80s, and n=4

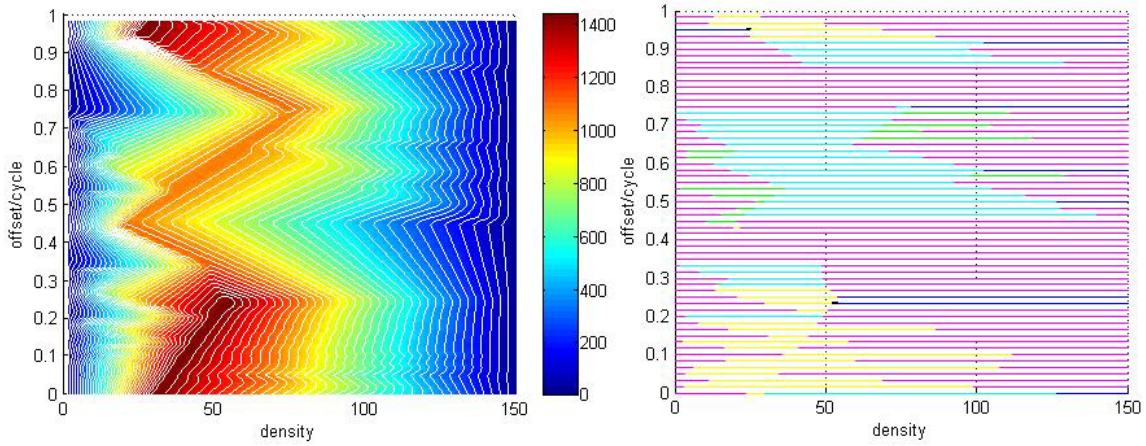

(a) L=100m, G=80%C, C=96s, n=30

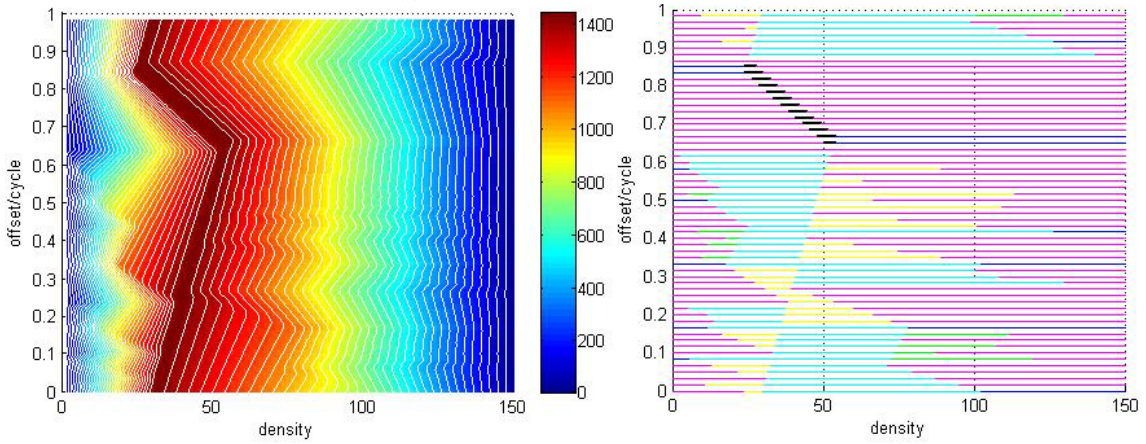

(b) L=266.67m, G=80%C, C=96s, n=30

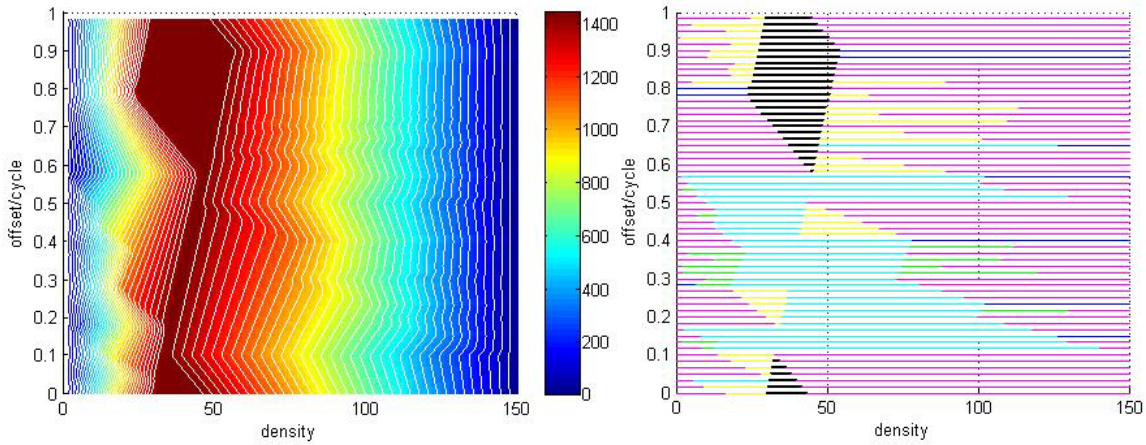

(c) L=360m, G=80%C, C=96s, n=30

Figure 4.7 Approximation of MFD based on VT theory and the corresponding effective cuts with G=80%C, C=96s, and n=30

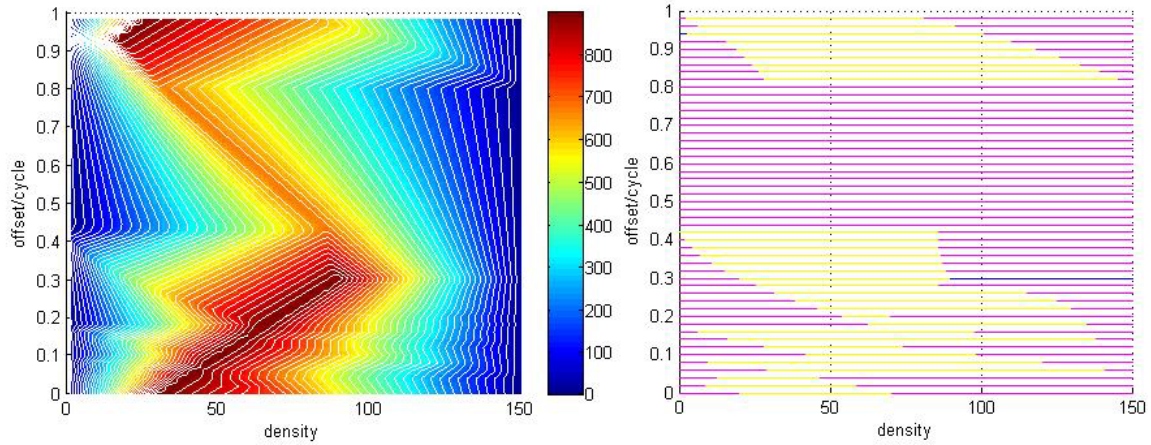

(a) L=100m, G=50%C, C=80s, n=30

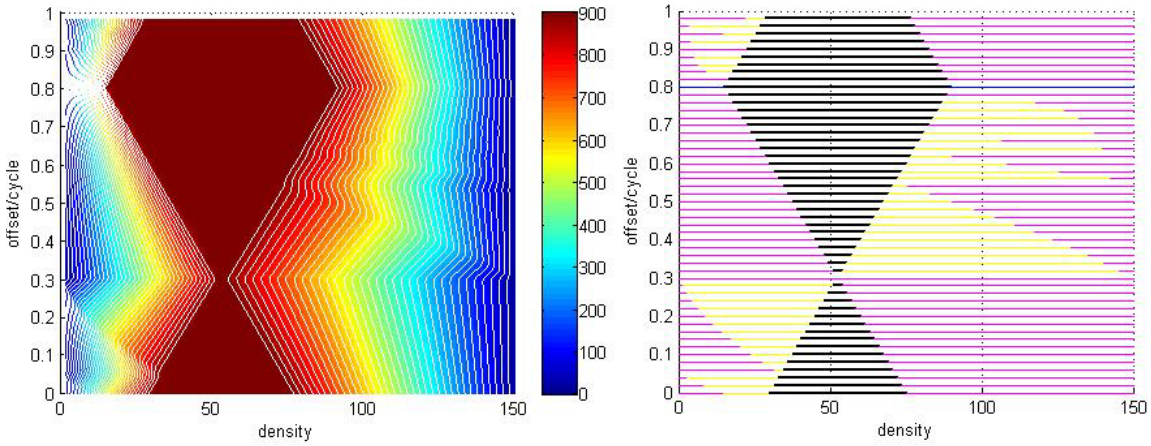

(b) L=266.67m, G=50%C, C=80s, n=30

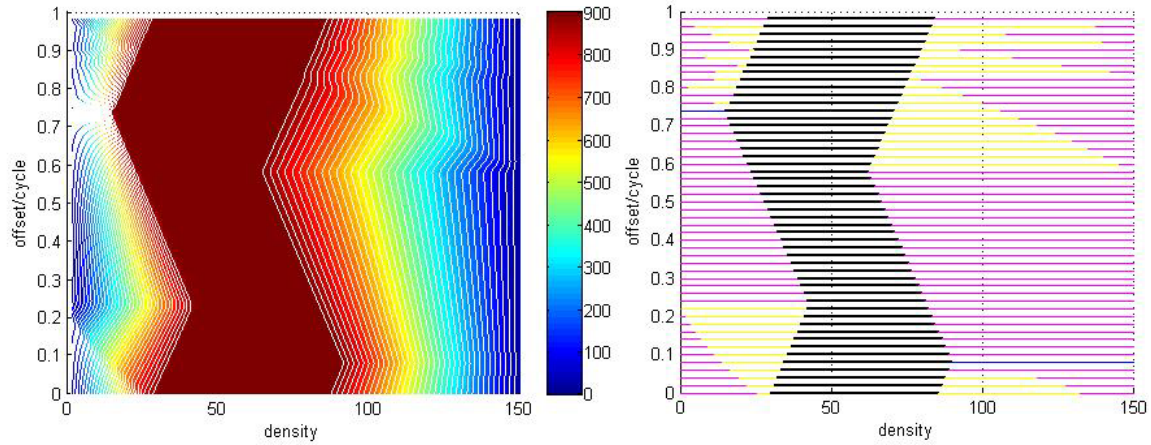

(c) L=360m, G=50%C, C=80s, n=30

Figure 4.8 Approximation of MFD based on VT theory and the corresponding effective cuts with G=50%C, C=80s, and n=30

4.5.2 Difference between Approximation and Simulation

The reliability of the MFD approximation is tested by simulation with CA(L) model The simulated flow and density are calculated every 320 seconds using Edie's formula (Edie, 1974). The standard deviation for the simulated samples from the approximation for the MFD is obtained by Equation (4.51).

$$Res = \sqrt{\frac{(q - \hat{q})^2}{n}} \tag{4.51}$$

A residence is calculated for each MFD. In Figure 4.9, the residences are plotted in related with m_f and m_b. For each map in Figure 4.9, we fix cycle, green phase, and road numbers, and each three-dimensional point $(\mathrm{m_f}, \mathrm{m_b}, \mathrm{Res})$ in the map is correspondent to a combination of (L, δ). Figure 4.9(a)(b)(c) are produced with $\{(L, \delta)|L \in [100,360], \delta \in [0,80)\}$, and Figure 4.9(d) is produced with $\{(L, \delta)|L \in [73.33,386.67], \delta \in [0,96)\}$. The simulated data that are best matched with the approximation for the MFD are colored dark blue and the MFD that are most deviated from the approximation are colored red in the heat maps. As shown in Figure 4.9, the residences stay quite low in the plotted map for most of the (m_f, m_b) pairs, however, large deviations over 50veh/hr do exist over several places. The greatest deviation occurs immediately left to $m_f = \frac{G}{C}, \frac{G}{2C}, \frac{G}{3C}, \ldots$ If $\frac{G}{C}$ can be divided by an m_f with no remainder, there will be large difference between the approximation and simulation when m_f a little smaller than that. The sum of m_f and m_b stays constant for almost all the times as the length of the road varies. As a result, the residence on a road with a fixed length can be found along a line tilted 45 degrees to the upper-left. The red lines in Figure 4.9 mark the residence for road chains with road length of 100 meters, the smallest length we have applied in the simulation. It can be observed that the difference is greater near the red line than anywhere else, which implies that shorter road lengths will be likely to generate greater errors in the approximation. Figure 4.9(c) bears the smallest residence among the 4 simulation runs. It

indicates that if the road links in the chain is large and the green phase is relatively small, the approximation result would be more compatible with the simulation.

Figure 4.10 goes further to explore the relation between the compatibility and the density. It shows the difference in flow between the simulated data and the approximation, which is mapped with offset/cycle and density as x-y plane. The simulated flow tends to be underestimated in areas where the yellow, green and cyan cuts dominate. The existence of cuts that are formed by stopping at an intersection before the γ_{max}th intersection is the major reason for the deviation with the simulated data. In contrast, the simulated data are often overestimated where the S-cuts dominate. The simulated maximum flow is usually smaller than the capacity of $\frac{G}{c} * q_c$.

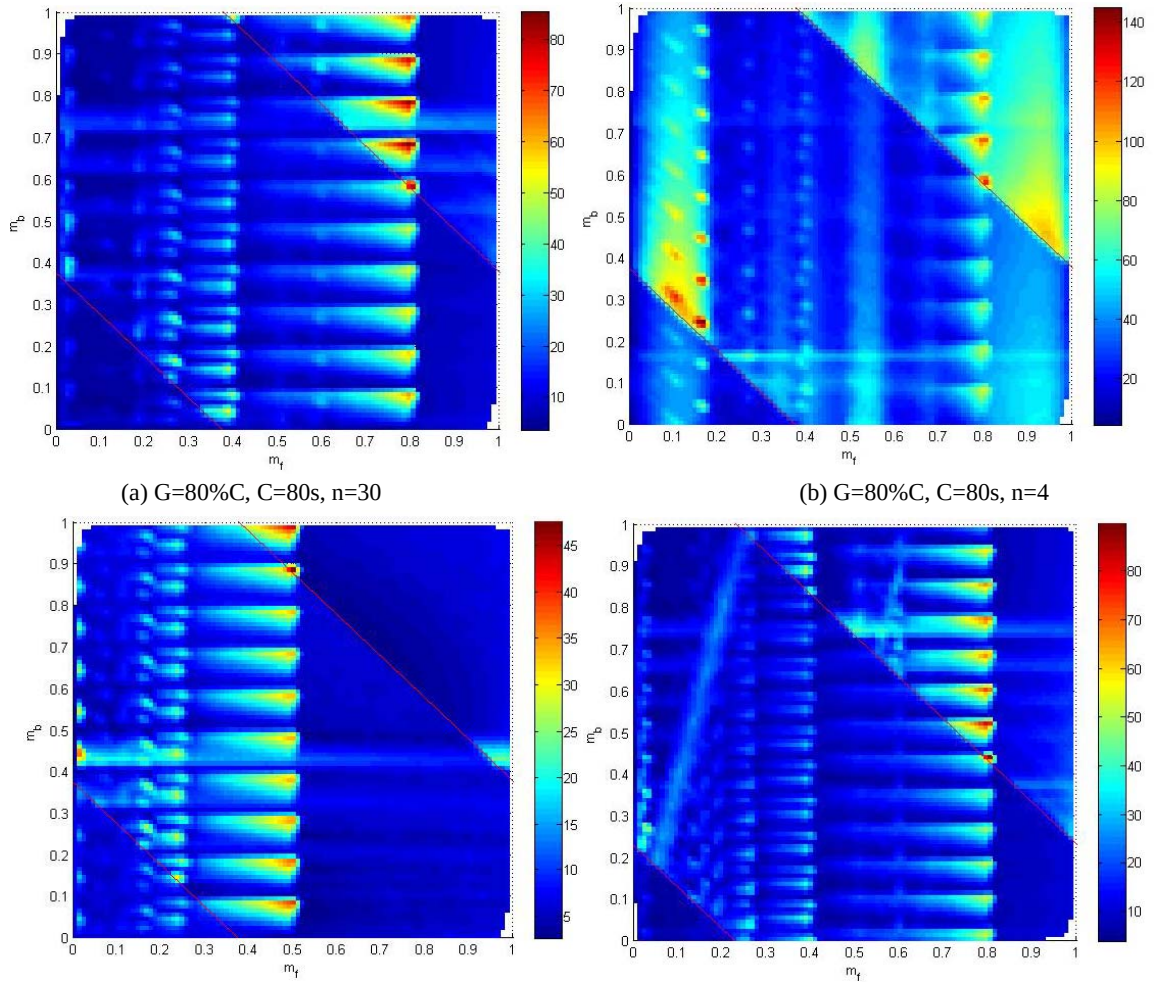

(a) G=80%C, C=80s, n=30

(b) G=80%C, C=80s, n=4

(c) G=50%C, C=80s, n=30

(d) G=80%C, C=96s, n=30

Figure 4.9 Error of estimation for combinations of various $\{(\mathbf{m_f}, \mathbf{m_b})\}$

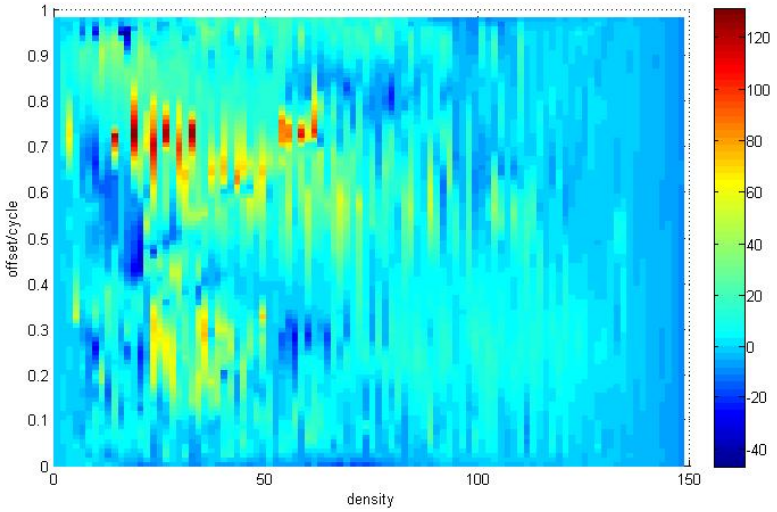

(a) L=100m, G=80%C, C=80s, n=30

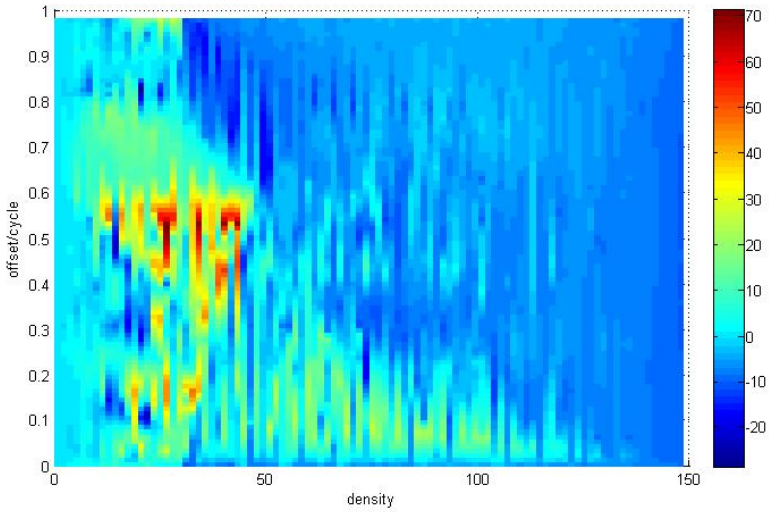

(b) L=266.67m, G=80%C, C=80s, n=30

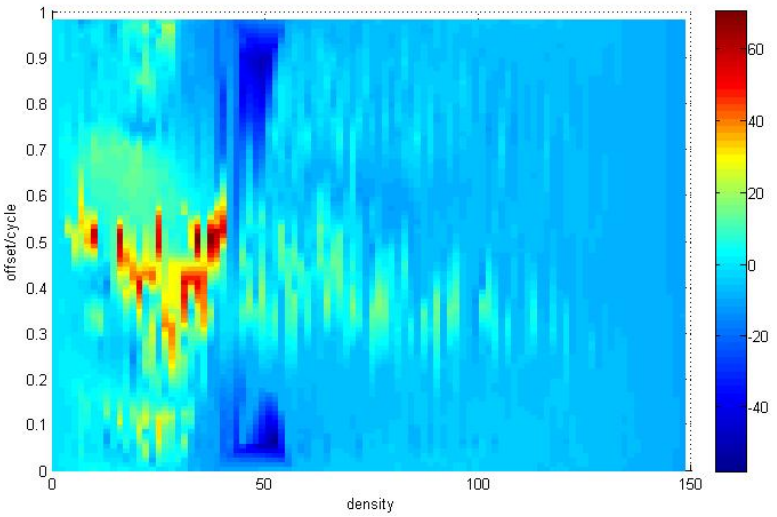

(c) L=360m, G=80%C, C=80s, n=30

Figure 4.10 Error of estimation for combination of various $\{(\boldsymbol{\delta}, \mathbf{k})\}$

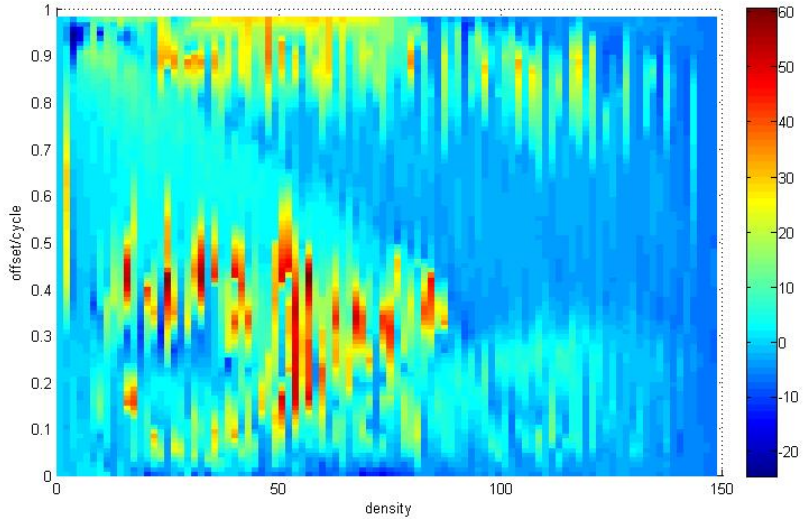

(d) L=100m, G=50%C, C=80s, n=30

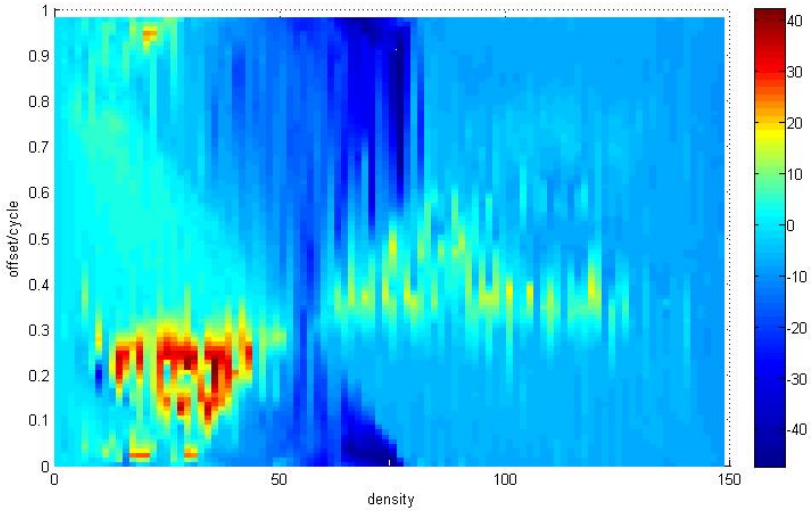

(e) L=266.67m, G=50%C, C=80s, n=30

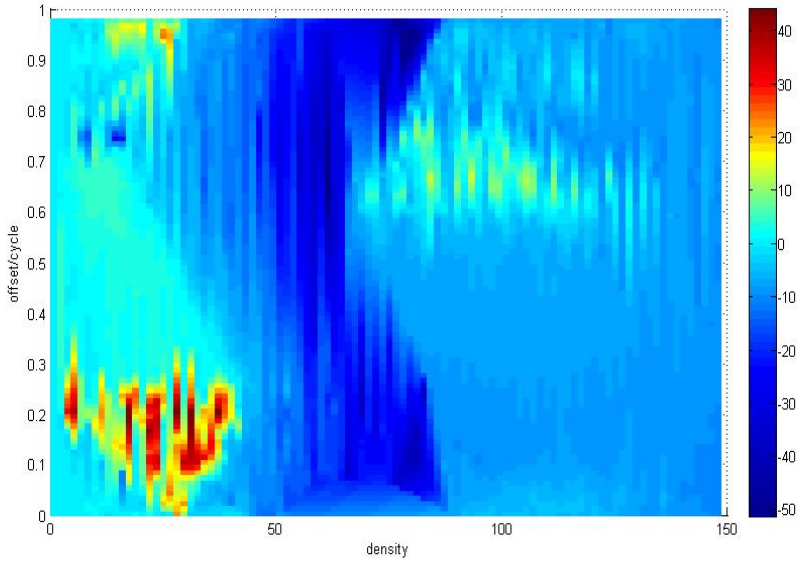

(f) L=360m, G=50%C, C=80s, n=30

Figure 4.10 Error of estimation for combination of various (Continued)

4.5.3Discussion on the Variance of Density

The traffic density is not necessarily uniformly distributed on every road in the chain, even in the equilibrium status. It is found that the variance of density on a road chain is largely determined by the slope of the effective cuts. Several figures for flow versus standard deviation of density are shown in Figure 4.11. The standard deviations of density measured in free-flow status are marked with red, and the ones measured in congested status are marked with blue. In simulations on a road chain that doesn't allow turnings and endogenous traffics, the standard deviation in density is usually smaller than 7 veh/km, except near the flow capacity of $\frac{G}{C} * q_c$. Large variance can be produced when the outflow of the system is slightly reduced at the maximum performance of the system. The road link shortly retain the maximum flow in a very unstable status and produce large variance in density before it falls onto the congested branch. It needs to be noted that after the maximum performance is reached, the performance of the system won't go along the S-cut or to the congested curve without any outer triggers.

It is observed that the variance in free-flow status is often bigger than the variance in congested status. However, this phenomenon is explained by that the slope for the forward cuts are often greater than the slope for the backward cuts in most cases. As shown in Figure 4.11, in either free-flow status or congested status, the variance of density is 0 when the flow is 0. The variance grows as the flow increases and the rate of the variance growth is determined by the first cut in the MFD diagram. If the absolute value of the cut slope is bigger, the variance density will rise more quickly. The rate of the variance increasing is changed where the second cut intersects. If the maximum flow is $\frac{G}{C} q_c$, the variance will drop to 0 at the maximum flow. Otherwise, the variance will be greater than 0 at the maximum flow.

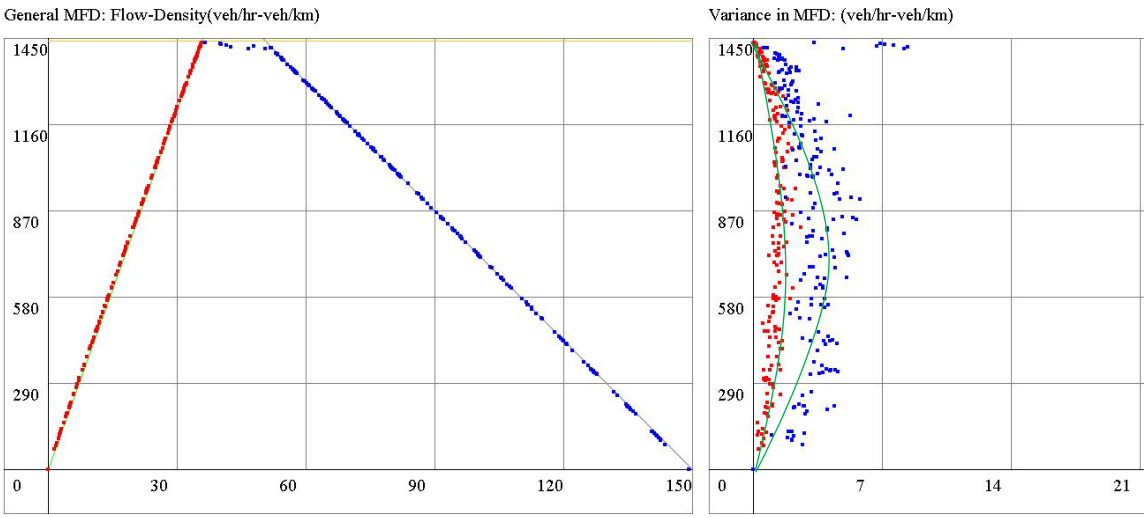

(a) L=266.67m, G=80%C, C=80s, δ=56s, n=30

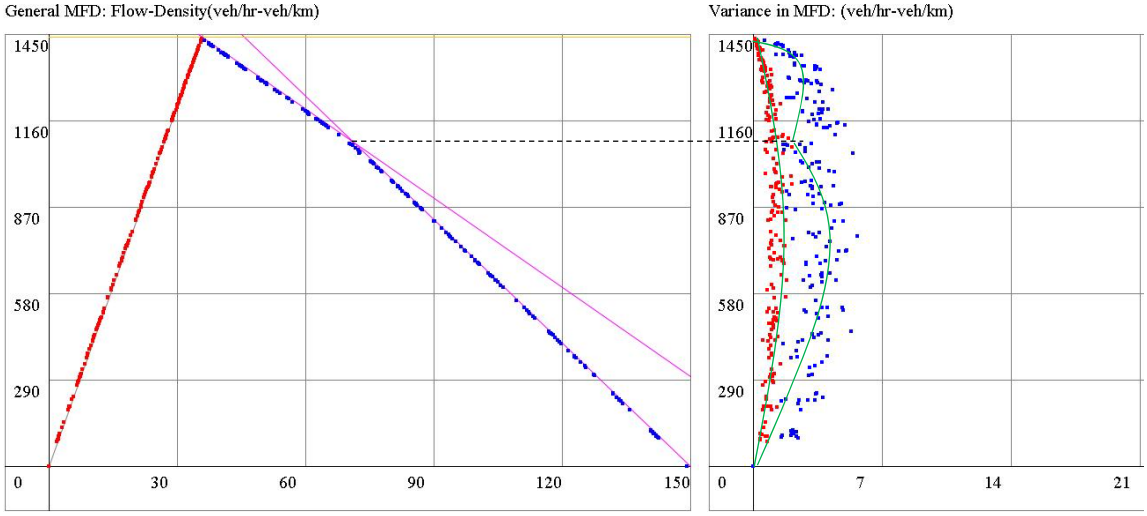

(b) L=266.67m, G=80%C, C=80s, δ=16s, n=30

Figure 4.11 Flow versus standard deviation in density on road chains

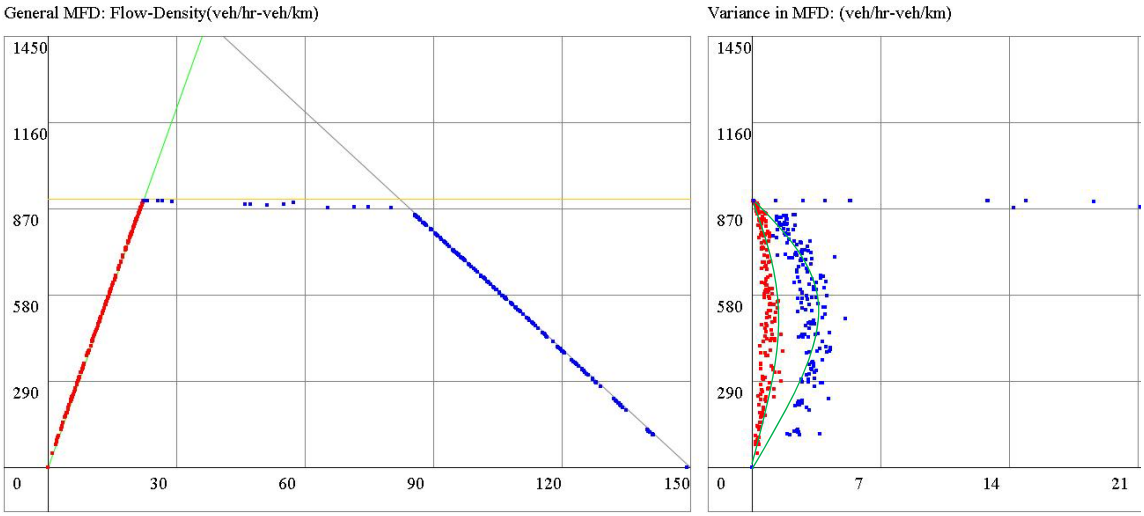

(c) L=266.67m, G=50%C, C=80s, δ=56s, n=30

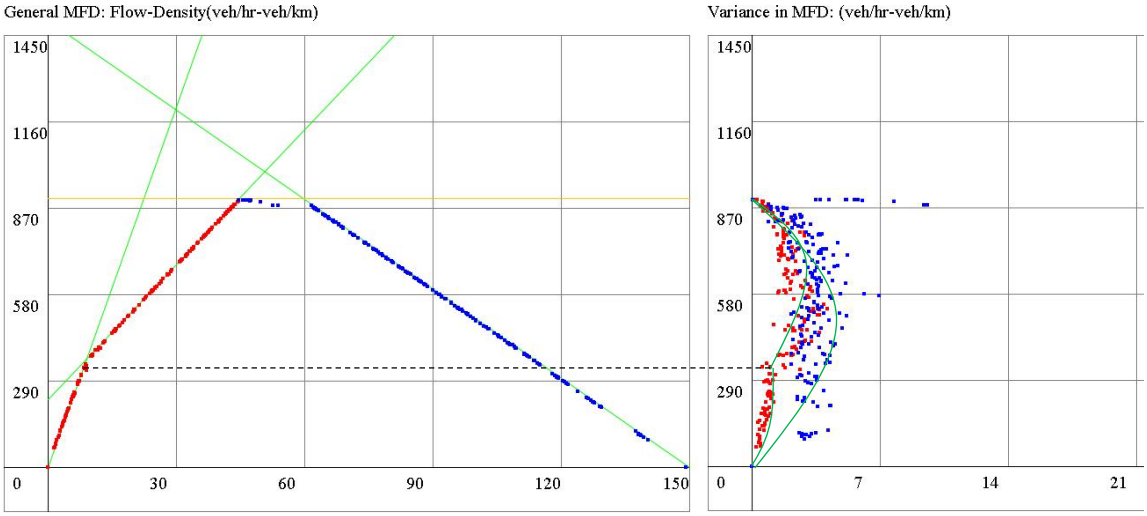

(d) L=266.67m, G=50%C, C=80s, δ=16s, n=30

Figure 4.11 Flow versus standard deviation in density on road chains (Continued)

CHAPTER 5

APPLICATION WITH URBAN NETWORKS

5.1 Network with turning rates

5.1.1 Deterministic Turning Rates

The approximation model doesn't deal with the existence of turning rates, but the turning behaviors universally exist in urban networks. The turning behavior is an important factor that will impact the appearance of the MFD and its existence cannot be neglected while in application in networks. It is interesting to compare the MFDs generated in a network that allows for turning at intersections with the ones generated on the road chain. We test with deterministic turning rates in a 10*10 network composed of single-way roads of the same length $l = 100m$ in all directions. The traffic is only allowed to be bound for south or east in this network (see Figure 3.1(a)). Figure 5.1 show a series of simulated MFDs and their corresponding flow versus standard variance in density when the green phase is 50% of the cycle. To focus on the effect of turning behaviors, simulations in this section set the same road length, offsets and green phase for the NS and EW directed roads so that the approximation for the NS and EW directed roads are identical. In Section 4.5, we have already shown that the simulated MFDSs on a road chain are compatible with the approximation. However, when a deterministic turning rate of 0.1 is introduced (see Figure 5.1(a)(c)(e)), the geometric shape of the MFD deviates from the approximation. Moreover, its maximum capacity, critical density, the distribution of the simulated sample dots along the curve, and the map of variance are all shifted. In simulation tests using single road length of 100m and 200m with a signal cycled 50 seconds and a 50% green time, the maximum capacity of MFD would drop if it is estimated to be $\frac{G}{C} q_c$ in the approximation (see Figure 5.1(a)) or retain the original level if it is estimated to be smaller than $\frac{G}{C} q_c$ in the approximation (see Figure 5-1(c)(e)). Although the turning rate causes the maximum

performance to drop, it brings benefits to enhance the stability of the traffic. The MFD generated with a deterministic turning rate are smoother than the approximation. The MFD no longer clutches to the straight line cuts as shown in Chapter 4; instead the lines are slightly bulged into curves and are smoothly connected to each other. The derivatives near the critical density become continuous and the simulated sample points tend to cluster near the maximum capacity. As a result, the flow at the densities near critical density is greatly improved when the approximated density is smaller than $\frac{G}{C} q_c$ as shown in Figure 5.1(c) to 5.1(f). Comparing Figure 5.1(a)(c)(e) with their counterparts of Figure 5.1(b)(d)(f) which apply a deterministic turning rate of 0.4 instead of 0.1, we find the curvature of the MFD curves becomes greater when the turning rate is larger. The comparison between Figure 5.1(a) and (b) also reveals that the drop from the maximum capacity would become more dramatic with a larger turning rate in the system.

The critical density for the MFD is also shifted under a deterministic turning rate and their shifting pattern is dependent on the tightest forward/backward cuts with the S-cut. Although without theoretical explanation, it is observed that the shift direction of the critical density is dependent on the slope of the approximated cuts. If the absolute value of the slope for the tightest forward cuts is greater than the tightest backward cuts, the critical density would divert from its approximated location to the side of the congested branch, and vice versa. As a result, when the slope of forward cuts is greater than that of the backward cuts, the critical density of the MFD would become bigger. Comparing Figure 5.1(a)(c)(e) with Figure 5.1 (b)(d)(f), we find the shifting distance is dependent on the value of the turning rate. A greater turning rate will cause a more obvious shift of the critical density. The diagrams of flow versus standard deviation in density are also shown in Figure 5.1 with their corresponding MFD diagrams. Since the MFD are curved, the standard deviation also become smoother at the connection of free-flow and congested status. The flow versus standard deviation points form a complete and smooth loop across the free-flow and congested status as shown in Figure 5.1(a)(b)(e)(f). However, it should also be noted that the loop is hard to form if the forward cut

is with a slope smaller than the backward cut. This situation may occur with roads of short length. In this case, the flow versus standard deviation points simulated under free flow status bend with a curvature equal to or greater than those simulated under congested status and the loop is not possible to be constructed.

It is interesting to note that the MFD generated with a turning rate shows clear signs of data cluster along its curve. As shown by Figure 5.1, the MFD curves are not dotted uniformly. The status with low traffic flows on the curve is sparsely dotted and the dots are densest near the critical density. On the congested branch of the MFD, samples cluster and dot the curve with space. The phenomenon of data cluster suggests that the traffic status change in the system is not changed along the MFD curve continuously; instead the traffic status jumps along the curve. Some traffic density and flow are easier to be obtained then other. And the phenomenon of data cluster become more severe as the deterministic turning rate grows.

Figure 5.2 shows the simulation with green phases of 70%C for the EW-directed streets and 30%C for the NW-directed streets. The other environmental settings are the same with the simulations for Figure 5.1. The curve in red is the averaged MFD for the system. The magenta curve is the averaged MFD for all EW-directed roads in the system, while the green curve is the averaged MFD for all NS-directed roads. The flow-density dots on all three curves representing the status at a same time are connected together. In other words, the dot on the red curve should be the average of the two points connected to it on the magenta and green curves. It should be noted that the averaged MFD curve lies between the MFDs for NW and EW-directed roads, but it isn't a simple weighted average between the two curves. That's because the sample points on the NW and EW MFDs that are used to be average the general MFD are not located at the same density nor at the same flow. The complexity lies in the fact that there is yet no known methodology to predict the traffic status in the NW MFDs when the traffic status in the EW MFDs is given. However, it is obvious that when the level of congestion is not evenly distributed in the two road groups. As shown in Figure 5.2, the lines that connect the corresponding points on three curves are always sloped upper right with a significant angle. Due

to the difference in green time, the EW roads always retain a traffic status much less congested than the NS roads. The comparison between Figure 5.2(a)(c)(e) and Figure 5.2(b)(d)(f), when the deterministic turning rate becomes larger, the flow for the MFD on EW roads drops and the flow for the MFD on NS roads increases. The turning rate could eliminate the difference of MFD between the two road systems. However, it should be noticed that the elimination is to reduce the difference in flow on EW and NS roads, and it doesn't help to eliminate the imbalanced distribution of traffic density. This observation is supported by the fact that the variance in density is lifted up when a larger turning rate is applied.

As a conclusion for this section, the deterministic turning rates affect the shape of MFD by designate a curvature to the MFD lines and smooth the approximated MFD into a derivable curve. As a result for its change in shape, the MFD may experience a drop of capacity if its maximum capacity is defined by the S-cut in approximation model. But the stability of the system to retain the maximum performance is greatly strengthened by the introduction of turning behaviors. The critical density and the curvature are also shifted under the influence of turning behaviors. In a traffic system with two groups of road with different MFDs, the turning rate is essential in eliminating the flow difference between the two groups.

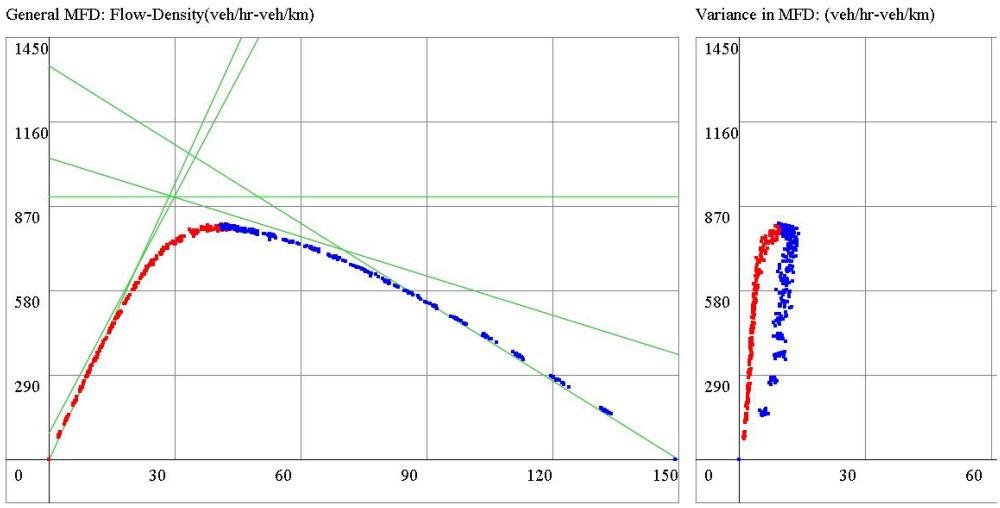

(a) MFD and $\sigma(k)$: L=100m, C=80s, G=50%C, offset=0s, turning rate=0.1

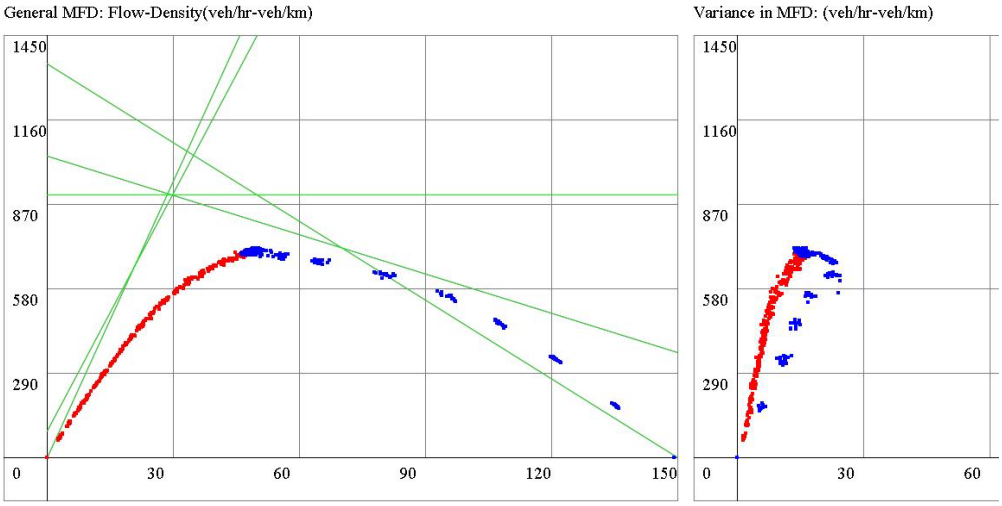

(b) MFD and $\sigma(k)$: L=100m, C=80s, G=50%C, offset=0s, turning rate=0.4

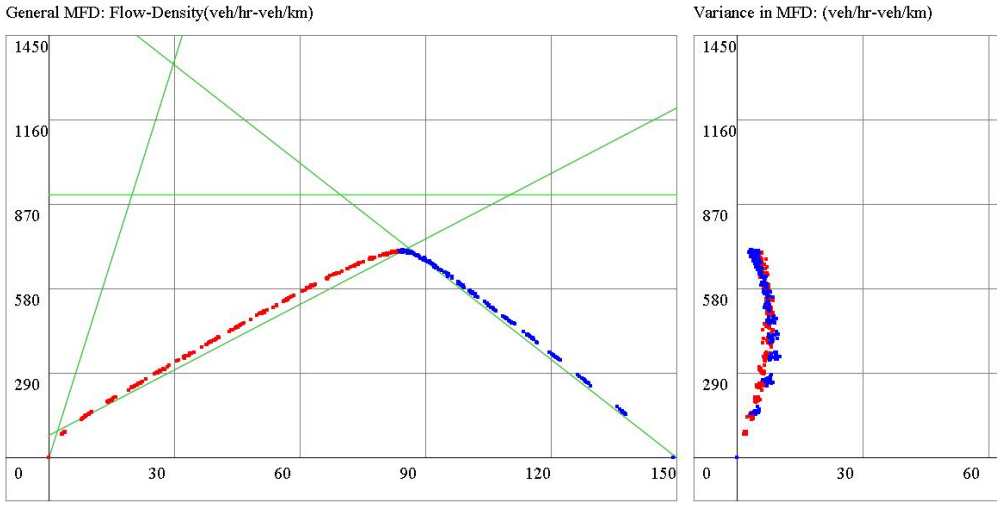

(c) MFD and $\sigma(k)$: L=100m, C=80s, G=50%C, offset=20s, turning rate=0.1

Figure 5.1 Simulations with deterministic turning rates in single-way network with G=50%C

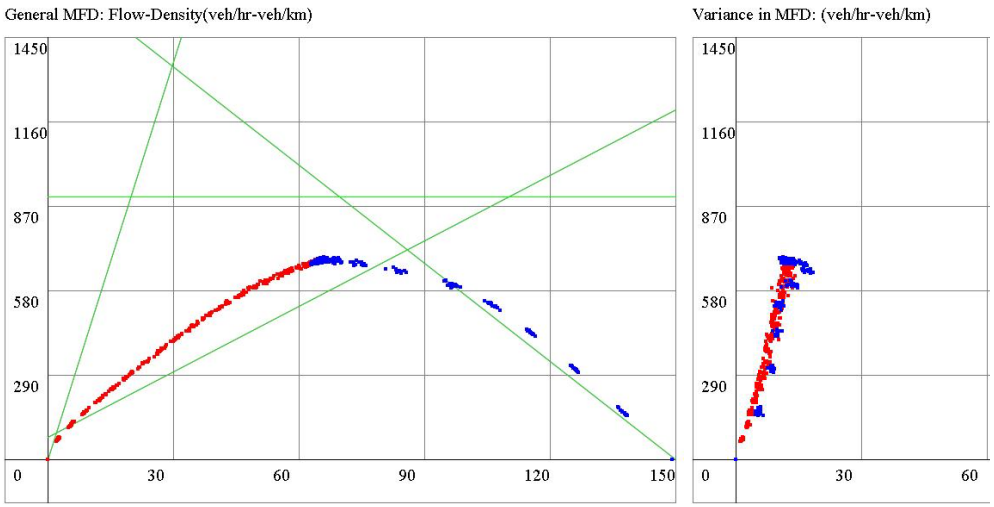

(d) MFD and $\sigma(k)$: L=100m, C=80s, G=50%C, offset=20s, turning rate=0.4

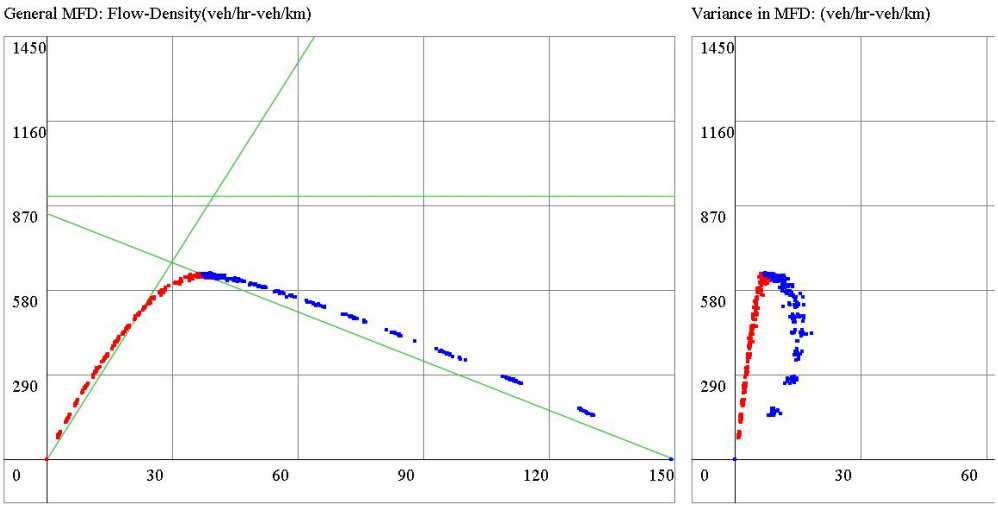

(e) MFD and $\sigma(k)$: L=100m, C=80s, G=50%C, offset=40s, turning rate=0.1

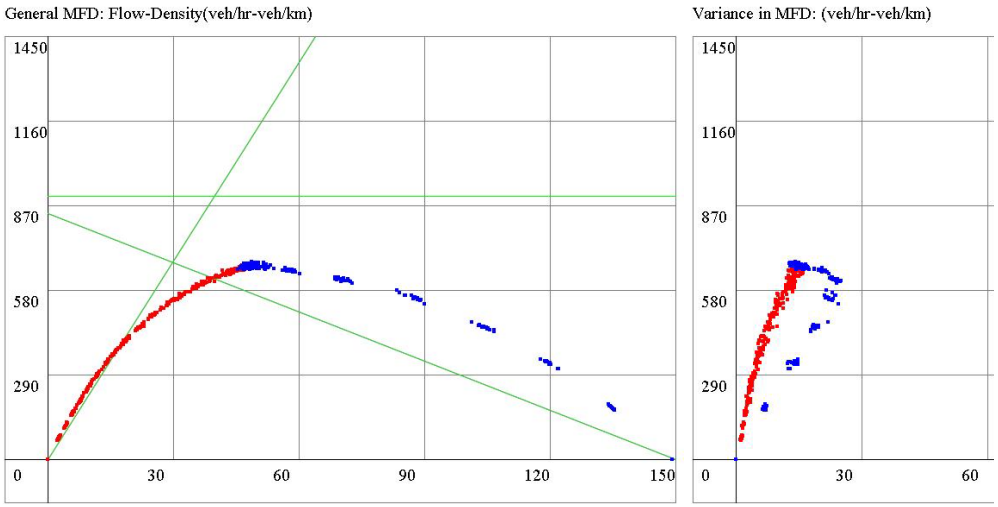

(f) MFD and $\sigma(k)$: L=100m, C=80s, G=50%C, offset=40s, turning rate=0.4

Figure 5.1 Simulations with deterministic turning rates in single-way network with G=50%C (Continued)

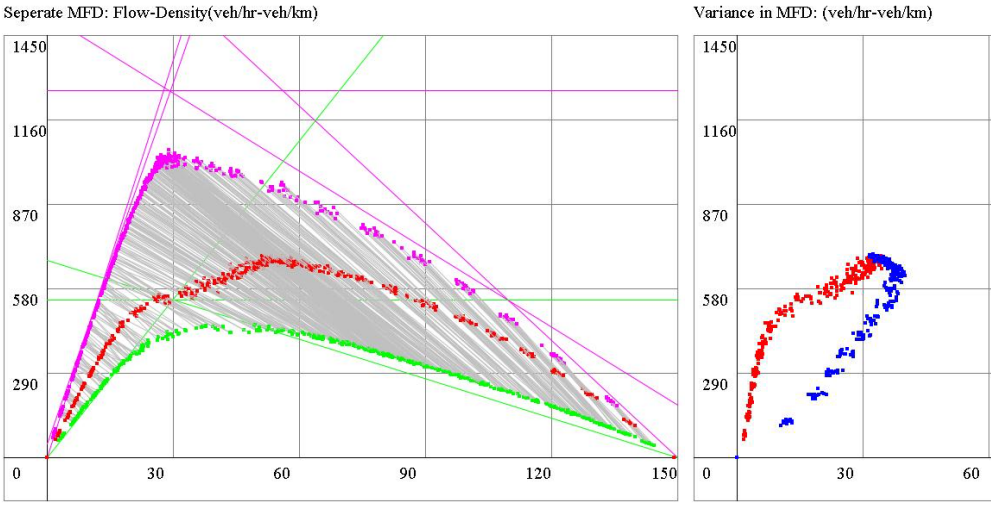

(a) MFD and $\sigma(k)$: L=100m, C=80s, G=50%C, offset=0s, turning rate=0.1

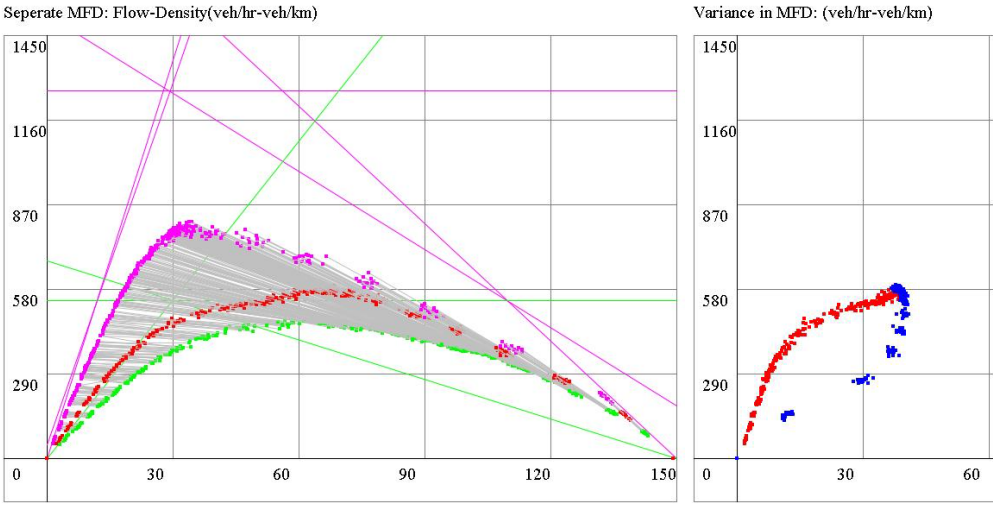

(b) MFD and $\sigma(k)$: L=100m, C=80s, G=50%C, offset=0s, turning rate=0.4

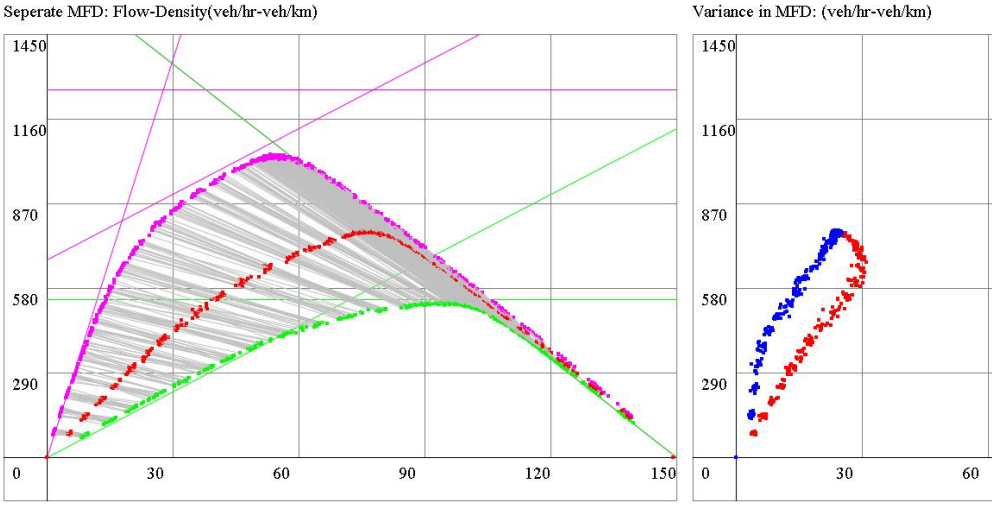

(c) MFD and $\sigma(k)$: L=100m, C=80s, G=50%C, offset=20s, turning rate=0.1

Figure 5.2 Simulations with deterministic turning rates in single-way network with G=70%C

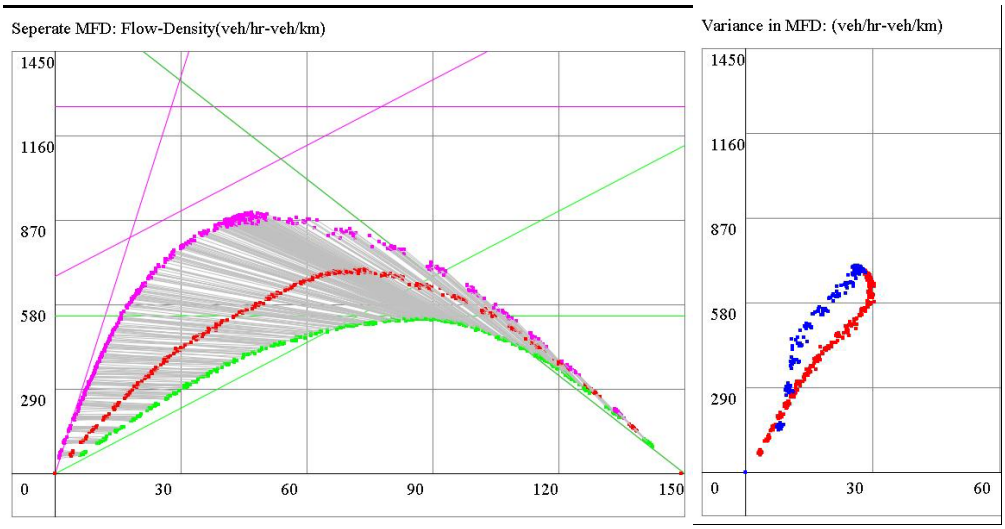

(d) MFD and $\sigma(k)$: L=100m, C=80s, G=50%C, offset=20s, turning rate=0.4

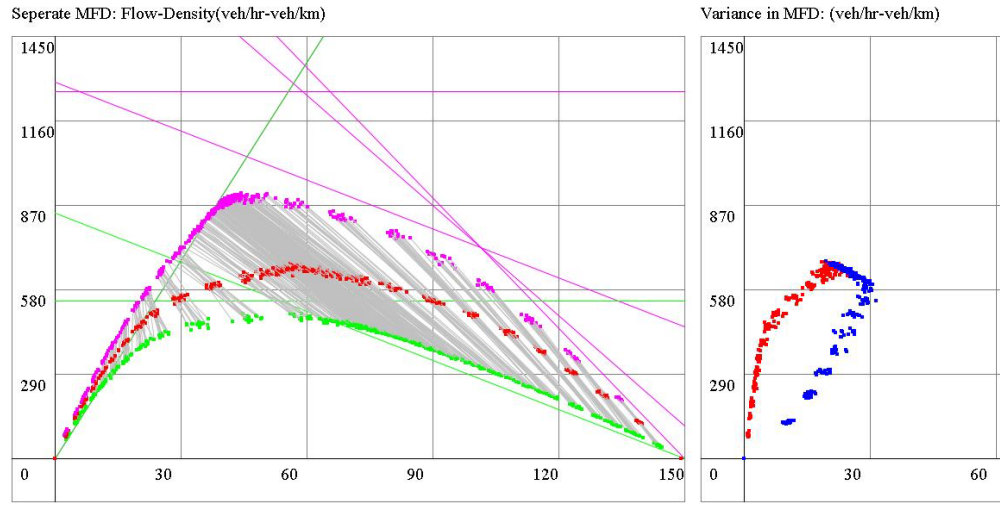

(e) MFD and $\sigma(k)$: L=100m, C=80s, G=50%C, offset=40s, turning rate=0.1

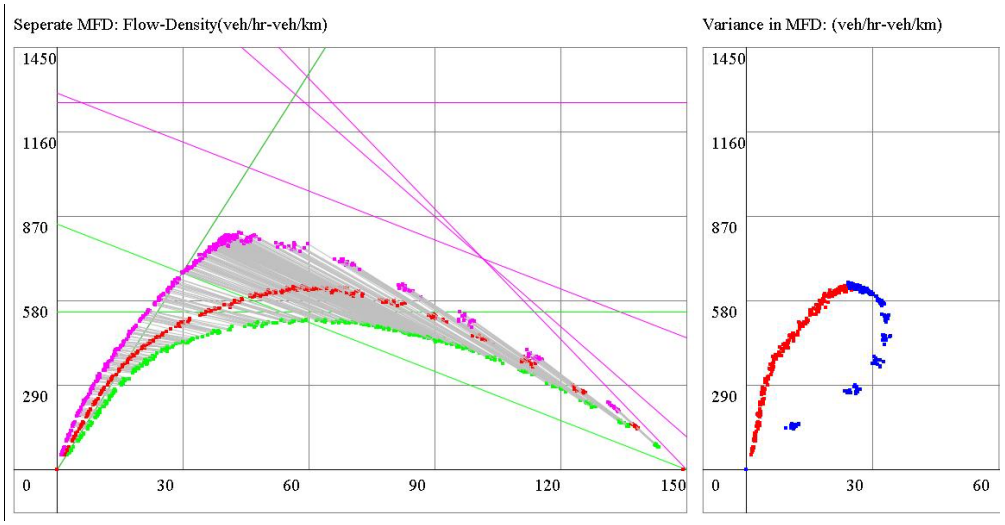

(f) MFD and $\sigma(k)$: L=100m, C=80s, G=50%C, offset=40s, turning rate=0.4

Figure 5.2 Simulations with deterministic turning rates in single-way network with G=70%C (Continued)

5.1.2 Stochastic Turning Rates and Exogenous Demands

Now we repeat the simulation completed in Section 5.1.1 in a stochastic scenario. We suppose the exogenous traffic entering the system through each road conform to a uniform distribution with c.o.v.=20%. If we denote the average demand of flow as μ_{flow} and the uniform distribution $U(\mu_{flow} - d, \mu_{flow} + d)$, the value of d can be deduced to be:

$$d = \mu_{flow}\sqrt{3 * cov^2} \tag{5.1}$$

As the average exogenous traffic demand is increased in the system by fixed step, we set a stochastic exogenous traffic flow rate for each street on the border of the network. We apply this stochastic model with exogenous traffic assuming that the turning rate in the network is 0.1. All the other parameters are the same as described in Section 5.1.1. The simulated results with stochastic exogenous traffic are shown in Figure 5.3. Compared with Figure 5.2, there is a slight drop with the flow in MFD in Figure 5.3 (a)(b)(c), but the shapes of MFD are retained the same. The slight drop is generated because the MFD curve on EW roads experienced a drop in its capacity. The MFD curve on EW roads deviates from its original shape in Figure 5.2 because a majority of stochastic points are produced with this curve. The points related with this curve are dispersed and the phenomenon of data clustering becomes more obvious. In contrast, the MFD on NS roads is little affected by the stochastic exogenous traffic. No obvious drop of capacity or change in curve shape is observed with the MFD for NS roads. It indicates that the stochastic exogenous traffic inputs tend to affect roads with higher maximum capacity. The variance of density shows no sign of general increase or decrease due to the exogenous traffic, except that the points with the flow-standard variation in density loops become more dispersed and tend to cluster.

Now, we apply the stochastic model with the turning rate in the system. The turning rate at each intersection in the network is a stochastic value conforming to the uniform distribution $U(\mu_{turn} - d, \mu_{turn} + d)$. We assume that the average turning rate in the system is $\mu_{turn} = 0.4$ and the c.o.v. is 40%. The value of d can be calculated using Equation (5.1). The simulated

results with stochastic turning rates are shown in Figure 5.4. When the generalized MFDs shown in Figure 5.4 are compared with the MFDs in Figure 5.2, the most obvious difference between the two is a slight drop of the flow in the MFD. For all densities, the flow that can obtained with that density is lower than the flow generated using deterministic turning rates for every intersection. Although the maximum value of the variance in density isn't affected, the variance in density drops more quickly on the congested branch as the flow drops. The stochastic turning rates expedite the uniform spread of congestion in the network. The effect of stochastic turning rate is a universal drop in flow at all densities. However, this impact is very trivial and can only be noticed when the turning rate and the c.o.v. are both quite large.

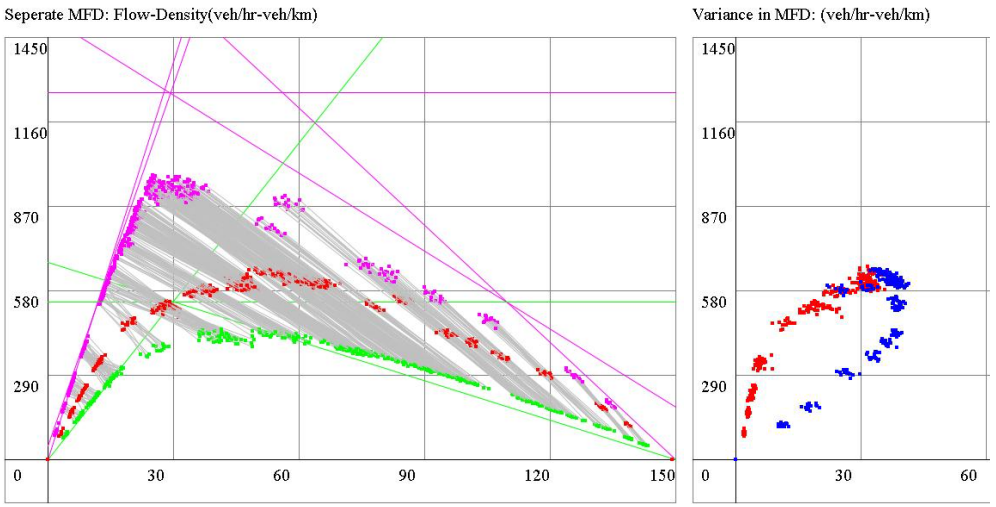

(a) MFD and $\sigma(k)$: L=100m, C=80s, G=70%C, offset=0s, turning rate=0.1, cov (exogenous traffic)=0.2

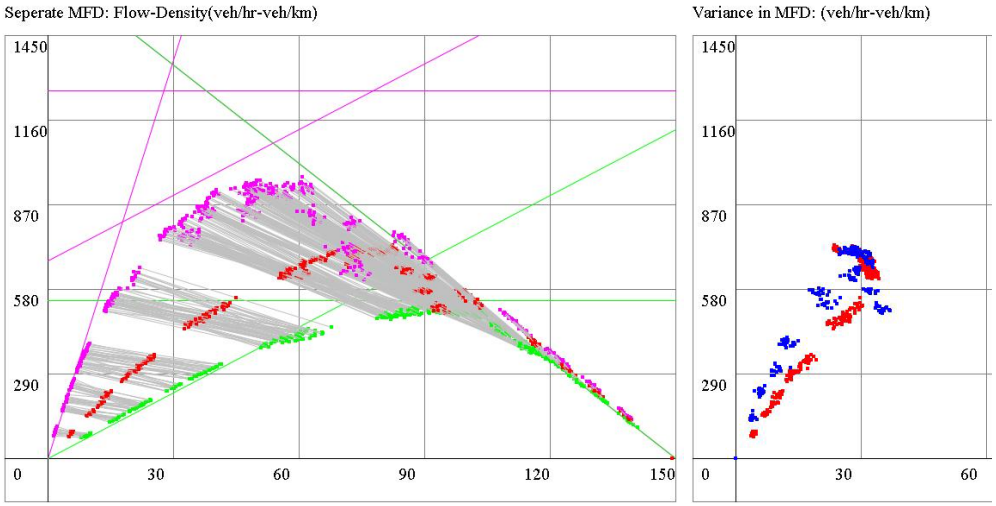

(b) MFD and $\sigma(k)$: L=100m, C=80s, G=70%C, offset=20s, turning rate=0.1, cov (exogenous traffic)=0.2

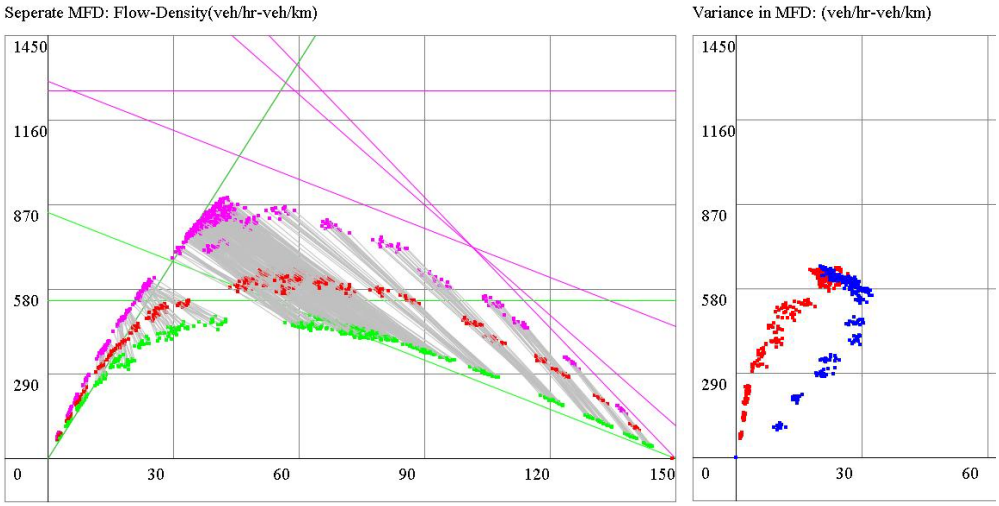

(c) MFD and $\sigma(k)$: L=100m, C=80s, G=70%C, offset=40s, turning rate=0.1, cov (exogenous traffic)=0.2

Figure 5.3 Simulations with stochastic exogenous traffic in one-way network

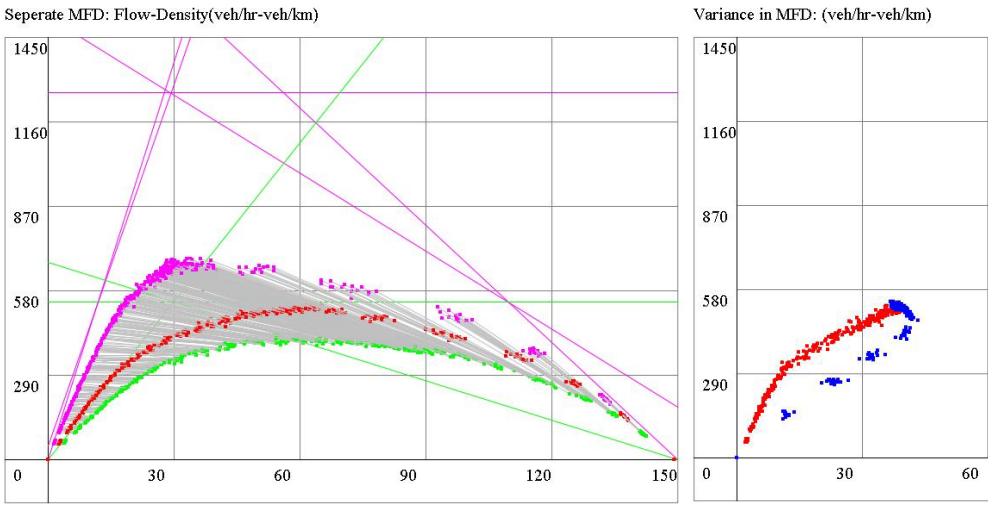

(a) MFD and $\sigma(k)$: L=100m, C=80s, G=70%C, offset=0s, turning rate=0.4, cov (exogenous traffic)=0.4

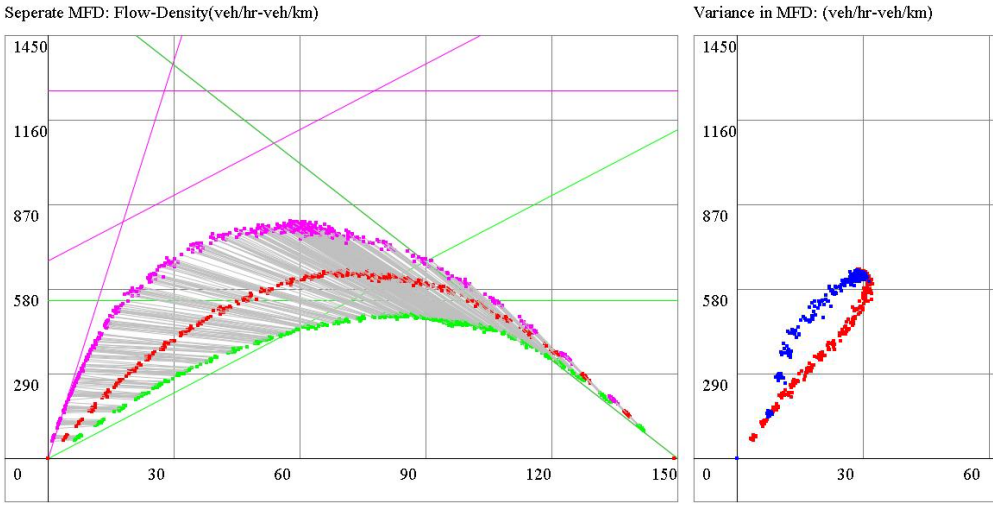

(b) MFD and $\sigma(k)$: L=100m, C=80s, G=70%C, offset=20s, turning rate=0.4, cov (exogenous traffic)=0.4

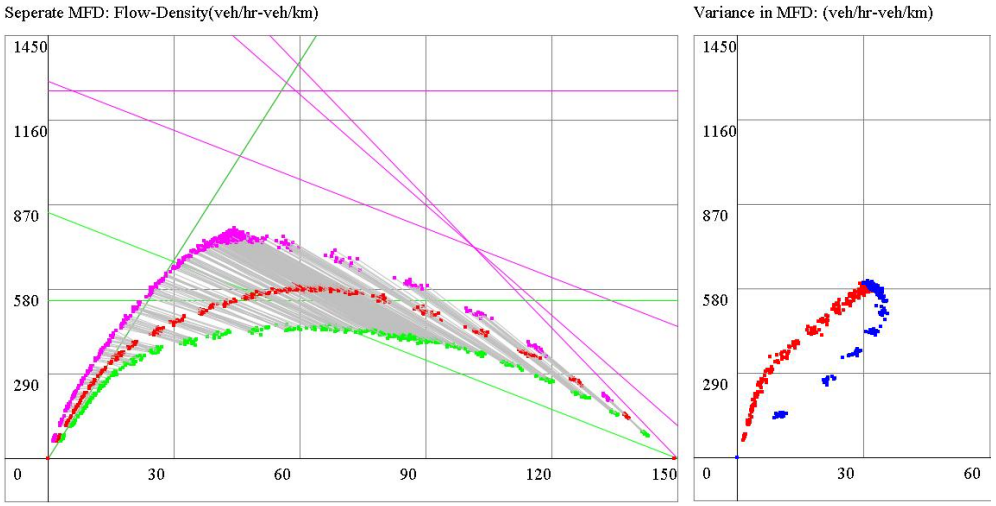

(c) MFD and $\sigma(k)$: L=100m, C=80s, G=70%C, offset=40s, turning rate=0.4, cov (exogenous traffic)=0.4

Figure 5.4 Simulations with stochastic turning rates in one-way network

5.2 Network with Endogenous Traffic

This section conducts simulation experiments to test with the effect of endogenous traffic in the network. The endogenous exit traffic is tested using the homogeneous network described in Section 5.1.1. Just for now, this model doesn't assume any existence of endogenous generated traffic in the network. The density of exit opportunity on roads is set as $\lambda = 0.3$/road unit cell. The deterministic turning rate is set as 0.1. The simulated results are shown in Figure 5.5. The capacity of the network is greatly reduced due to the endogenous exit traffic. The maximum capacity for EW and NS streets are capped when the flow has increased to around 700 veh/hr and 430 veh/hr separately. The capacity of the system retains at the level it is capped before falling into congestion status. The further increasing of exogenous traffic demands doesn't lift the circulating flow in the network. It is interesting to notice that although the maximum flow is capped, the maximum free-flow speed in the system is improved. The traffic is allowed to travel faster with the existence of exogenous traffic. The stability of the system to retain its performance at the maximum flow is greatly strengthened that the simulated sample points concentrate near the free-flow branch and the maximum capacity. As the restrictions on the outflow are strengthened, the maximum capacity is retained at the expense of an enlarged variance in density. The traffic status on the congested branch is extremely unstable that if the system fails to retain at its maximum performance when the outflows are restricted, it quickly fall to the congested status. The critical density shifts towards the free-flow branch where the flow is capped.

Recall the methods to generate and terminate endogenous traffic in network from Section 3.2.4. Now, the endogenous traffic demands are added to the model in the existence of the endogenous exit traffic. We keep all the parameter settings in the simulation as the simulation with endogenous exit opportunity, and add an endogenous traffic demand rate of $\rho = 3/10000$. The value of ρ is the chance that a new vehicle enters the system at each length cell on roads within one time step. As shown in Figure 5.6, in the existence of endogenous exit traffic, the endogenous generated traffic increases the capacity of the MFD and the MFD shape is close to

what is shown as their counterparts in Figure 5.2. Although the maximum capacity is restored, the endogenous traffic generated within the network could disturb the homogenous distribution of congestion, especially in free-flow status. The figures for the flow versus standard variance indicate that the endogenous generated traffic cause the variance in free-flow branch to become bigger sharply near the critical density. Moreover, the lines connecting points on the generalized MFD curve and the MFD curves on NS and EW roads are flatter, which indicates that the difference of the density in both systems becomes larger. In the existence of endogenous exit traffic, the endogenous generated traffic improves the continuity of change in traffic status on the congested branch. Interestingly, when the endogenous generated traffic is included in the model, the traffic status for the system is able to shrink into congestion without imposing environmental restrictions on the traffic outflow. Endogenous traffic enables the system to self-lock into congestions.

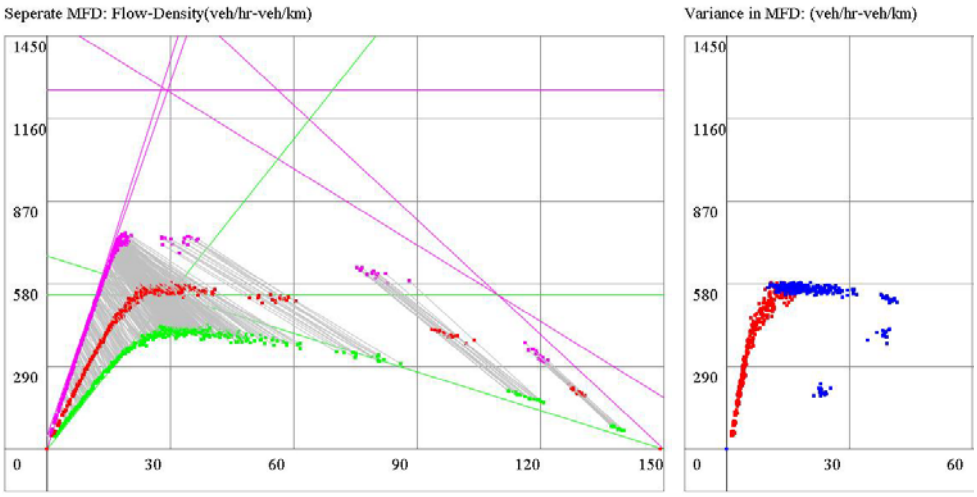

(a) MFD and $\sigma(k)$: L=100m, C=80s, G=70%C, offset=0s, turning rate=0.1, exit density=0.3

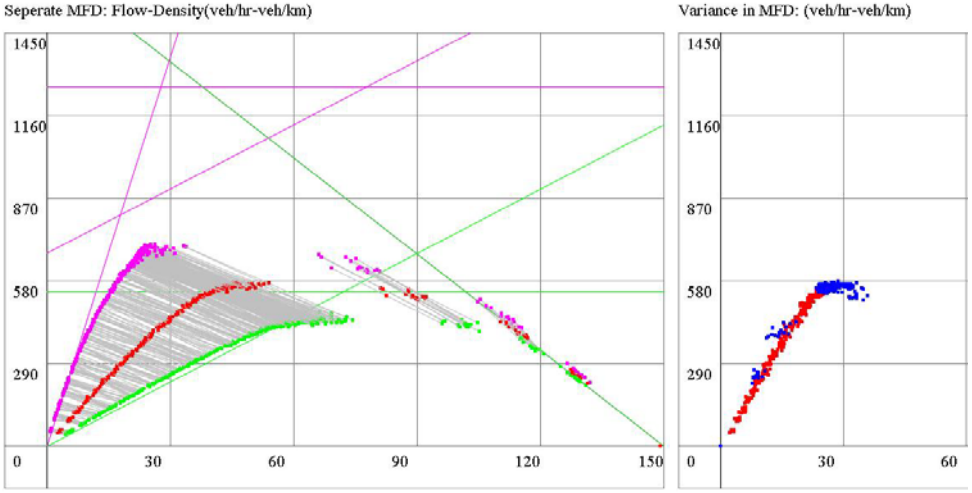

(b) MFD and $\sigma(k)$: L=100m, C=80s, G=70%C, offset=20s, turning rate=0.1, exit density=0.3

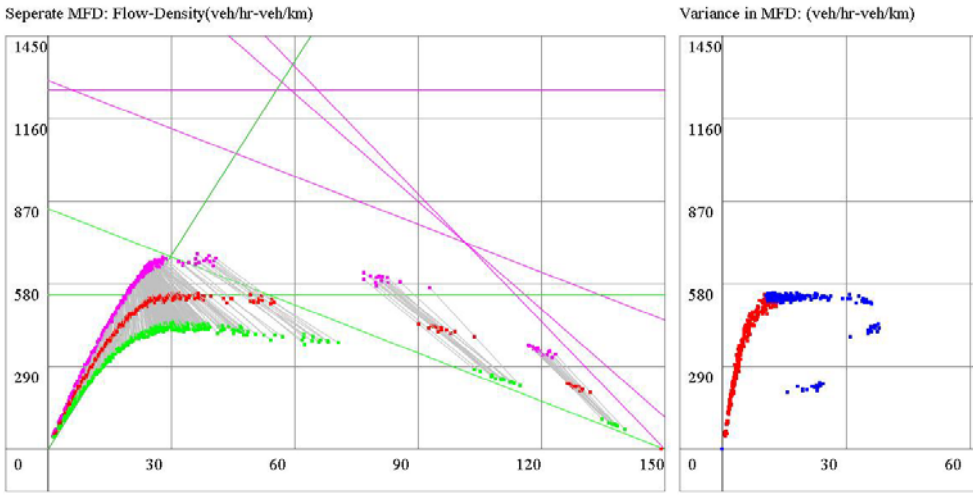

(c) MFD and $\sigma(k)$: L=100m, C=80s, G=70%C, offset=20s, turning rate=0.1, exit density=0.3

Figure 5.5 Simulations with endogenous exit traffic in one-way network

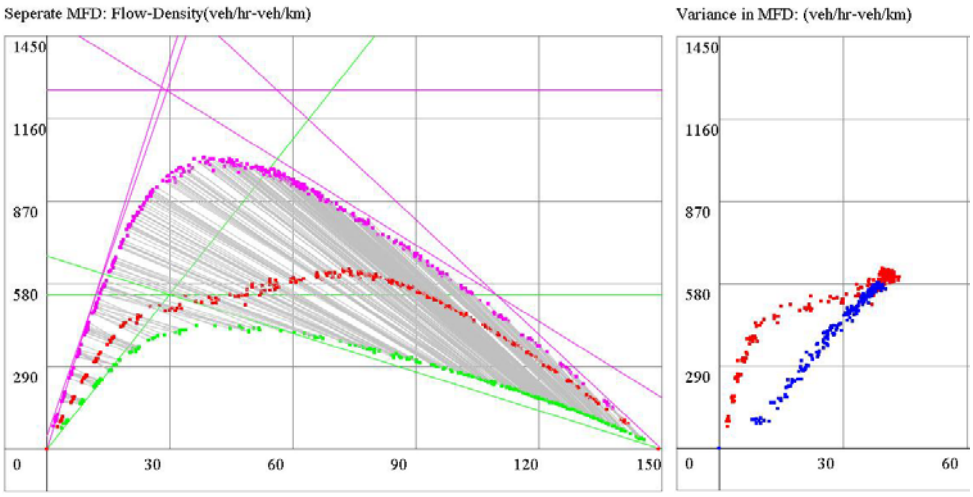

(a) MFD and $\sigma(k)$: L=100m, C=80s, G=70%C, offset=0s, turning rate=0.1, exit density=0.3, generating rate/inflow rate=3/10000

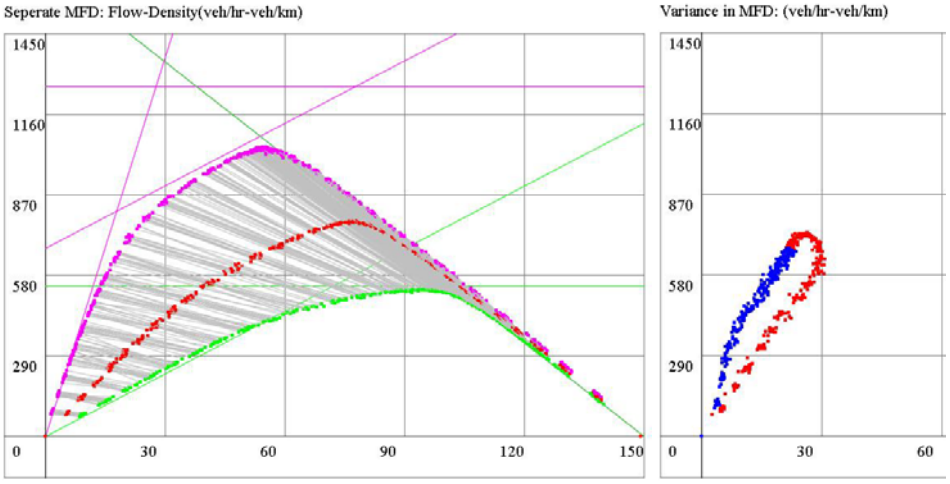

(b) MFD and $\sigma(k)$: L=100m, C=80s, G=70%C, offset=20s, turning rate=0.1, exit density=0.3, generating rate/inflow rate=3/10000

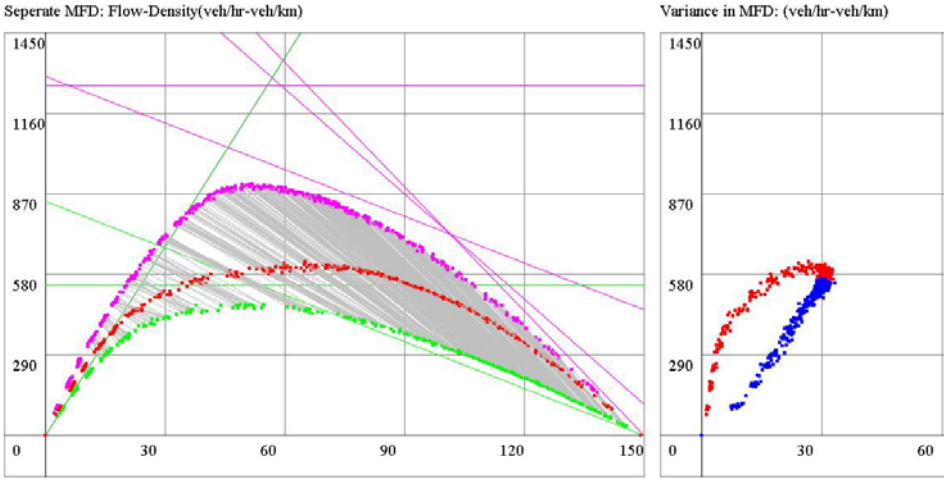

(c1) MFD and flow-standard variance: L=100m, C=80s, G=70%C, offset=40s, turning rate=0.1, exit density=0.3, generating rate/inflow rate=3/10000

Figure 5.6 Simulations with endogenous generated and exit traffic in one-way network

5.3 Network with Two-Way Roads

The networks simulated in Section 5.3 are composed of two-way roads, which allows for traffic traveling in all directions just like normal networks in real life. An O-D map is extracted when the simulation is done for the area. The whole area is divided into 9 areas as shown in Figure 5.7. Area 4 can be seen as a local center of the network. The exogenous traffics flow enters the system from Area 9-20 outside of the network. Each area among area 1-9 is designated a value for endogenous traffic generating rate and endogenous traffic exit rate by multiplying the average endogenous traffic rates by a regional factor from 0 to 2. Each area among area 9-20 are designated a value for outflow control and boundary traffic inputs by multiplying the average exogenous traffic flow rates by a regional factor from 0 to 2. The average density for endogenous exit is 0.03 and the generating rate for endogenous traffic at any vacant cell of length during one time step in simulation is 0.00003#/unit/timestep. The network is made of 10*10 block and each road is 100m. The area 4 is made of 2*2 blocks. The signal cycle is 80 seconds in the system and the green phase is 50% in all directions. There are two parts of factors that decide the turning rate for each road lane at its end. The first part is a deterministic value of 0.8 for going straight, 0.1 for turning left and 0.1 for turning right. The second part is decided by endogenous exit opportunities a vehicle can expect to reach when it takes a certain road. It is supposed that the drivers tend to turning towards the direction that most exit opportunities are offered. The two parts are averaged with a weight of 0.4 for the first part and 0.6 for the second part to make the turning choice rate for drivers at each intersection.

The model is run under four scenarios: (1) all parameters are homogeneous in the network; (2) the density of exit opportunity is 13:4 in the Area 4 to other areas (i.e. the density of exit opportunity is the highest in Area 4); (3) the exogenous inflow is 13:4 in Area 10,13,16,19 to other outer areas (i.e. the exogenous inflow is higher in the middle of each network border); (4) not only the density of exit opportunity is 13:4 in the Area 4 to other areas, but the endogenous traffic generation rates in other areas is 13:4 to the rate in Area 4 (i.e. the endogenous exit rate is high in Area 4, but the endogenous traffic generation is high in other areas). The simulated

results for the 4 scenarios are shown in order in Figure 5.8 to Figure 5.11, and each figure shows the general MFD in the system, the flow versus standard variance in density, and the MFDs for four types of roads that bounded for east, west, south, and north separately. The MFD for all roads bounded for east is colored magenta, the MFD for roads bounded for south is colored green, the MFD for roads bounded for west is colored blue, and the MFD for roads bounded for north is colored orange.

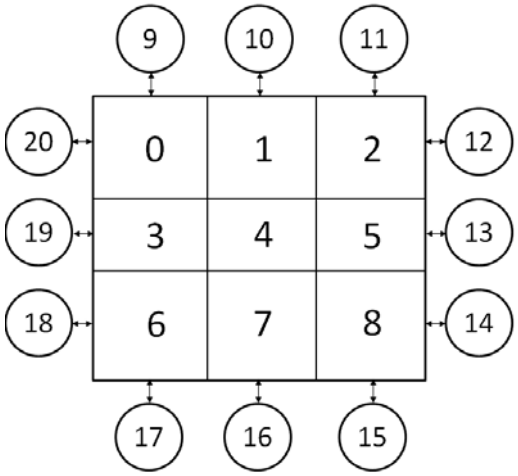

Figure 5.7 Division of regions in a network composed of two-lane roads.

The generated four MFDs don't show obvious difference between each other in their shape of MFD. It verifies that in a two-way network, the diversity in traffic input/output settings between areas is not major factor in determining the shape of the MFD. However, there exist difference in the density of dots distributed along the MFD curves. Comparing among Figure 5.8 to Figure 5.11, Figure 5.9 is the most sparsely dotted in the free-flow status. In Figure 5.9, the sampled dots are sparse when the density is small in the network. This indicates that the two-way network would more quickly obtain its maximum performance when traffic demand has been produced, if the endogenous exit opportunities are located at the central area. Figure 5.10 is not dotted with the MFD curve that is low on the congested branch. It shows that when the exogenous traffic demand is not evenly distributed along the border, the system would retain at a certain range of performance level and does not fall to jammed congestion until the very end.

It is also interesting to point out that there is an overlap between the free-flow and congested traffic status reflected on the MFD. The overlap occurs due to the existence of endogenous generated traffics. It is assumed in the model that the demand for endogenous traffic increases with the demand for exogenous traffic. When the restriction on the outflow is exerted, the number of vehicles in the system increases and it suppressed the generation of endogenous traffics. As a result the flow increases and the density drops.

Table 5.1 to Table 5.4 are the normalized OD map for the network in the simulation. The travelled vehicles are counted in their numbers with the region for them to start the trips and the region to end their trips. The counting for each OD pair is divided by the total number of vehicle counts that have travelled in the system over the whole simulation process to make the normalized value. The traffic flows are paired between the area 0 to 8 in the network and an external environment of the network (area 9-20). The external environment is shorthand as E in the OD tables. No matter which scenario it is, in all four models, the traffics that come from outer environment and travel through the network without ending in the network is takes about 29% to 35% of the total traffics. This result is quite consistent with the discovery in the MFD research in Yokohama (Geroliminis & Daganzo, 2008) that the outflow is likely to be a fixed percentage in the total traffic flow. Although the OD tables vary from each other in the value for each OD pairs as the parameters for exogenous and endogenous traffic vary, the MFD and density variance maps are identical. It proposes that the shape of MFD has little relationship with the OD structure for the network.

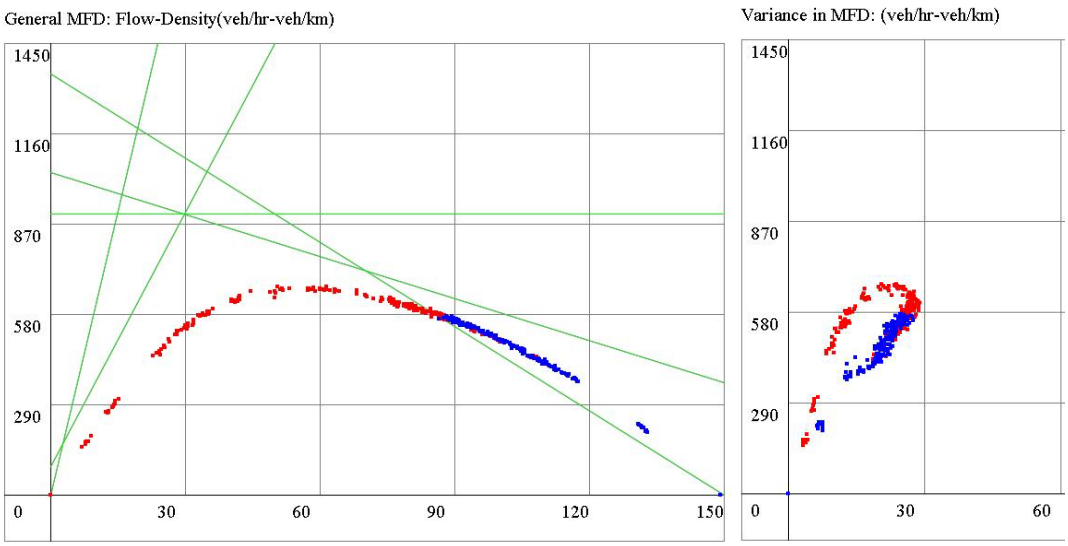

(a) MFD and flow-standard variance: L=100m, C=80s, G=50%C, offset=40s, turning rate=0.1, exit density=0.3, generating rate/inflow rate=3/10000

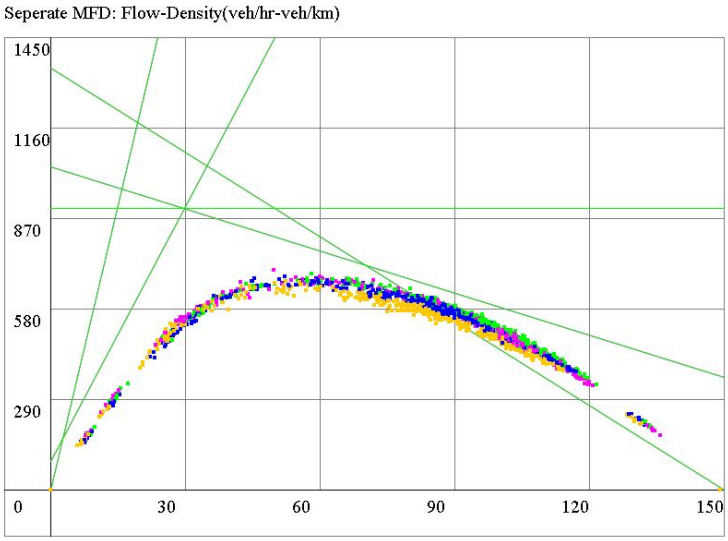

(b) MFDs for EW/NS double directed roads: L=100m, C=80s, G=50%C, offset=40s, turning rate=0.1, exit density=0.3, generating rate/inflow rate=3/10000

Figure 5.8 MFD with deterministic parameters in two-way network

Table 5.1 Normalized O-D map based on area divisions in the network with deterministic parameters

D\O	0	1	2	3	4	5	6	7	8	E
0	0.65	0.17	0.19	0.20	0.09	0.17	0.07	0.04	0.09	0.98
1	0.11	0.26	0.17	0.07	0.09	0.14	0.04	0.03	0.07	0.54
2	0.12	0.14	1.25	0.09	0.09	0.59	0.05	0.05	0.22	1.64
3	0.18	0.09	0.14	0.64	0.18	0.24	0.19	0.09	0.18	1.08
4	0.19	0.13	0.28	0.27	0.50	0.46	0.19	0.13	0.32	1.26
5	0.14	0.13	0.47	0.18	0.19	1.35	0.11	0.10	0.51	1.90
6	0.08	0.04	0.07	0.28	0.10	0.14	0.69	0.14	0.19	1.15
7	0.04	0.03	0.06	0.10	0.09	0.13	0.12	0.26	0.18	0.60
8	0.08	0.06	0.20	0.16	0.14	0.52	0.18	0.21	1.41	2.03
E	4.21	2.10	6.61	4.05	2.04	6.46	4.30	2.06	6.75	31.71

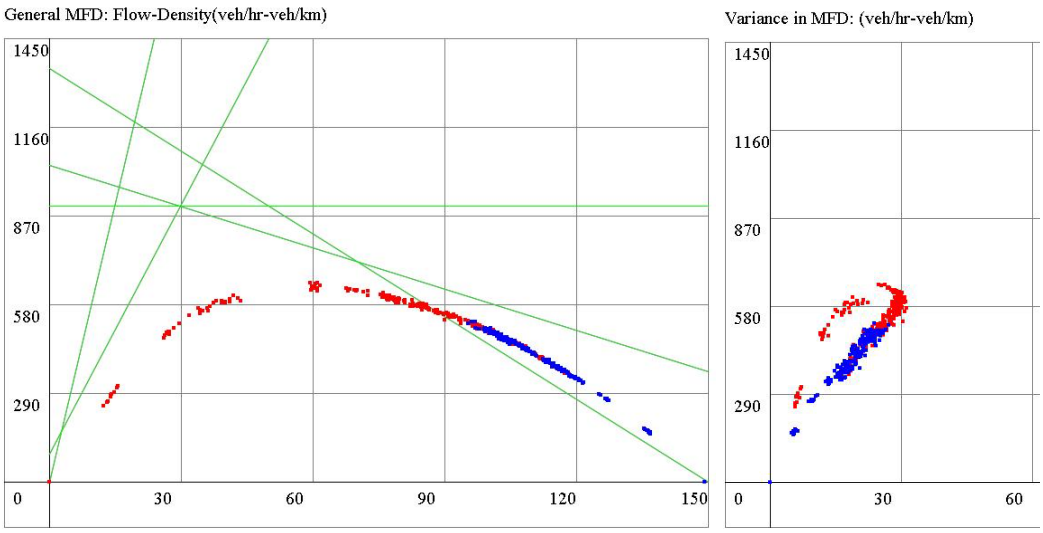

(a) MFD and flow-standard variance: L=100m, C=80s, G=50%C, offset=40s, turning rate=0.1, exit density=0.3, generating rate/inflow rate=3/10000, endogenous exit rate at area4: other areas=13:4

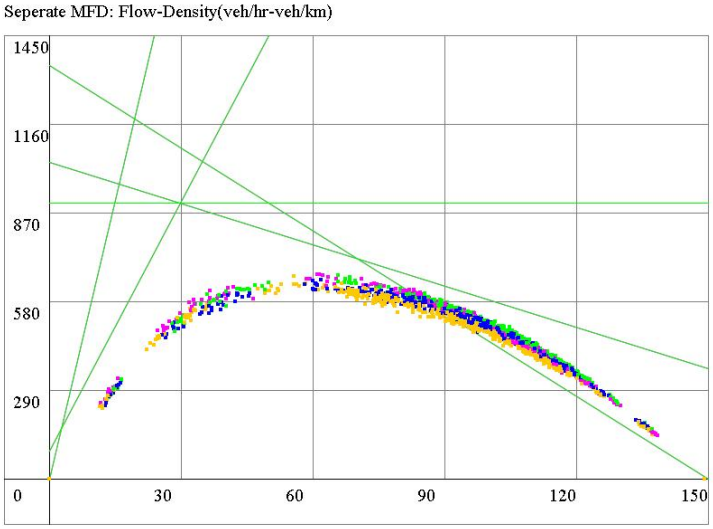

(b) MFDs for EW/NS double directed roads: L=100m, C=80s, G=50%C, offset=40s, turning rate=0.1, exit density=0.3, generating rate/inflow rate=3/10000, endogenous exit rate at area4: other areas=13:4

Figure 5.9 MFD with higher exogenous input in the middle of each boundary in two-way network

Table 5.2 O-D map based on area divisions in the network with higher exogenous input in the middle of each boundary

D\O	0	1	2	3	4	5	6	7	8	E
0	0.28	0.08	0.09	0.09	0.05	0.09	0.04	0.02	0.05	0.47
1	0.05	0.11	0.08	0.04	0.05	0.07	0.02	0.01	0.04	0.26
2	0.06	0.06	0.54	0.05	0.04	0.29	0.03	0.02	0.11	0.76
3	0.09	0.05	0.07	0.29	0.09	0.13	0.09	0.04	0.10	0.54
4	0.28	0.19	0.43	0.41	0.73	0.69	0.30	0.19	0.50	1.93
5	0.07	0.06	0.21	0.10	0.09	0.60	0.06	0.05	0.25	0.90
6	0.04	0.02	0.04	0.14	0.05	0.07	0.31	0.06	0.09	0.55
7	0.02	0.02	0.03	0.05	0.04	0.06	0.06	0.11	0.08	0.29
8	0.04	0.03	0.10	0.09	0.07	0.24	0.09	0.10	0.63	0.94
E	4.83	2.46	7.59	4.82	2.37	7.70	4.98	2.40	7.89	36.95

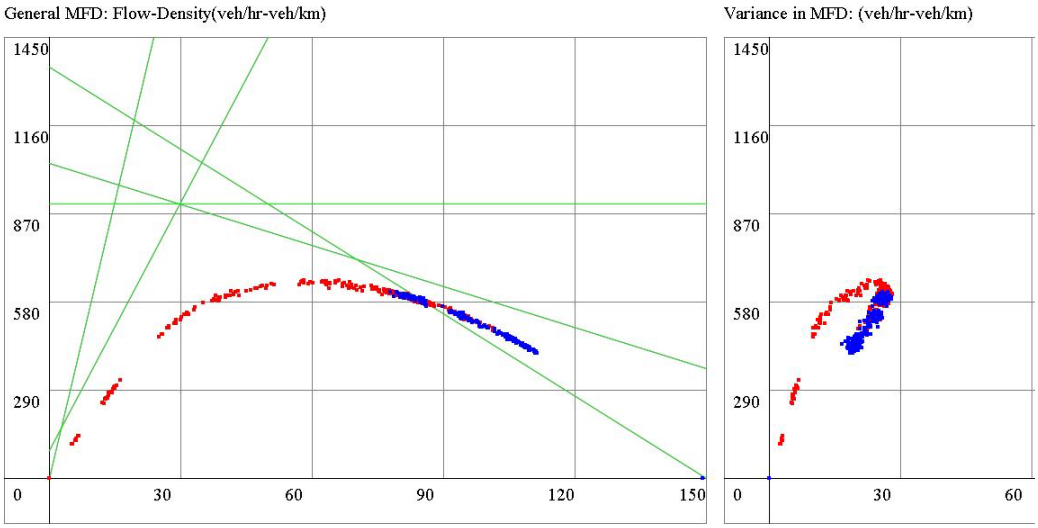

(a) MFD and flow-standard variance: L=100m, C=80s, G=50%C, offset=40s, turning rate=0.1, exit density=0.3, generating rate/inflow rate=3/10000, exogenous input rate to area1,3,5,7: other areas=13:4

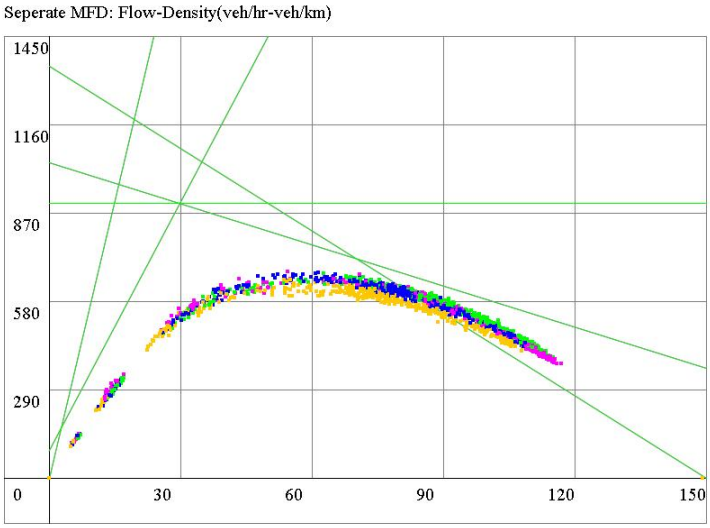

(b) MFDs for EW/NS double directed roads: L=100m, C=80s, G=50%C, offset=40s, turning rate=0.1, exit density=0.3, generating rate/inflow rate=3/10000, exogenous input rate to area1,3,5,7: other areas=13:4

Figure 5.10 MFD with higher endogenous input in areas surrounding the urban core in two-way network

Table 5.3 O-D map based on area divisions in the network with higher endogenous input in areas surrounding the urban core

D\O	0	1	2	3	4	5	6	7	8	E
0	0.79	0.20	0.23	0.24	0.11	0.19	0.09	0.04	0.11	1.06
1	0.13	0.31	0.21	0.09	0.11	0.16	0.05	0.03	0.08	0.59
2	0.15	0.18	1.52	0.11	0.10	0.68	0.07	0.05	0.27	1.76
3	0.22	0.11	0.16	0.75	0.21	0.28	0.24	0.11	0.21	1.19
4	0.17	0.12	0.25	0.25	0.46	0.42	0.18	0.12	0.30	1.09
5	0.17	0.15	0.57	0.21	0.22	1.57	0.13	0.12	0.62	2.08
6	0.10	0.05	0.09	0.32	0.11	0.17	0.85	0.17	0.24	1.23
7	0.05	0.04	0.08	0.11	0.11	0.15	0.15	0.31	0.22	0.66
8	0.10	0.08	0.25	0.19	0.17	0.62	0.22	0.25	1.73	2.16
E	4.19	2.05	6.58	3.93	1.98	6.25	4.29	2.02	6.72	28.65

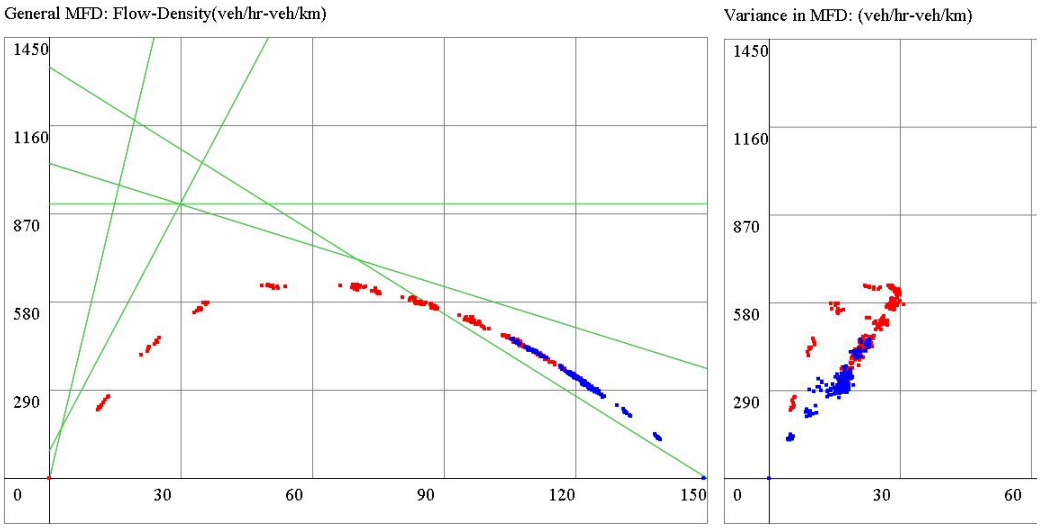

(a) MFD and flow-standard variance: L=100m, C=80s, G=50%C, offset=40s, turning rate=0.1, exit density=0.3, generating rate/inflow rate=3/10000, exogenous input rate to area1,3,5,7: other areas=4:13

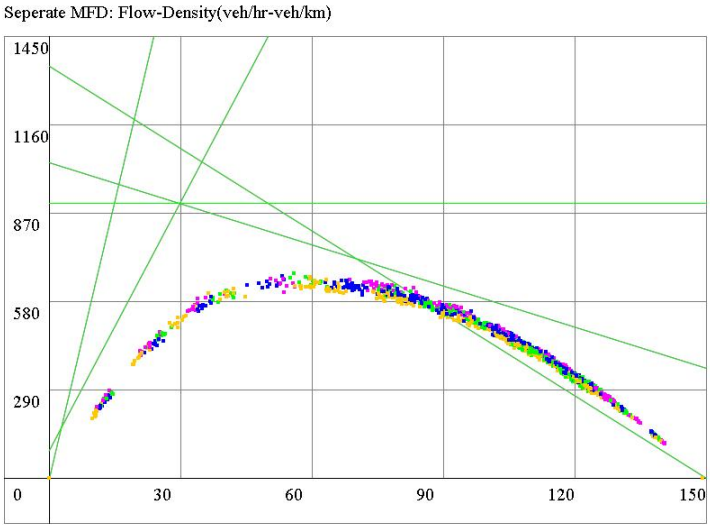

(b) MFDs for EW/NS double directed roads: L=100m, C=80s, G=50%C, offset=40s, turning rate=0.1, exit density=0.3, generating rate/inflow rate=3/10000, exogenous input rate to area1,3,5,7: other areas=4:13

Figure 5.11 MFD with higher exogenous input at the network's corners in two-way network

Table 5.4 O-D map based on area divisions in the network with higher exogenous input at the network's corners

D\O	0	1	2	3	4	5	6	7	8	E
0	0.32	0.08	0.08	0.09	0.03	0.08	0.01	0.02	0.04	0.36
1	0.05	0.12	0.07	0.04	0.03	0.07	0.00	0.01	0.03	0.19
2	0.05	0.06	0.58	0.04	0.03	0.28	0.00	0.02	0.09	0.56
3	0.09	0.05	0.07	0.34	0.07	0.12	0.02	0.05	0.10	0.43
4	0.20	0.14	0.30	0.32	0.41	0.52	0.04	0.15	0.37	1.11
5	0.06	0.05	0.20	0.08	0.06	0.61	0.01	0.05	0.22	0.66
6	0.05	0.03	0.05	0.22	0.05	0.10	0.08	0.11	0.14	0.57
7	0.02	0.01	0.03	0.05	0.03	0.06	0.01	0.13	0.09	0.24
8	0.04	0.03	0.09	0.08	0.05	0.24	0.01	0.10	0.69	0.72
E	6.30	2.96	9.50	6.44	1.96	9.03	1.21	3.19	10.03	34.89

5.4 Discussion on Other Factors

5.4.1 Driver Adaptation

The driver adaption is adopted in the simulations in previous chapters and sections. Now, we run the simulation in a 10*10 network composed of single-way roads to show the importance of driver adaptation in the characteristics of MFDs. If the drivers stick to their choice of a jammed road at an intersection, and refuse to move for other optional roads, the network can quickly fall into the jammed congested status. As shown in Figure 5.12, the simulated MFD for a network is scattered on the congested branch. The MFD on EW directed roads is close to the approximation but the MFD on NS directed roads is very unstable with its congested branch. It shows that when the driver is inadaptable in their choice of route, the MFD for the roads with low capacities are disturbed heavily. As a result of the scattered MFD on NS directed roads, the averaged MFD for the system is dispersed instead of converge with the congested branch. As the turning rates increase from 0.1 to 0.15, the MFD for the NS roads become more unstable and shrink with its jamming density. When the deterministic turning rate increases to 0.2, the shape for MFD is greatly distorted. And it can be verified in the simulation, that the MFD becomes distorted more easily with networks of larger scales. This result is quite understandable because that if the turning rate is large or the scale of the network is large, the number of vehicles coming from west directions that desire to make a turn and enter the first crossing NS directed road will be large. The first crossed EW road is congested very quickly when the exogenous flow is sufficiently large. When the road is congested and vehicles cannot turn onto the first crossing NS directed roads, serious congestion begins to happen on the roads at the border of the network. Since these roads serve as the boundary entrance for exogenous traffic, the congestion would soon result in zero exogenous traffic inputs. As a result, the network system quickly falls to a jammed status while the average density in the network is very small.

In real practice, the characteristics of drivers fall between a complete stubborn and a complete adaptation, so it is likely that the shape of MFD will bear a slight scatter on the congested branch.

5.4.2 Disturbance of Slow Movers

In urban networks, there are often slow movers mixed in the traffic stream, such as the school bus and large trucks. The existence of such slow movers would also exert an impact on the shape for MFD. To identify this impact, we fix the percentage of slow movers in regular traffic as 10%, and test with a slow movers' speed of $\frac{3}{4}v_f$ and $\frac{1}{2}v_f$ separately. The simulated MFDs are shown in Figure 5.13 and they are compared with their counterpart in Figure 5.1. The existence of slow movers suppresses the average speed in the network and causes a drop in the free-flow speed and maximum capacity. But the slow movers don't affect the shape of the congested branch. With a fixed percentage of slow movers in traffic, the critical density for MFD is shifted towards jamming density. The slower speed for those slow movers, the greater the capacity drops and the critical density shifts.

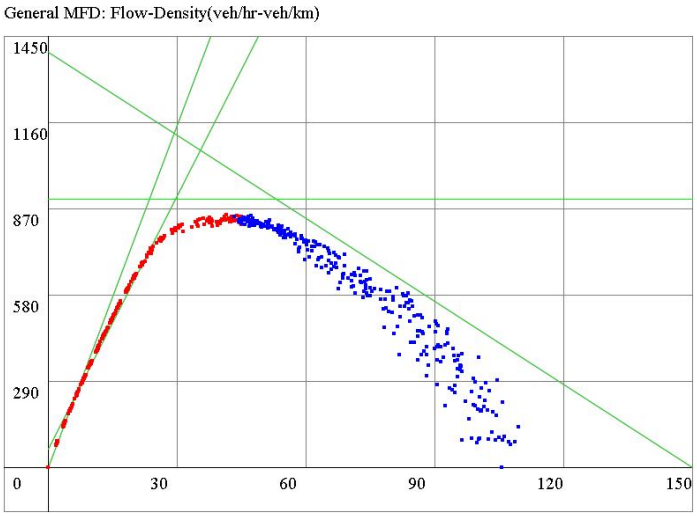

(a) MFD: L=100m, C=80s, G=50%C, offset=0s, turning rate=0.1

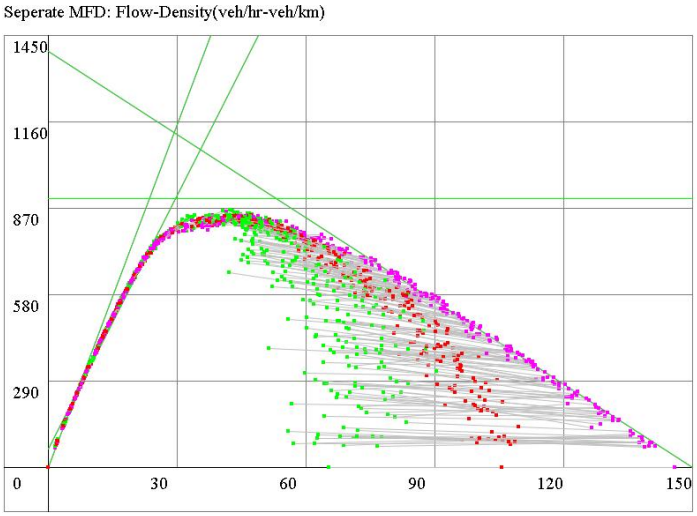

(b) MFD and EW/NS MFD: L=100m, C=80s, G=50%C, offset=0s, turning rate=0.1

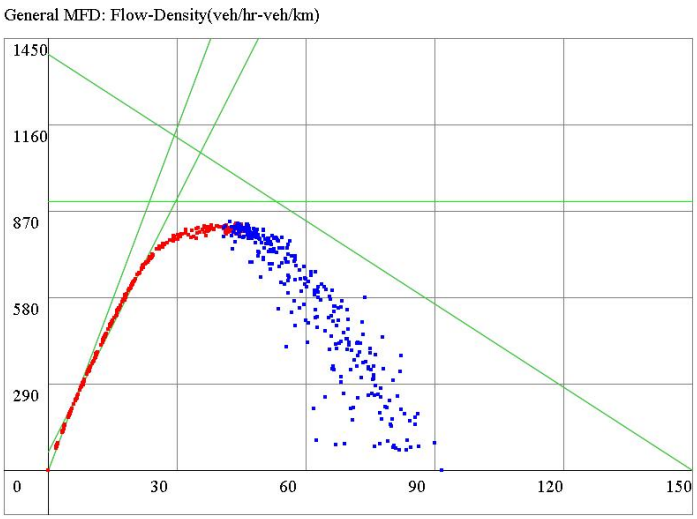

(c) MFD: L=100m, C=80s, G=50%C, offset=0s, turning rate=0.15

Figure 5.12 MFD in network with drivers that are not adaptive in route selection

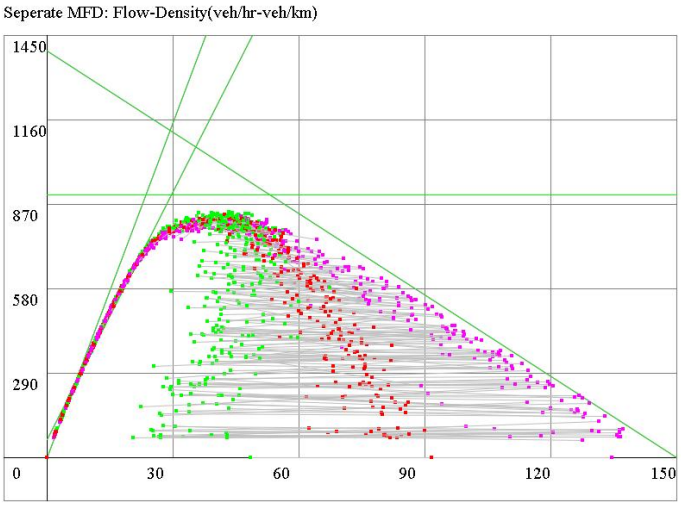

(d) MFD and EW/NS MFD: L=100m, C=80s, G=50%C, offset=0s, turning rate=0.15

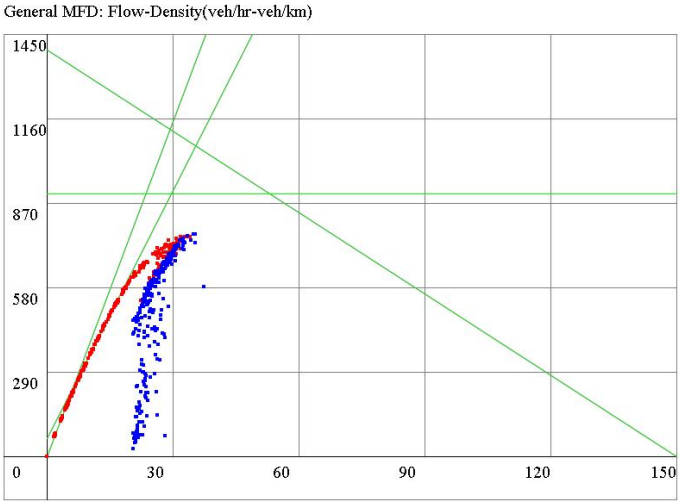

(e) MFD: L=100m, C=80s, G=50%C, offset=0s, turning rate=0.2

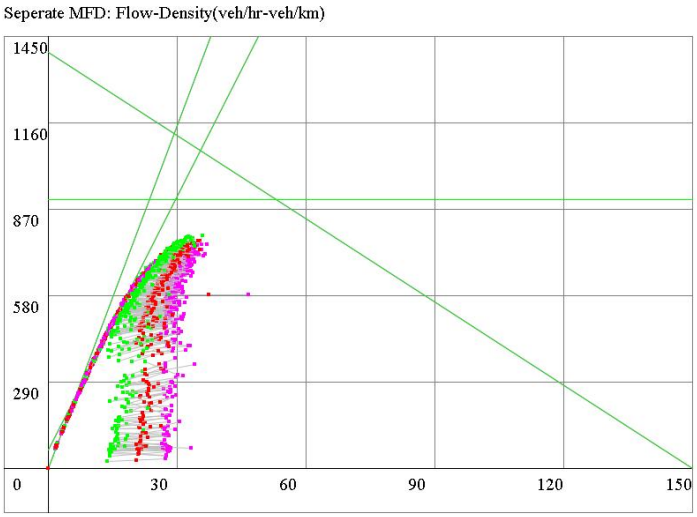

(f) L=100m, C=80s, G=50%C, offset=0s, turning rate=0.2

Figure 5.12 MFD in network with drivers that are not adaptive in route selection (Continued)

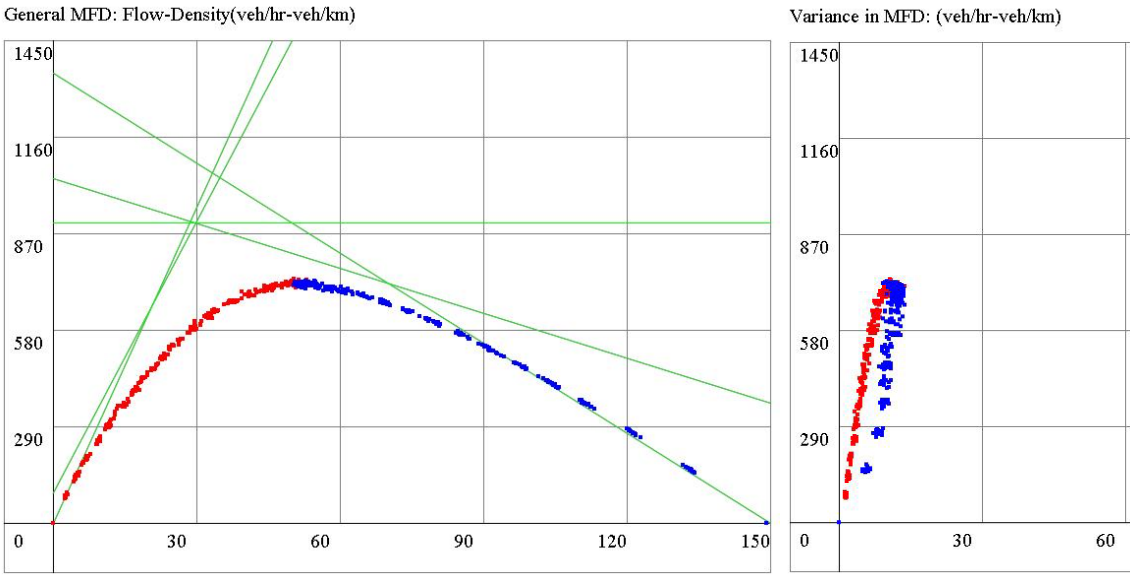

(a) MFD: L=100m, C=80s, G=50%C, offset=0s, turning rate=0.1, slow mover speed=0.75v_f

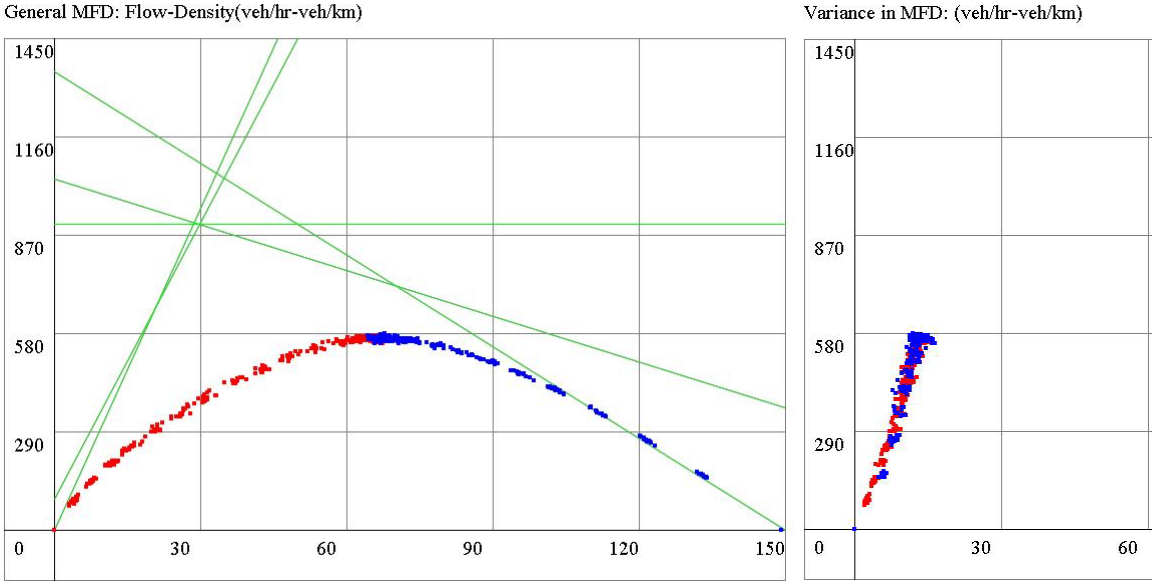

(b) MFD: L=100m, C=80s, G=50%C, offset=0s, turning rate=0.1; slow mover speed=0.5v_f

Figure 5-13 MFD in network with slow movers

CHAPTER 6

CONCLUSION AND OUTLOOKS

6.1 Major Findings

The thesis has conducted analysis with the approximated model for MFD as suggested by Daganzo in 2008. It has made progress in two regards: first, it simplifies the approximation model by reducing the cuts needed, and secondly, it makes tests with situations that the approximation model fails to deal with. With the first discovery, the future studies just need to focus on the characteristics of a very limited number of cuts to make the prediction for the appearance of MFD. It has revealed that instead of concerning with all kinds of traditional factors such as road length, cycle, green phase, and offset, the approximation actually relies only on three parameters: D_1, D_1^b and G/C. The application of Daganzo's model is studied first in a scenario of a road chain, where each road is connected to each other from end to end. When all the roads in the chain is homogeneous in their length, the model of Daganzo can be improved in reducing the cuts it requires to construct an upper approximation. The improvements proposed by the thesis promises to reduce the total cuts required for MFD approximation to at most 7 cuts. The total number of desired cuts are dependent on three parameters: for D_1, D_1^b and G/C as described in Chapter 4. The approximation suggests that regardless of the road lengths and signal designs, the MFD developed with an offset=0 can always approximate with a maximum capacity $\frac{G}{C} q_c$. The length of road determines whether the range for the maximum capacity $\frac{G}{C} q_c$ can possibly exist by choosing appropriate offsets. We have shown in Section 4.5 that if $L \geq \frac{Gwv}{w+v}$, such range exists.

Comparing the approximation with the simulated results, we find that when Edie's formula (1974) is applied for the calculation for flow and density in the simulation, the simulation generate results that are highly compatible and consistent with

the prediction given by the approximation. The critical density obtained from the simulation is exactly the same what the approximation predicts. However, when a range for the capacity $\frac{G}{C} q_c$ exist, the simulation is very difficult to retain traffic status performing with the maximum capacity. In such as simulated model, the traffic either stay with the free-flow branch or with the congested branch. It is also found that the simulation tends to overpass the predicted value where the value of $\frac{D_1}{C} mod 1$ is a little less than the one that can divide the green phase rate in a cycle without remainder. The cuts formed by stopping at intersections before the first intersection the observer has to stop are the major causes for the difference between simulation and prediction. The number of and the length of roads in the system would also contributing to the deviation, because the road chain with fewer roads and short roads are more likely to be underestimated by the approximation.

When the improved approximation model is compared with simulation, it shows that the approximation and simulation are highly compatible with each other, although some large deviations may occur near the situation where the value $\frac{D_1}{C} mod 1$ can divide $\frac{G}{C}$ without remainder and when the road length is small.

The MFD approximation has assumed a very small turning rate and that no trip begins or ends in the middle of the system. This thesis has looked into those two problems by testing them with simulation Turning rate can play an important role to smooth the linear cuts in the approximation into curves by lowering the maximum capacity in the system and at the same time bulge the curve near the critical density. When turning rate is introduced, the system's ability to keep stabilized near the critical density is greatly strengthened. The stability becomes stronger with larger deterministic turning rates, so that sample points tend to gather near the critical density in those cases. The critical density is also shifted if turning rates apply, and the shift direction of the critical density from its original predicted location is determined by the cuts that are cut

closest with the S-cut. The critical density would shift towards the side with a less steep cut.

The endogenous traffics bring instability to the equilibrium of the system. The endogenous exit rate plays a role in cap the maximum flow in the MFD. It also brings greater variance for the congested branch. The endogenous traffic generation can increase the maximum flow in the MFD in the existence of endogenous exit rate. But it also create greater variance density for the free-flow branch. A summary for the effects for various factors in play are shown as follows in Table 6.1.

Table 6.1 Impacts exerted on MFD by various factors

	Reduce capacity	**Increase capacity**	**Reduce critical density**	**Increase critical density**	**Reduce difference between MFDs**	**Change variance in density**
Turning rate	Y		Sometimes	Sometimes	Y	Y
Stochastic exogenous input	Y				Y	Y
Stochastic turn	Y		Sometimes	Sometimes	Y	Y
Endout	Y		Y		Y	Y
End in		Y		Y		Y

The simulations without driver adaption strategy show that the driver's adaptation in avoiding congestion in their route choice determines the value of average density when the system is completely jammed. The low capability for drivers to avoid congested roads will cause great variance in density in the system, and cause a dispersed MFD in congested status and make the system fall to jammed congestion even at low average system density.

6.2 Outlooks on the Research

The thesis has discussed the research of MFD with the approximation model. It has suggested improvements on the approximation model that reduce the required calculation and can easily give explicit formula for the approximated MFD and verifies the consistency between the approximation and simulation with CA model. This discovery enables future researchers to better focus a few cuts that can effectively decide

the MFD. The discussion on turning rates and endogenous traffic makes up for the common situations in network that the approximation model fail to consider. The thesis also expound on the effect that these factors can bring on the approximation. And it points out that some effects of these impacts are dependent with the slope of the cuts that are employed in the approximation model. It indicates that modification based on the effect of turning rates and endogenous traffic can be applied to the approximated results in the approximation to make a prediction for the MFD under these situations.

The discussion on the application of the MFD can be implemented with future studies to improve. The improved model for MFD approximation can be further strengthened. A majority of results in approximation suggests that although the improved approximation model has greatly reduced the cuts required in road chain prediction, there may still be some redundant cuts generated under this model. And although the effect of various factors on the MFD is verified in Chapter 5, more studies are required to quantify the results to give a precise formula to modify with the approximated results.

APPENDIX A

PROGRAMMING SCRIPT FOR THE MFD APPROXIMATION

Java Programming

```
public void estimation(int length, int offset, int green, int cycle, int stnum){
      double greentime=green*1.6;
      double cycletime=cycle*1.6;
      double offsettime=offset*1.6;
      double reachtime=length*0.4;
      double wreachtime=length*1.6;
      int maxforward=stnum+1, maxback=stnum+1;
      mf1=(length*0.4+offsettime)%cycletime/cycletime;mb1=(length*1.6+cycletime-
offsettime)%cycletime/cycletime;
      double mf=((double)length/4+offset)%cycle; int mb=(length+cycle-offset)%cycle;
      for (int i=1;i<=stnum;i++){if
(Double.valueOf(fds.format((i*mf)%cycle))>=green){maxforward=i;break;}}
      for (int i=1;i<=stnum;i++){if ((i*mb)%cycle>=green){maxback=i;break;}}
      ParaMFD.resultprint("Maxforward",maxforward,"Maxbackward=",maxback);
      ParaMFD.resultprint("m_f",mf1,"m_b=",mb1);
      double judgejumpf;int judgejumpb;
      if (mf!=0){judgejumpf=((int)Math.floor(green/mf)+1)*mf;}else{judgejumpf=2*cycle;}
      if (mb!=0){judgejumpb=((int)Math.floor(green/mb)+1)*mb;}else{judgejumpb=2*cycle;}
      if (judgejumpf==2*cycle){
         bgmfd.setColor(Color.cyan);cutf++;
         double obspeed=60;
         double passrate=0;
         int[] linepoint=plots.linebrush(obspeed, passrate);
         bgmfd.drawLine(linepoint[0], linepoint[1], linepoint[2], linepoint[3]);
         ParaMFD.resultprint("slope",obspeed,"intercept=",passrate);
         uf[0]=obspeed;cf[0]=passrate;tf[0]=1;
      }else if ((judgejumpf>=cycle)&&(Double.valueOf(fds.format(green%mf))!=0)){
         bgmfd.setColor(Color.magenta);cutf++;
         int n=1, prevjump=0;
         if (Math.ceil(Double.valueOf(fds.format(1/mf1)))<=maxforward){
            int r=(int)Math.ceil(Double.valueOf(fds.format(1/mf1)))-1;
            double beforeredtime=greentime-(r*mf)%cycle*1.6;
            double obspeed=length*r/(reachtime*r+beforeredtime+cycletime-greentime)*24;
            double passrate=1800*(beforeredtime)/(reachtime*r+beforeredtime+cycletime-greentime);
            int[] linepoint=plots.linebrush(obspeed, passrate);
            bgmfd.drawLine(linepoint[0], linepoint[1], linepoint[2], linepoint[3]);
            ParaMFD.resultprint("slope",obspeed,"intercept=",passrate,"Stopped Intersection=",r);
            cutf++;
            uf[2]=obspeed;cf[2]=passrate;tf[2]=5;
         }
         n=(int)Math.floor(Double.valueOf(fds.format(maxforward*mf1)));
         if (n>=1){
            int r=(int)Math.ceil(Double.valueOf(fds.format(n/mf1)))-1;
            int i=1;
            while (Math.ceil(Double.valueOf(fds.format((n-i)/mf1)))>=1){
               if (Math.ceil(Double.valueOf(fds.format((n-i)/mf1)))-1==r-1){r--;i++;}else{break;}
            }
```

```
        if ((r>(int)Math.ceil(Double.valueOf(fds.format(1/mf1)))-1)&&(r<maxforward)){
            double beforeredtime=greentime-(r*mf)%cycle*1.6;
            double obspeed=length*r/(reachtime*r+beforeredtime+cycletime-greentime)*24;
            double passrate=1800*(beforeredtime)/(reachtime*r+beforeredtime+cycletime-greentime);
            int[] linepoint=plots.linebrush(obspeed, passrate);
            bgmfd.drawLine(linepoint[0], linepoint[1], linepoint[2], linepoint[3]);
            ParaMFD.resultprint("slope",obspeed,"intercept=",passrate,"Stopped Intersection=",r);
            cutf++;
            uf[1]=obspeed;cf[1]=passrate;tf[1]=4;
        }
    }
    if (maxforward<=stnum){
        int r=maxforward;
        double beforegreentime=cycletime-(r*mf)%cycle*1.6;
        double obspeed=length*r/(reachtime*r+beforegreentime)*24;
        double passrate=0;
        int[] linepoint=plots.linebrush(obspeed, passrate);
        bgmfd.drawLine(linepoint[0], linepoint[1], linepoint[2], linepoint[3]);
        ParaMFD.resultprint("slope",obspeed,"intercept=",passrate,"Stopped Intersection=",r);
        uf[0]=obspeed;cf[0]=passrate;tf[0]=2;
    }else{
        double obspeed=60;
        double passrate=0;
        int[] linepoint=plots.linebrush(obspeed, passrate);
        bgmfd.drawLine(linepoint[0], linepoint[1], linepoint[2], linepoint[3]);
        ParaMFD.resultprint("slope",obspeed,"intercept=",passrate);
        uf[0]=obspeed;cf[0]=passrate;tf[0]=1;
    }
}else if ((judgejumpf<cycle)&&(Double.valueOf(fds.format(green%mf))!=0)){
    bgmfd.setColor(Color.green);cutf++;
    int r=maxforward-1;
    if (r>0){
        double beforeredtime=greentime-(r*mf)%cycle*1.6;
        double obspeed=length*r/(reachtime*r+beforeredtime+cycletime-greentime)*24;
        double passrate=1800*(beforeredtime)/(reachtime*r+beforeredtime+cycletime-greentime);
        int[] linepoint=plots.linebrush(obspeed, passrate);
        bgmfd.drawLine(linepoint[0], linepoint[1], linepoint[2], linepoint[3]);
        ParaMFD.resultprint("slope",obspeed,"intercept=",passrate,"Stopped Intersection=",r);
        cutf++;
        uf[1]=obspeed;cf[1]=passrate;tf[1]=3;
    }
    if (maxforward<=stnum){
        r=maxforward;
        double beforegreentime=cycletime-((r*mf)%cycle)*1.6;
        double obspeed=length*r/(reachtime*r+beforegreentime)*24;
        double passrate=0;
        int[] linepoint=plots.linebrush(obspeed, passrate);
        bgmfd.drawLine(linepoint[0], linepoint[1], linepoint[2], linepoint[3]);
        ParaMFD.resultprint("slope",obspeed,"intercept=",passrate,"Stopped Intersection=",r);
        uf[0]=obspeed;cf[0]=passrate;tf[0]=2;
    }else{
        double obspeed=60;
        double passrate=0;
        int[] linepoint=plots.linebrush(obspeed, passrate);
        bgmfd.drawLine(linepoint[0], linepoint[1], linepoint[2], linepoint[3]);
        ParaMFD.resultprint("slope",obspeed,"intercept=",passrate);
```

```
            uf[0]=obspeed;cf[0]=passrate;tf[0]=1;
          }
        }else if (Double.valueOf(fds.format(green%mf))==0){
          bgmfd.setColor(Color.gray);
          if (maxforward<=stnum){
            int r=maxforward;
            double beforegreentime=cycletime-(r*mf)%cycle*1.6;
            double obspeed=length*r/(reachtime*r+beforegreentime)*24;
            double passrate=0;
            int[] linepoint=plots.linebrush(obspeed, passrate);
            bgmfd.drawLine(linepoint[0], linepoint[1], linepoint[2], linepoint[3]);
            ParaMFD.resultprint("slope",obspeed,"intercept=",passrate,"Stopped Intersection=",r);
            uf[0]=obspeed;cf[0]=passrate;tf[0]=2;
          }else{
            double obspeed=60;
            double passrate=0;
            int[] linepoint=plots.linebrush(obspeed, passrate);
            bgmfd.drawLine(linepoint[0], linepoint[1], linepoint[2], linepoint[3]);
            ParaMFD.resultprint("slope",obspeed,"intercept=",passrate);
            uf[0]=obspeed;cf[0]=passrate;tf[0]=1;
          }
        }
        if (judgejumpb==2*cycle){
          bgmfd.setColor(Color.cyan);cutb++;
          double obspeed=-15;
          double passrate=2250;
          int[] linepoint=plots.linebrush(obspeed, passrate);
          bgmfd.drawLine(linepoint[0], linepoint[1], linepoint[2], linepoint[3]);
          ParaMFD.resultprint("slope",obspeed,"intercept=",passrate);
          ub[0]=obspeed;cb[0]=passrate;tb[0]=1;
        }else if ((judgejumpb>=cycle)&&(green%mb!=0)){
          bgmfd.setColor(Color.magenta);cutb++;
          int n=1,prevjump=0;
          if (Math.ceil(Double.valueOf(fds.format(1/mb1)))<=maxback){
            int r=(int)Math.ceil(Double.valueOf(fds.format(1/mb1)))-1;
            double beforeredtime=greentime-(r*mb)%cycle*1.6;
            double obspeed=-length*r/(wreachtime*r+beforeredtime+cycletime-greentime)*24;
            double
passrate=(1800*beforeredtime+2250*wreachtime*r)/(wreachtime*r+beforeredtime+cycletime-greentime);
            int[] linepoint=plots.linebrush(obspeed, passrate);
            bgmfd.drawLine(linepoint[0], linepoint[1], linepoint[2], linepoint[3]);
            ParaMFD.resultprint("slope",obspeed,"intercept=",passrate,"Stopped Intersection=",r);
            cutb++;
            ub[2]=obspeed;cb[2]=passrate;tb[2]=5;
          }
          n=(int)Math.floor(Double.valueOf(fds.format(Math.min(maxback,stnum)*mb1)));
          if (n>=1){
            int r=(int)Math.ceil(Double.valueOf(fds.format(n/mb1)))-1;
            int i=1;
            while (Math.ceil(Double.valueOf(fds.format((n-i)/mb1)))>=1){
              if (Math.ceil(Double.valueOf(fds.format((n-i)/mb1)))-1==r-1){r--;i++;}else{break;}
            }
            if (r>(int)Math.ceil(Double.valueOf(fds.format(1/mb1)))-1){
              double beforeredtime=greentime-(r*mb)%cycle*1.6;
              double obspeed=-length*r/(wreachtime*r+beforeredtime+cycletime-greentime)*24;
```

```
                double
passrate=(1800*beforeredtime+2250*wreachtime*r)/(wreachtime*r+beforeredtime+cycletime-greentime);
                int[] linepoint=plots.linebrush(obspeed, passrate);
                bgmfd.drawLine(linepoint[0], linepoint[1], linepoint[2], linepoint[3]);
                ParaMFD.resultprint("slope",obspeed,"intercept=",passrate,"Stopped Intersection=",r);
                cutb++;
                ub[1]=obspeed;cb[1]=passrate;tb[1]=4;
              }
            }
            if (maxback<=stnum){
              int r=maxback;
              double beforegreentime=cycletime-(r*mb)%cycle*1.6;
              double obspeed=-length*r/(wreachtime*r+beforegreentime)*24;
              double passrate=2250*wreachtime*r/(wreachtime*r+beforegreentime);
              int[] linepoint=plots.linebrush(obspeed, passrate);
              bgmfd.drawLine(linepoint[0], linepoint[1], linepoint[2], linepoint[3]);
              ParaMFD.resultprint("slope",obspeed,"intercept=",passrate,"Stopped Intersection=",r);
              ub[0]=obspeed;cb[0]=passrate;tb[0]=2;
            }else{
              double obspeed=-15;
              double passrate=2250;
              int[] linepoint=plots.linebrush(obspeed, passrate);
              bgmfd.drawLine(linepoint[0], linepoint[1], linepoint[2], linepoint[3]);
              ParaMFD.resultprint("slope",obspeed,"intercept=",passrate);
              ub[0]=obspeed;cb[0]=passrate;tb[0]=1;
            }
          }else if ((judgejumpb<cycle)&&(green%mb!=0)){
            bgmfd.setColor(Color.green);cutb++;
            int r=maxback-1;
            if (r>0){
              double beforeredtime=greentime-(r*mb)%cycle*1.6;
              double obspeed=-length*r/(wreachtime*r+beforeredtime+cycletime-greentime)*24;
              double
passrate=(1800*beforeredtime+2250*wreachtime*r)/(wreachtime*r+beforeredtime+cycletime-greentime);
              int[] linepoint=plots.linebrush(obspeed, passrate);
              bgmfd.drawLine(linepoint[0], linepoint[1], linepoint[2], linepoint[3]);
              ParaMFD.resultprint("slope",obspeed,"intercept=",passrate,"Stopped Intersection=",r);
              cutb++;
              ub[1]=obspeed;cb[1]=passrate;tb[1]=3;
            }
            if (maxback<=stnum){
              r=maxback;
              double beforegreentime=cycletime-(r*mb)%cycle*1.6;
              double obspeed=-length*r/(wreachtime*r+beforegreentime)*24;
              double passrate=2250*wreachtime*r/(wreachtime*r+beforegreentime);
              int[] linepoint=plots.linebrush(obspeed, passrate);
              bgmfd.drawLine(linepoint[0], linepoint[1], linepoint[2], linepoint[3]);
              ParaMFD.resultprint("slope",obspeed,"intercept=",passrate,"Stopped Intersection=",r);
              ub[0]=obspeed;cb[0]=passrate;tb[0]=2;
            }else{
              double obspeed=-15;
              double passrate=2250;
              int[] linepoint=plots.linebrush(obspeed, passrate);
              bgmfd.drawLine(linepoint[0], linepoint[1], linepoint[2], linepoint[3]);
              ParaMFD.resultprint("slope",obspeed,"intercept=",passrate);
              ub[0]=obspeed;cb[0]=passrate;tb[0]=1;
```

```
        }
      }else if (green%mb==0){
        bgmfd.setColor(Color.gray);
        if (maxback<=stnum){
          int r=maxback;
          double beforegreentime=cycletime-(r*mb)%cycle*1.6;
          double obspeed=-length*r/(wreachtime*r+beforegreentime)*24;
          double passrate=2250*wreachtime*r/(wreachtime*r+beforegreentime);
          int[] linepoint=plots.linebrush(obspeed, passrate);
          bgmfd.drawLine(linepoint[0], linepoint[1], linepoint[2], linepoint[3]);
          ParaMFD.resultprint("slope",obspeed,"intercept=",passrate,"Stopped Intersection=",r);
          ub[0]=obspeed;cb[0]=passrate;tb[0]=2;
        }else{
          double obspeed=-15;
          double passrate=2250;
          int[] linepoint=plots.linebrush(obspeed, passrate);
          bgmfd.drawLine(linepoint[0], linepoint[1], linepoint[2], linepoint[3]);
          ParaMFD.resultprint("slope",obspeed,"intercept=",passrate);
          ub[0]=obspeed;cb[0]=passrate;tb[0]=1;
        }
      }
      bgmfd.setColor(Color.orange);
      double obspeed=0;
      double passrate=greentime/cycletime*1800;
      int[] linepoint=plots.linebrush(obspeed, passrate);
      bgmfd.drawLine(linepoint[0], linepoint[1], linepoint[2], linepoint[3]);
      ParaMFD.resultprint("slope",obspeed,"intercept=",passrate);
      ParaMFD.resultprint("forward cuts",cutf,"backward cuts=",cutb);
      scut=passrate;
      repaint();
      }
```

3-d Interpolation for MFD Mapping in Matlab

```
clear;
load('l37c50g40n30.mat');       %%can be replace by other documents
figure;grid;hold on;
xlabel('density');ylabel('offset/cycle');zlabel('flow');
cycle=50;          %%set correct cycle
t=l37c50g40n30;         %%can be replace by other documents
uf=t(:,4:6);cf=t(:,7:9);tf=t(:,16:18);ub=t(:,10:12);cb=t(:,13:15);tb=t(:,19:21);
scut=t(1,22);offset=t(:,23);
SimuX=0;SimuY=0;SimuZ=0;
for i=1:cycle
   us=uf(i,:);cs=cf(i,:);ts=tf(i,:);ubs=ub(i,:);cbs=cb(i,:);tbs=tb(i,:);
   for j=3:-1:1
      if us(j)==80
         us(j)=[];cs(j)=[];ts(j)=[];
      end
      if ubs(j)==-30
         ubs(j)=[];cbs(j)=[];tbs(j)=[];
      end
   end
   xf=0;xb=0;
   temp1=size(us);temp2=temp1(2);
```

```
if temp2==1
   xf(1)=0;xf(2)=scut/us(1);
elseif temp2==2
   xf(1)=0;xf(2)=-(cs(2)-cs(1))/(us(2)-us(1));xf(3)=(scut-cs(2))/us(2);
elseif temp2==3
   test1=-(cs(2)-cs(1))/(us(2)-us(1));test2=-(cs(3)-cs(2))/(us(3)-us(2));
   if abs(test2-test1)>=0.004
      xf(1)=0;xf(2)=test1;xf(3)=test2;xf(4)=(scut-cs(3))/us(3);
   else
      xf(1)=0;xf(2)=-(cs(3)-cs(1))/(us(3)-us(1));xf(3)=(scut-cs(3))/us(3);
      us(2)=[];cs(2)=[];ts(2)=[];
   end
end
temp1=size(ubs);temp2=temp1(2);
if temp2==1
   xb(1)=150;xb(2)=-(cbs(1)-scut)/ubs(1);
elseif temp2==2
   xb(1)=150;xb(2)=-(cbs(2)-cbs(1))/(ubs(2)-ubs(1));xb(3)=-(cbs(2)-scut)/ubs(2);
elseif temp2==3
   test1=-(cbs(2)-cbs(1))/(ubs(2)-ubs(1));test2=-(cbs(3)-cbs(2))/(ubs(3)-ubs(2));
   if abs(test1-test2)>=0.004
      xb(1)=150;xb(2)=test1;xb(3)=test2;xb(4)=-(cbs(3)-scut)/ubs(3);
   else
      xb(1)=150;xb(2)=-(cbs(3)-cbs(1))/(ubs(3)-ubs(1));xb(3)=-(cbs(3)-scut)/ubs(3);
      ubs(2)=[];cbs(2)=[];tbs(2)=[];
   end
end
temp1=size(xf);temp2=size(xb);
leng1=temp1(2);leng2=temp2(2);
if xf(leng1)-xb(leng2)>0
   xf(leng1)=-(cs(leng1-1)-cbs(leng2-1))/(us(leng1-1)-ubs(leng2-1));
   xb(leng2)=xf(leng1);
   if leng1>=3&xf(leng1-1)>xb(leng2)
      xf(leng1)=[];us(leng1-1)=[];cs(leng1-1)=[];ts(leng1-1)=[];
      xf(leng1-1)=-(cs(leng1-2)-cbs(leng2-1))/(us(leng1-2)-ubs(leng2-1));
      xb(leng2)=xf(leng1-1);
      if leng1>=4&xf(leng1-2)>xb(leng2)
         xf(leng1-1)=[];us(leng1-2)=[];cs(leng1-2)=[];ts(leng1-2)=[];
         xf(leng1-2)=-(cs(leng1-3)-cbs(leng2-1))/(us(leng1-3)-ubs(leng2-1));
         xb(leng2)=xf(leng1-2);
      end
   end
   temp1=size(xf);temp2=size(xb);
   leng1=temp1(2);leng2=temp2(2);
   if leng2>=3&xf(leng1)>xb(leng2-1)
      xb(leng2)=[];ubs(leng2-1)=[];cbs(leng2-1)=[];tbs(leng2-1)=[];
      xb(leng2-1)=-(cs(leng1-1)-cbs(leng2-2))/(us(leng1-1)-ubs(leng2-2));
      xf(leng1)=xb(leng2-1);
      if leng2>=4&xf(leng1)>xb(leng2-2)
         xb(leng2-1)=[];ubs(leng2-2)=[];cbs(leng2-2)=[];tbs(leng2-2)=[];
         xb(leng2-2)=-(cs(leng1-1)-cbs(leng2-3))/(us(leng1-1)-ubs(leng2-3));
         xf(leng1)=xf(leng2-2);
      end
   end
else
```

```
        X=[xf(leng1),xb(leng2)];Y=[(i-1)/cycle,(i-1)/cycle];Z=[us(leng1-1)*xf(leng1)+cs(leng1-1),ubs(leng2-
1)*xb(leng2)+cbs(leng2-1)];
        plot3(X,Y,Z,'y');
    end
    temp1=size(us);temp2=temp1(2);
    for j=1:temp2
        X=[xf(j),xf(j+1)];Y=[(i-1)/cycle,(i-1)/cycle];Z=[us(j)*xf(j)+cs(j),us(j)*xf(j+1)+cs(j)];
        if ts(j)==1
            plot3(X,Y,Z,'r');
        elseif ts(j)==2
            plot3(X,Y,Z,'m');
        elseif ts(j)==3
            plot3(X,Y,Z,'b');
        elseif ts(j)==4
            plot3(X,Y,Z,'g');
        elseif ts(j)==5
            plot3(X,Y,Z,'c');
        end
    end
    temp1=size(ubs);temp2=temp1(2);
    for j=1:temp2
        X=[xb(j),xb(j+1)];Y=[(i-1)/cycle,(i-1)/cycle];Z=[ubs(j)*xb(j)+cbs(j),ubs(j)*xb(j+1)+cbs(j)];
        if tbs(j)==1
            plot3(X,Y,Z,'r');
        elseif tbs(j)==2
            plot3(X,Y,Z,'m');
        elseif tbs(j)==3
            plot3(X,Y,Z,'b');
        elseif tbs(j)==4
            plot3(X,Y,Z,'g');
        elseif tbs(j)==5
            plot3(X,Y,Z,'c');
        end
    end
    for j=1:150
        SimuX=[SimuX,j];
        SimuY=[SimuY,(i-1)/cycle];
        Tempq(1)=uf(i,1)*j+cf(i,1);
        Tempq(2)=uf(i,2)*j+cf(i,2);
        Tempq(3)=uf(i,3)*j+cf(i,3);
        Tempq(4)=ub(i,1)*j+cb(i,1);
        Tempq(5)=ub(i,2)*j+cb(i,2);
        Tempq(6)=ub(i,3)*j+cb(i,3);
        Tempq(7)=scut;
        SimuZ=[SimuZ,min(Tempq)];
    end
end
figure;grid;hold on;xlabel('density');ylabel('offset/cycle');zlabel('flow');
[PX,PY,PZ]=griddata(SimuX,SimuY,SimuZ,linspace(0,150)',linspace(0,1));
surf(PX,PY,PZ);shading flat;
contour3 (PX,PY,PZ,35,'w')
```

REFERENCES

Buisson, C., & Ladier, C. (2009). Exploring the impact of homogeneity of traffic measurements on the existence of macroscopic fundamental diagrams. Transportation Research Record 2124, 127-136.

Daganzo, C. F. (2004). In Traffic Flow, Cellular Automata=Kinematic Waves. Transportation Research Part B 40, 396-403.

Daganzo, C. F. (2005). A variational formualtion of kinematic waves: Basic theory and complex boundary conidtions. Transportation Research Part B, 39(10), 187-196.

Daganzo, C. F. (2007). Urban gridlock: Macroscopic modeling and mitigation approaches. Trasnportation Research Part B 41, 49-62.

Daganzo, C. F., & Geroliminis, N. (2008). An analytical approximation for the macroscopic fundamental diagram of urban traffic. Transportation Research Part B: Methodological 42, 771-781.

Daganzo, C. F., Gayah, V. V., & Gonzales, E. J. (2011). Macroscopic relations of urban traffic variables: Bifurcations, multi-valuedness and instability. Transportation Research Part B: Methodological 45, 278-288.

Edie, L. C. (1965). Discussion of traffic stream measurements and definitions. OECD, Paris: Proc. Int. Symp. on the Theory of Traffic Flow, (J.Almond, ed.).

Edie, L. C. (1974). Traffic Science (D.C. Gazis, ed.). New York: Wiley.

Gayah, V., & Daganzo, C. (2011). Clockwise hysteresis loops in the macroscopic fundamental diagram: An effect of network instability. Transportation Research Part B.

Geroliminis, N., & Boyaci, B. (2012). The effect of variability of urban systems characteristics in the network capacity. Transportation Research Part B 46, 1607-1623.

Geroliminis, N., & Daganzo, C. (2007). Macrsocopic modeling of traffic in cities. Washington, D.C.: 86th Annual Meeting of the Transportation Research Board, Paper No. 07-413.

Geroliminis, N., & Daganzo, C. (2008). Existence of urban-scale macroscopic fundamental diagrams: some experimental findings. Transportation Research Part B: Methodological 42, 759-770.

Geroliminis, N., & Sun, J. (2011). Properties of a well-defined macroscopic fundamental diagram for urban traffic. Transportation Research Part B 45, 605-617.

Godfrey, J. W. (1969). The mechanism of a road network. Traffic Engineering and Control 11, 323-327.

Greenshields, B. D. (1935). A study in highway capacity. Highway Res. Board Proc. 14, 448-477.

Helbing, B. D. (2009). Derivation of a fundamental diagram for urban traffic flow. The European Physical Journal B 70, 229-241.

Herman, R., & Ardekani, S. (1984). Characterizing traffic conditions in urban areas. Transportation Science 18 (2), 101-140.

Herman, R., & Prigogine, I. (1979). A two-fluid approach to town traffic. Science, 204(4389), 148-151.

Knoop, V. L. (2012). The impact of traffic dynamics on the Macroscopic Fundamental Diagram. 92th Annual Meeting of the Transportation Research Board. Washington D.C.

Mazloumian, A., Geroliminis, N., & Helbing, D. (2010). The spatial variability of vehicle densities as determinant of urban network capacity. Philosophical Transactions of the Royal Society A 368, 4627-4647.